NO MODUS ADRIFT

by

E. G. Ward, R .S. Mercier, Offshore Technology Research Center
J. Zhang, M. H. Kim, C. Aubeny, Texas A&M University
R. B. Gilbert, University of Texas at Austin

Final Project Report

Prepared for the Minerals Management Service
Under the MMS/OTRC Cooperative Research Agreement
1435-01-04-CA-35515
Task Order 39735
MMS Project Number: 574

March 2008

OTRC Library Number: 3/08C188

"The views and conclusions contained in this document are those of the authors and should not be interpreted as representing the opinions or policies of the U.S. Government. Mention of trade names or commercial products does not constitute their endorsement by the U. S. Government".

For more information contact:

Offshore Technology Research Center
Texas A&M University
1200 Mariner Drive
College Station, Texas 77845-3400
(979) 845-6000

or

Offshore Technology Research Center
The University of Texas at Austin
1 University Station C3700
Austin, Texas 78712-0318
(512) 471-6989

A National Science Foundation Graduated Engineering Research Center

Table of Contents

List of Tables and Figures

Tables

Figures

NO MODUS ADRIFT

by

E.G. Ward, J. Zhang, M.H. Kim, R.B. Gilbert, C. Aubeny, R.S. Mercier

Executive Summary

Mooring failures during hurricanes Ivan, Katrina, and Rita caused 16 deepwater MODU's to go adrift. Drifting MODU's can potentially damage other critical elements of the offshore oil and gas infrastructure, e.g., colliding with floating or fixed production systems and transportation hubs, or damaging pipelines by dragging anchors. The health of this infrastructure has become a matter of national significance because of the importance of deepwater production for the US oil and gas supply and its influence on worldwide process.

The objective of this research project was to investigate technical solutions that could (1) prevent the total drift-off of a MODU by intervention during the progressive failure of a mooring system during a hurricane, and (2) control or reduce the drift of an unmoored MODU in a hurricane. The approach taken for this study was to

- develop & calibrate models that could describe the progressive failure of a mooring system and the movement of a drifting MODU,
- develop mitigation ideas to prevent total mooring failure and drift-off and to control drift
- use these models to assess the expected effectiveness and applicability of these and other mitigation ideas,
- formulate a plan to develop the more promising ideas into solutions that could be applied in MODU drilling practices

This project could lead to cost-effective technical options to mitigate MODU drift due to mooring failures in hurricanes and reduce the hazards and risks to the offshore

infrastructure (e.g., floating and fixed production structures, pipelines and flowlines, subsea well systems).

Phase 1 of this project was sponsored by the MMS and the OTRC Industry Consortia and addressed the first two items above. Available information on MODU's that either went adrift during these storms was studied. Capabilities to predict (1) the behavior of a MODU during the progressive failure of its mooring system and (2) a MODU's drift after loss of stationkeeping were successfully developed and verified against data available from hurricanes Ivan and Katrina. A list of technical solutions to mitigate against a total drift-off or control the drift of an unmoored MODU was developed and reviewed with the MMS and industry. This report documents the results from Phase 1.

Phase 1 provides the basis for Phase 2. In Phase 2 we would use these capabilities to assess the feasibility and effectiveness of mitigation measures to either prevent the total failure of the mooring system or control the drift of an unmoored MODU. That assessment would identify the more promising mitigation measures, and lead to developing solutions for field application. We anticipate proceeding with Phase 2 as a JIP.

The industry is currently completing a JIP on MODU Mooring Strength and Reliability that is being managed by American Bureau of Standards Consulting (ABSC) to assess methods to immediately strengthen MODU mooring systems before the next hurricane season, address the hazards and risks of drifting MODUs, assess current API standards to determine if mooring design criteria should be increased, and develop and recommend new criteria as warranted.

The project described here is complementary, and we have appreciated and benefited from opportunities to interact with that project. While the ABSC JIP has focused more on strengthening moorings and revising criteria and standards, this OTRC project focused on technical solutions to prevent a MODU from going adrift should the mooring system

fail in a hurricane, and methods to control, reduce, or stop a MODU that has gone adrift in a hurricane.

Introduction

The objective of this research project was to investigate technical solutions that could (1) prevent the total drift-off of a MODU by intervention during the progressive failure of a mooring system during a hurricane, and (2) control or reduce the drift of an unmoored MODU in a hurricane. In this Phase 1, the focus was to develop & calibrate models that could describe (1) the progressive failure of a mooring system and (2) the movement of a drifting MODU. These models would then be available to assess the expected effectiveness and applicability of mitigation ideas. Mitigation ideas to prevent total mooring failure and drift-off and to control drift would also be developed and discussed with industry in Phase 1.

The project was structured in the following tasks:

Task 1: Data Gathering
Task 2: Case Studies of Mooring and Foundation Failures
Task 3: Validate Global Analysis Tools to Predict Mooring Failure
Task 4: Generate Ideas to Prevent MODU Going Adrift
Task 5: Validate Global Analysis Tools to Predict MODU Drift
Task 6: Generate Ideas to Slow or Stop a Drifting MODU
Task 7: Review Alternatives & Select Promising Alternatives for detailed analysis

Results from these tasks will be addressed in the following sections.

Data Gathering & Case Studies

Case Selections. Available data was reviewed to select cases that could be used to calibrate the models being developed to (1) prevent the total drift-off of a MODU by intervention during the progressive failure of a mooring system during a hurricane, and

(2) control or reduce the drift of an unmoored MODU in a hurricane. Data needed to calibrate these models are

- specific MODU failures of interest that can serve as case studies for use in calibrating either the model of the progressive failure of the mooring system or (2) the model to describe the movement of a drifting MODU
- sufficiently detailed descriptions of the MODUs such that the structures could be modeled
- detailed information on the failures
- information on the metocean environment present during the failure

Table 1 (Sharples 2006a) shows the deepwater MODUs that went adrift or had partial mooring failures during hurricanes Ivan, Katrina, and Rita. Sixteen MODUs went adrift after suffering a complete mooring system failure, and two that were being towed went adrift after their towlines failed. Eight MODUs had partial mooring failures but remained on station.

Table 1. Deepwater MODUs that Went Adrift or Had Partial Mooring Failure during Hurricanes Ivan, Katrina, And Rita (Sharples 2006a)

Hurricane	MODU	Block	Depth	# Line Failures	Drift (approx miles)	Anchors Dragged	Remarks
Ivan	Ocean America	VN962	4677	total	10	?	
	Ocean Star	VN825	2423	total	25	?	
	Jim Thompson	MC383	5730	total	55	N	
	Nautilus	LR399	8989	total	70	N	
	Lorris Bouzigard	VN817	650	partial	0.5	?	
Katrina							
	Jim Thompson	**MC935**	**3865**	**total**	**20**	**Y**	
	Ocean Voyager	MC711	2975	total	10	N	
	Nautilus	GC434	3444	total	80	N	
	Arctic I	MC413	1750	total	25	N	
	Development Driller I	**GI92**	**240**	**partial**	**0.5**	**Y**	
	Development Driller II	**GI91**	**275**	**partial**	**0.3**	**Y**	
	Celtic Sea	**GC562**	**4040**	**partial**	**4**	**Y**	
	Ocean Quest	MC161	3200	minor	na	na	
	Ensco 7500	GC652		towline parted	na	na	under tow, broke towline
Rita							
	Paul Romano	**GC518**	**4049**	**total**	**115**	**Y, 0.5mi**	
	Ocean Saratoga	**GC157**	**2450**	**total**	**100**	**?**	
	Marianis	**GC882**	**3840**	**total**	**145**	**Y, 0.5mi**	
	Ocean Star	**GC768**	**5253**	**total**	**100**	**N**	
	Amos Runner	**GC765**	**5313**	**total**	**75**	**?**	
	Max Smith	**GC238**	**2346**	**total**	**123**	**Y**	
	Therald Martin	**GC236**	**2160**	**total**	**100**	**Y, 100**	
	Lorris Bouzigard	GB244	2114	partial	0.8	0.8	
	Celtic Sea	GI107	320	partial	1	1	
	Ocean Concord	GI106	342	partial, 6/8	0.5	0.5	
	F-100	GC6/50	660	partial	0.5	0.5, 4/8	
	Development Driller I	GI91	275	minor		na	
	Nautilus	GC 434	3444	towline parted	na	na	under tow, broke towline

Detailed analyses on the mooring system failures of the Deepwater Nautilus and the Noble Jim Thompson were presented by Shell and BP, respectively, at the 2005 API Hurricane Readiness and Recovery Conference (OTRC 2005). These and other mooring system failures during hurricane Ivan are also documented by Sharples (2006b, 2006c).

The completeness of the available data led us to select the Deepwater Nautilus and the Noble Jim Thompson mooring failures during hurricane Ivan as the best case studies to use in validating the model to predict the progressive failure of mooring systems. The location of these MODUs relative to hurricane Ivan's track is shown in Figure 1.

Figure 1. Hurricane Ivan & MODU Locations

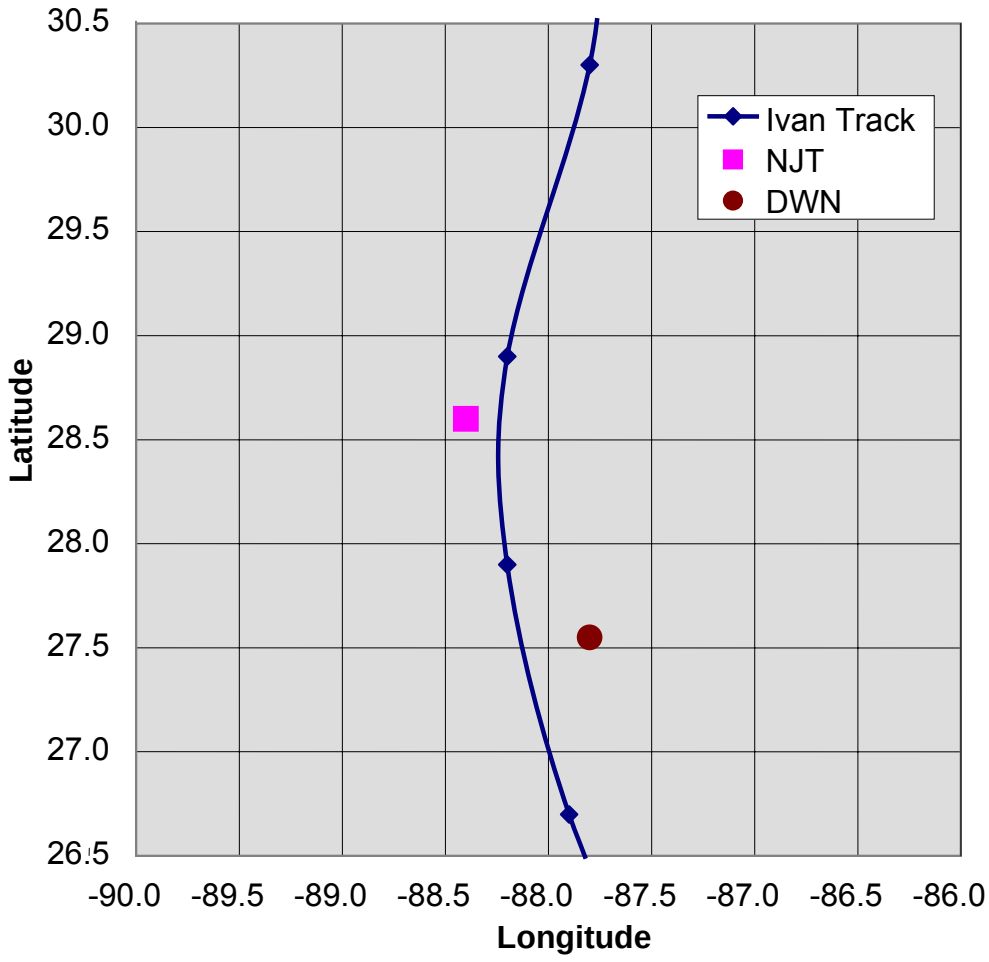

During hurricane Ivan, MODUs were generally not equipped with instrumentation that would provide data on their tracks when they went adrift. Following Ivan, MODU operators were encouraged to outfit MODUs with GPS systems that could broadcast their positions to shore receiving stations. Thus during hurricanes Katrina and Rita, there were tracks available for many of the MODUs that went adrift.

When hurricane Katrina passed close to the locations of the Deepwater Nautilus and Noble Jim Thompson, the mooring systems failed and these MODUs went adrift. GPS systems on each MODU provided data on their drift tracks as shown in Figure 2 (MMS 2006). The Deepwater Nautilus and the Noble Jim Thompson drift during hurricane Katrina were selected as cases to use in validating the model to predict MODU drift tracks. Aside from providing good cases for study, this allowed the use the same MODUs for both the progressive mooring failure and drift studies and avoid have to develop models of two additional MODUs.

Figure 2. Measured Drifts for the Noble Jim Thompson & the Deepwater Nautilus during Hurricane Katrina (30 minute intervals)

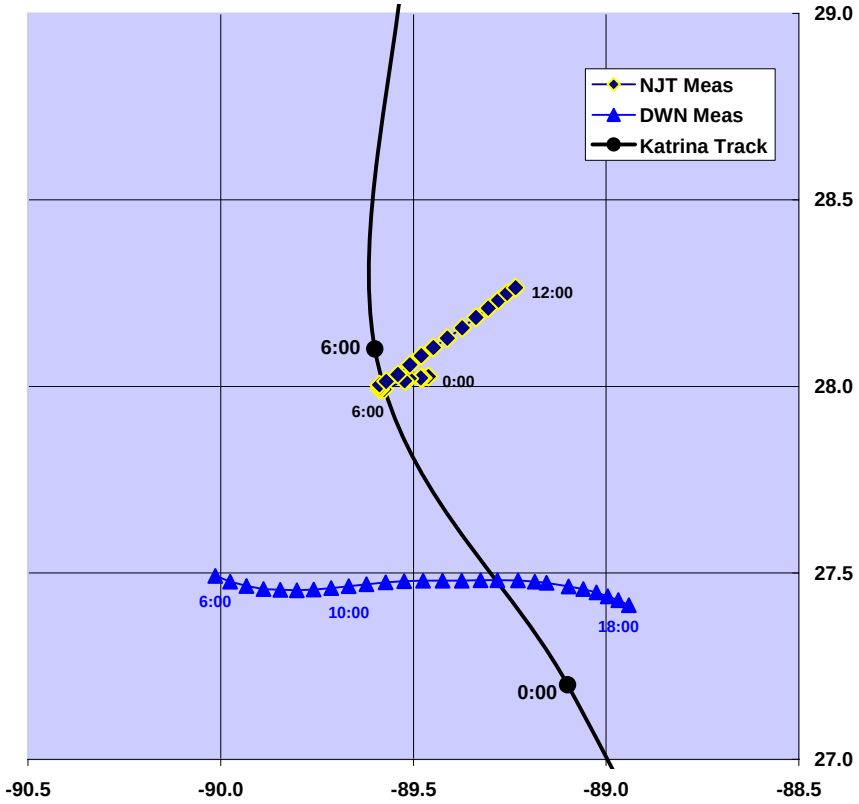

MODU Descriptions. The Noble Jim Thompson has a triangularly shaped hull. The Deepwater Nautilus' hull has four columns and pontoons. Detailed descriptions of these two MODUs were not available for this study. Delmar used Information taken from public literature to develop approximate descriptions for these two MODUs and provided this information for use in this study (Delmar 2006). These MODUs will be referred to as MODU 1 and MODU 2 in the remainder of this report. The hull models for MODU I and MODU II are shown in Figure 3. Information on mooring systems and wind load coefficients was also provided.

Figure 3. Hull Models

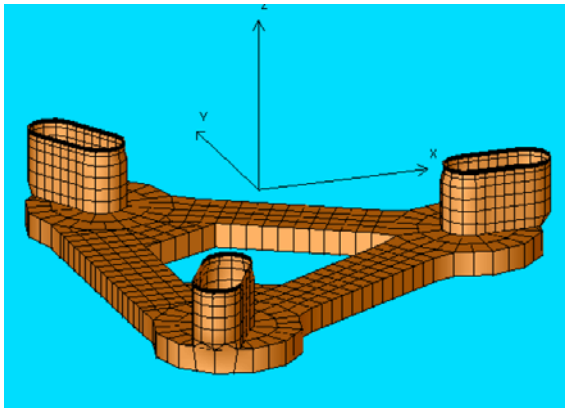

MODU I

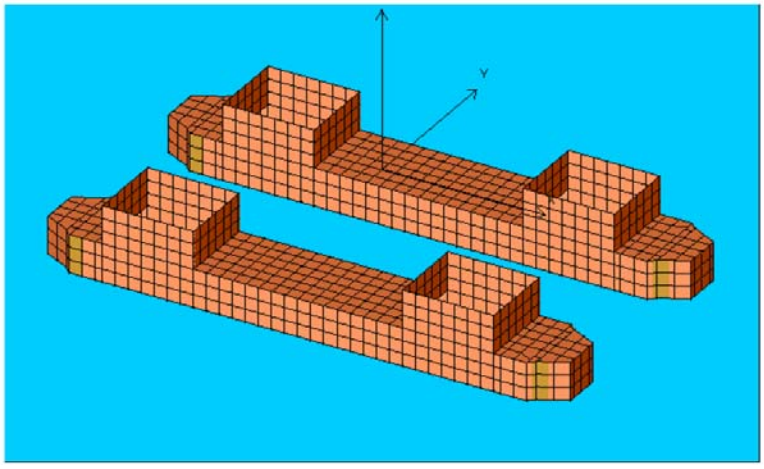

MODU II

Recall that a primary purpose of this study was to use available information to validate numerical models for the progressive mooring failure and the drift of a MODU, and not to do post-storm forensic analyses of the failure and subsequent behaviors of either Noble Jim Thompson or the Deepwater Nautilus. As the results will indicate, these approximate descriptions served the purpose well and led to a satisfactory validation of the numerical models.

Metocean Data. Hindcast data were available to describe the winds, waves, and currents throughout hurricanes Ivan and Katrina (Oceanweather (2004, 2005, 2006). Hurricane Ivan was hindcast twice - immediately after the storm (termed the Emergency Response Data or ERD hindcast) and again later once all available data could be gathered and incorporated in the windfield for the hindcast (termed the Revised Data or RD hindcast). Because of the timing of the hindcasts and project schedule, some analyses were carried out using both hindcasts.

The Hurricane Katrina was hindcast was completed with a detailed windfield that incorporated all available data. However a different current model was used to improve the hindcast of near surface currents.

The hindcasts provided predicted winds, wave, and currents at times and grid point locations throughout the storms, which were interpolated to the MODU locations. Waves were described by statistical parameters and directional spectra.

Drifting MODUs

The numerical model DRIFT was developed to predict the drift of an unmoored MODU in hurricane winds, waves, and currents. The equation describing the horizontal motion of the MODU due to steady wind, wave (mean drift), and current forces is written as

$$(\mathbf{M}_S + \mathbf{M}_{add})\, d^2\mathbf{x}(t)/dt^2 = \mathbf{F}_{wind} + \mathbf{F}_{Current} + \mathbf{F}_{WMDF}$$

where **x** = surge, sway, and yaw and $\mathbf{M}_S$ and $\mathbf{M}_{add}$ are the MODU mass and added mass, respectively. The forces **F** are computed from MODU properties and the winds, waves, and currents at the current locations. This equation solved numerically using the metocean parameters at the MODUs current location to predict the MODU's movement to a new position **x**. Appendix A provides more details of the solution method and provides detailed results. Some of the important results and conclusions are summarized here.

MODU I. As shown in Figure 2, MODU I went adrift as Katrina's eye approached, was blown WSW, likely passed through the eye, and then reversed directions and drifted ENE under the influence of the winds on the backside of the storm. Hindcasts were made from the initial position ahead of the storm tracked the MODU I though the eye The drift track for MODU I was initially completed based on the hindcast hurricane winds, waves, and currents, and started as the storm was approaching. The predicted track looped to the south rather than the north as it passed though the eye or Katrina. Uncertainties and the large temporal and spatial changes of the winds, waves, and currents within the eye likely contributed to errors in the predicted track. The track was predicted again starting from a position just after eye passage (6:30 UDT). That track (labeled "Predicted with No Loop Current or Anchor Drag") is shown along with the measured track in Figure 4. The predicted track was significantly farther north than the measured track.

The potential impact of the loop current was investigated since it was known that the Loop Current was also in this vicinity as shown in Figure 5. Though detailed data are not available, a easterly current of 3 fps was assumed. It was also leaned that perhaps 1 or 2 anchors had dragged, and a dragging force for the anchors was estimated and applied in the direction opposing the drift. The drift track for MODU I with the hurricane winds, waves, and currents plus the Loop Current and anchor drag is also shown in Figure 4. It should be noted that the predicted trajectory of MODU I without considering Loop Currents and Dragging Anchor was terminated at 10:30 while the measured trajectory and the related prediction with the consideration of Loop Current and Dragging Anchor

were terminated at 12:00. The addition of the effects of the Loop Current and the anchor drag significantly improved the comparison between the predicted and measured tracks.

Figure 4. Predicted and Measured Drifts for MODU I (30 minute intervals)

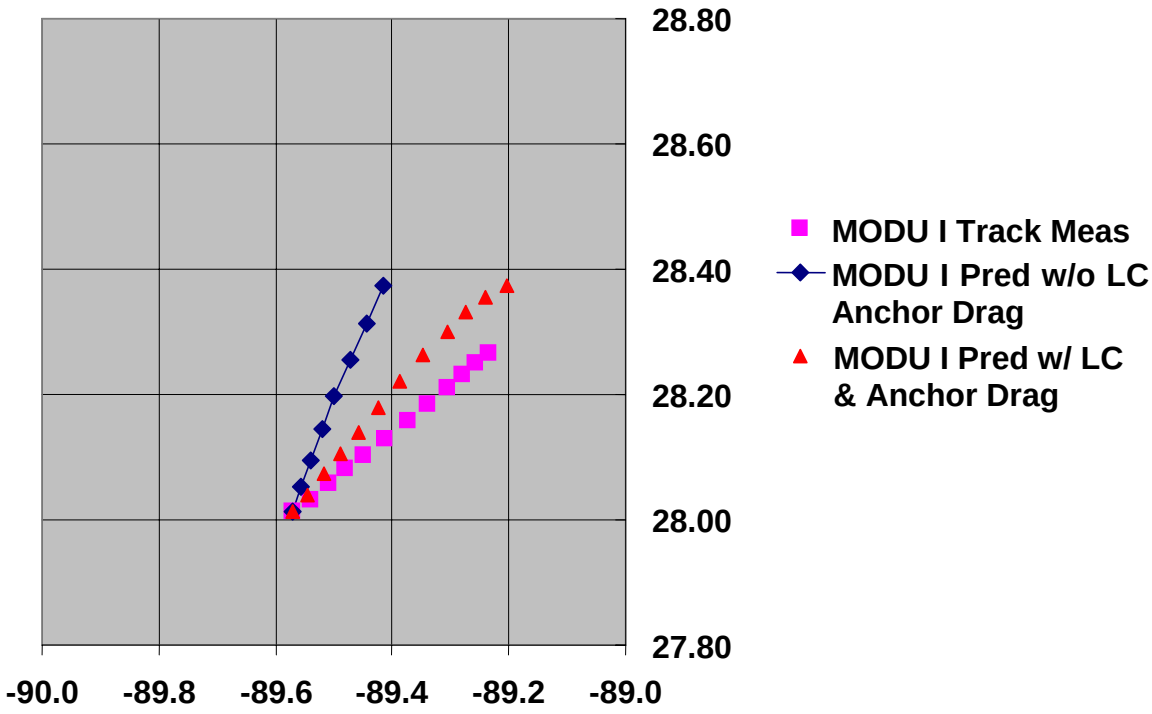

Figure 5. Loop Current near MODUs I & II during Hurricane Katrina

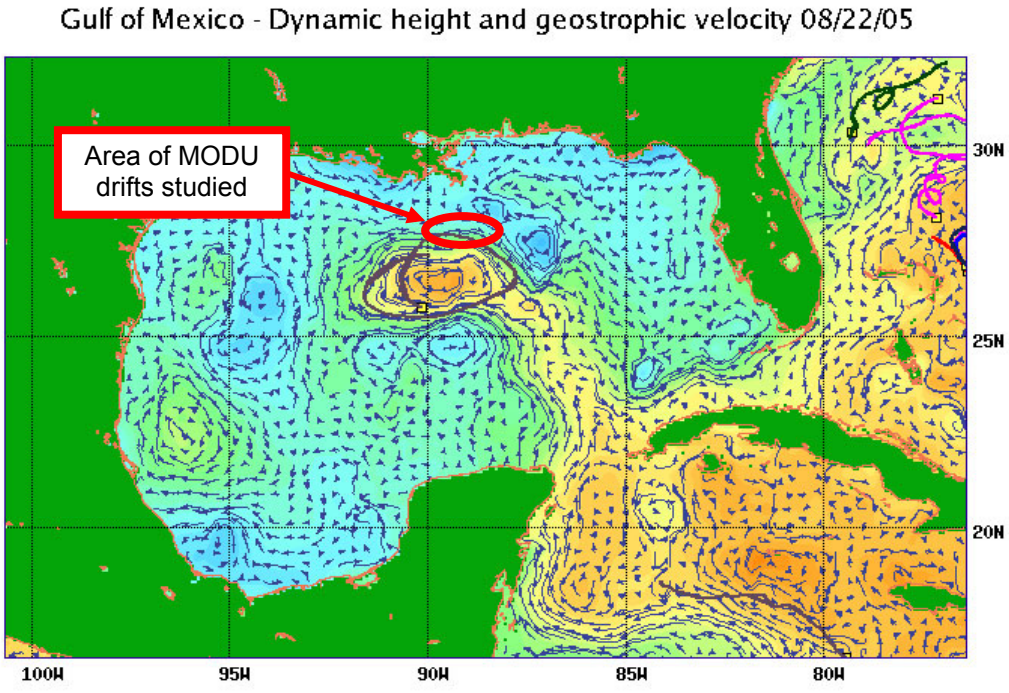

MODU II. As shown in Figure 2, MODU II went adrift after Katrina's eye had passed to east of the location and was about 30 n mi north. It was subjected to winds on the backside of the hurricane which blew from the southeast initially and became more easterly as the storm moved further north. The track was predicted from 6:00 to 10:00, at which time the eye was then more than 100 n mi north of the location. The predicted track is compared with the measured track in Figure 6.

Figure 6. Predicted and Measured Drifts for MODU II (30 minute intervals)

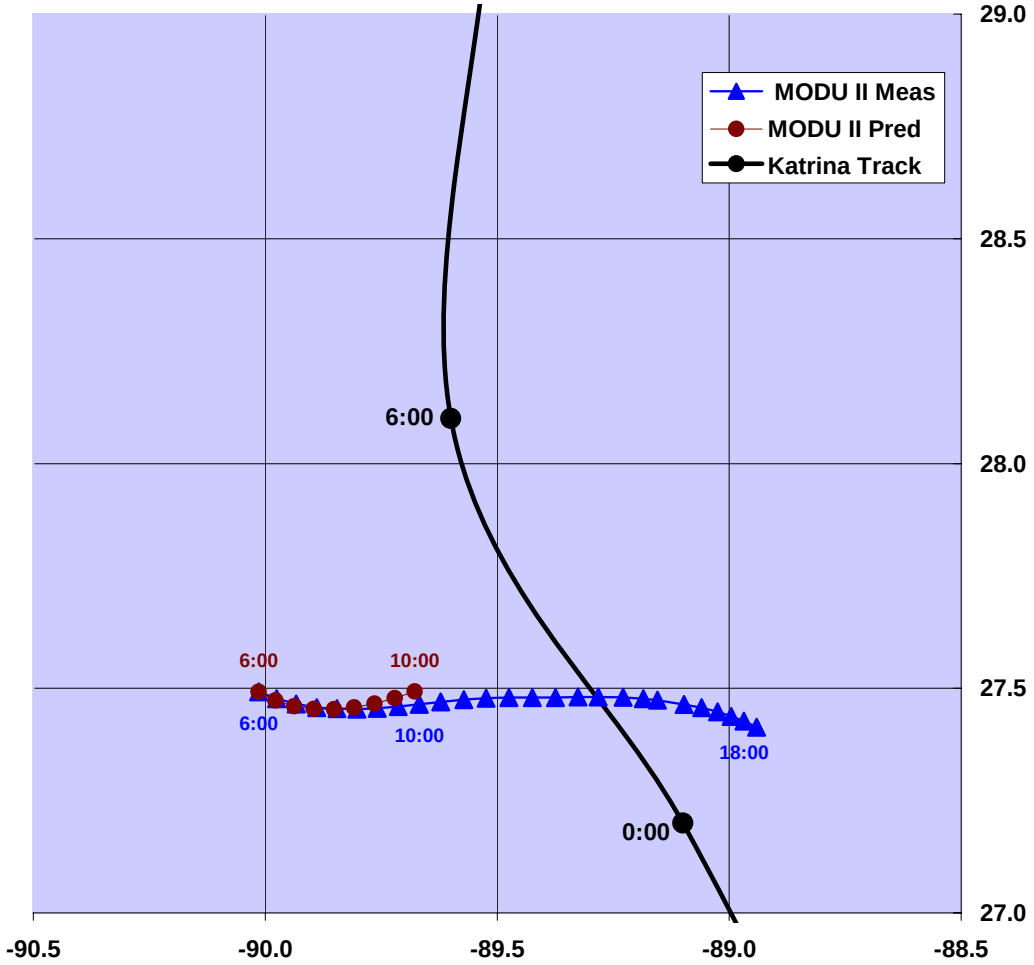

Summary. Final results for the predicted and measured drift tracks for MODU I and MODU II are shown in Figure 7. These results show that the mathematical models used in this study can satisfactorily predict the drift tracks of MODUs adrift in a hurricane and are adequate to assess mitigation options control drift.

The accuracy of a predicted track is of course directly influenced by the accuracy of the wind, wave, and current conditions that a MODU encounters along its path. In strong wind conditions, wind forces dominate MODUs drift. Hurricane hindcast models developed and primarily calibrated to predict the winds and resulting waves in the severe portion of the storms.

Hurricane winds diminish rapidly away from the eye, and winds at these more distant locations are influenced by the surrounding atmospheric and oceanographic conditions as well as the hurricane. The relative importance of wind in the overall wind, wave, and current force balance on the MODU becomes diminished such that wind is no longer the single dominant force driving a MODU's drift and more information is needed on currents and waves. These factors result in it being more difficult to accurately predict a MODU's drift track from its starting location over a long period of time as the distance between the hurricane and the MODU increases. As shown in Appendix A, predictions of the long term MODU drift that were periodically corrected to the measured location and the associated environment were significantly more accurate.

Figure 7. Predicted and Measured Drifts for MODUs I and MODU II (30 minute intervals)

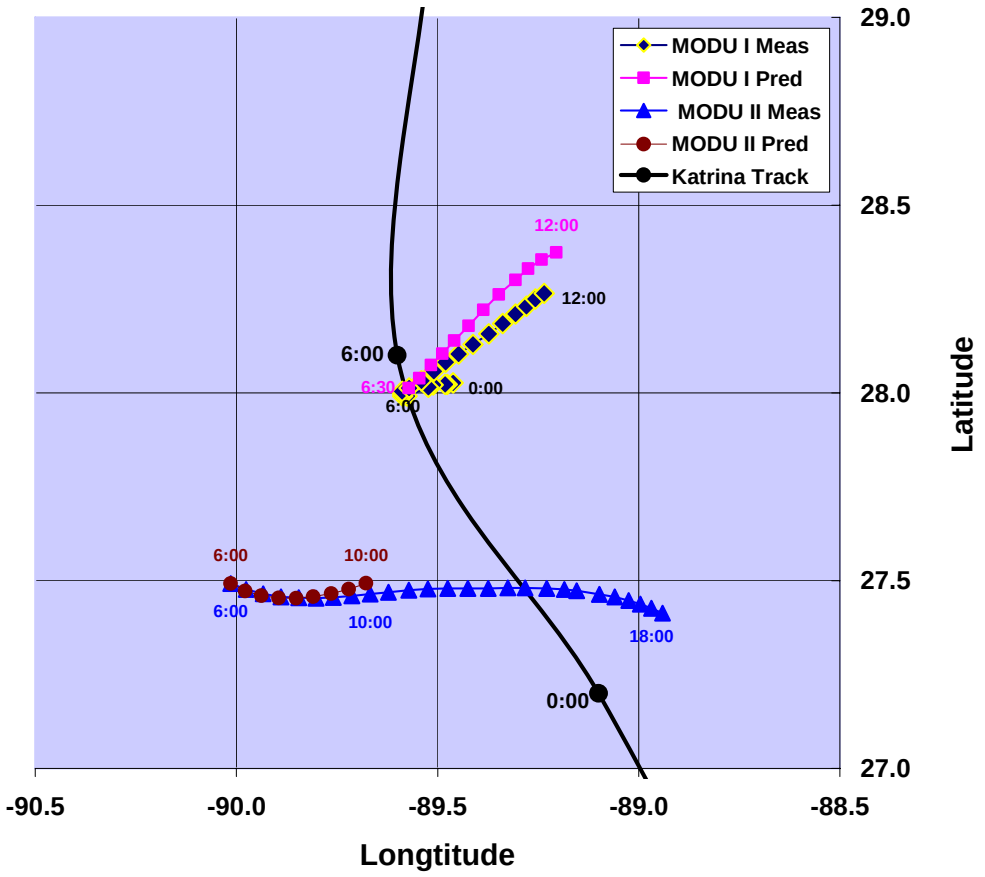

Progressive Failure of a MODU Mooring System during a Hurricane

A time-domain vessel-mooring coupled dynamic analysis computer program TAMU-WINPOST (Kim 2001) was used to simulate the sequence of progressive mooring-line failures of MODU I and MODU II during hurricane Ivan. TAMU-WINPOST has been extensively verified through comparisons of predicted and measured responses of in-place floating structures and their mooring systems from both laboratory and offshore data (Kim 1999, Halkyard 2004).

The MODU motions and mooring line loads were simulated in the time domain. A mooring line was assumed to fail when the predicted tensions exceeded the minimum break load (MBL) specified for the line. No connection or weak links were modeled, so that line failure always was assumed to occur at the fairlead were the line tension was largest. After failure, its tension was then no longer applied to the MODU, the stiffness of the mooring system changed, and the loads in other mooring lines increased. On occasion, there were large transient responses that resulted in a sudden tension increase in neighboring lines. Using this time-domain approach, the progressive line-by-line failure of the mooring system was simulated.

The total simulation time was 5000 seconds (83 minutes). The environmental loads were ramped up from zero to their actual value over the first 250 seconds to minimize start-up transient responses.

Appendix B provides more details of the solution method and detailed results. Some of the important results are summarized here.

Hindcast wind, wave, and currents were used for the simulations. For a specific location, the hindcast data provided wind (speed and direction), wave (directional spectra and statistics), and currents every 3 hours. We represented the environments as a non-collinear environment with winds, waves, and currents approaching from different directions. Wind speed time series were simulated using spectral methods and the hindcast average wind speed, and the direction was taken as constant. Wave time series

was simulated from the hindcast unidirectional spectra, and the direction was taken as constant in the mean direction of the total variance of the wave energy. Current speed and directions were available at the surface, mid-depth, and bottom of the mixed layer.

MODU I. MODU I was modeled as a triangular hull with a 9 line omni-spread semi-taut chain-wire system in 5800 ft.

The metocean conditions at the time the maximum waves occurred were selected for analysis, since no information on when the mooring system failed during the storm shown in Table 1.

Table 2. Maximum Conditions at Location of MODU I during Hurricane Ivan

	Parameter	Value	Depth (m)
Wave	Sig. Wave Height	15.2 m	na
	Peak Period	16.2 sec	na
Wind	Speed at 10 m	38.9 m/sec	na
Current	Surface	2.3 m/sec	0
	Mid-depth	1.7 m/sec	48
	Zero level	0	97

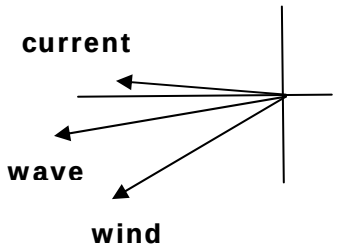

The time series for the MODU's responses and mooring line tensions are shown in Figures 8 and 9. Mooring line breaks are indicated when the line tension reaches the MBL and thereafter is shown as a straight line. As the mooring lines break, the MODU begins to move laterally as shown in Figure 8 (see the surge and sway responses). Other responses indicate large transients immediately following a line break, e.g. see yaw. The sequence and timing of the line breaks are shown in Table 3. The progressive failure from the first line break (line 5) to the last occurs over a 40 minute period.

The progression of failed lines is also compared with Sharples' and Delmar's forensic studies in Table 3. The agreement with the result of this study is good.

Table 3. Line Break Sequence for MODU I

Present Study		Sharples	Delmar
Sequence	Time (sec)	Sequence	Sequence
5	263	5	5
6	265	4	4
4	309	6	6
7	469	7	7
3	991	3	8
8	1647	8	3
2	1664	2	2
1	2276	1	9
9	2685	9	1

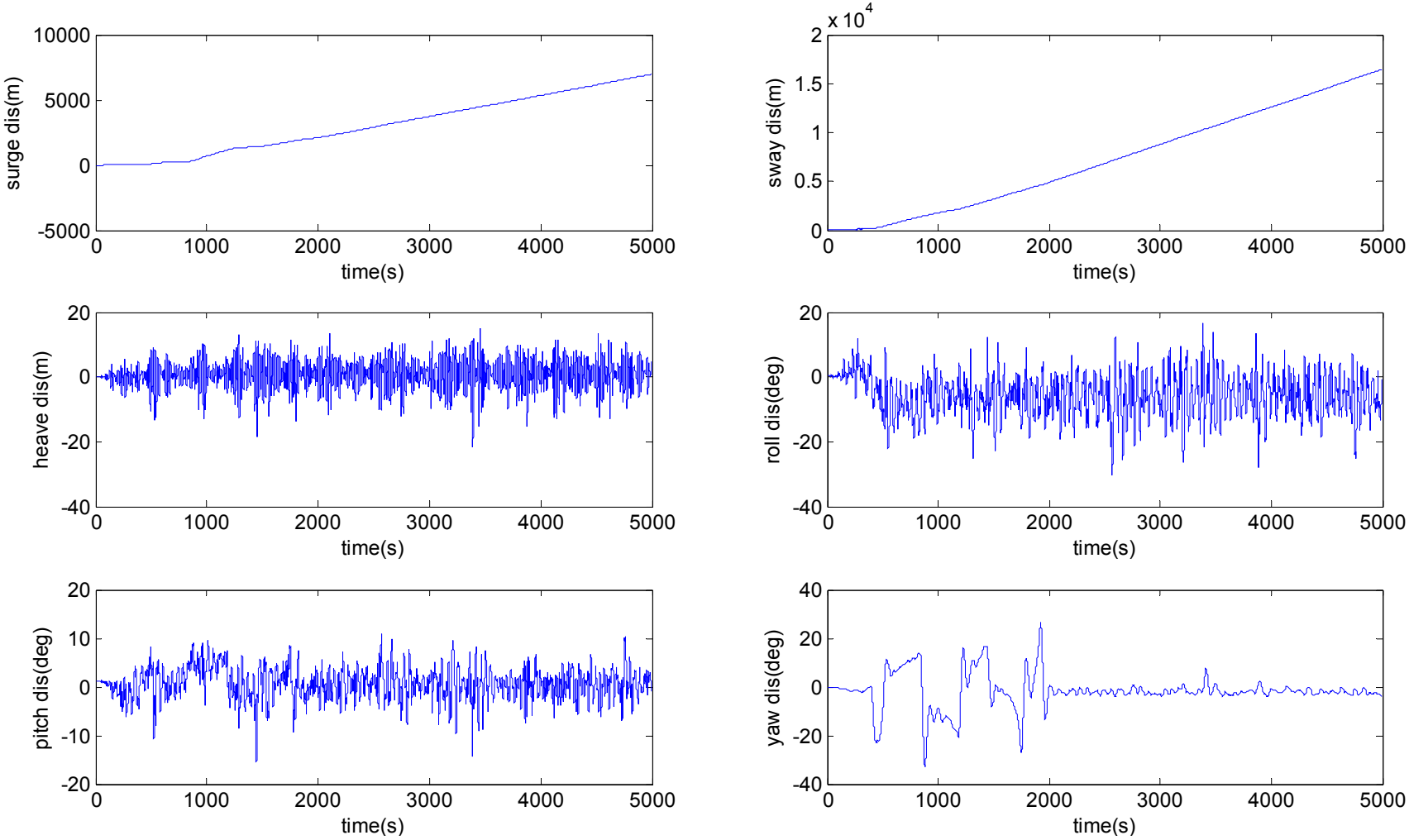

Figure 8. Motion Responses of MODU I during the Progressive Failure of the Mooring System

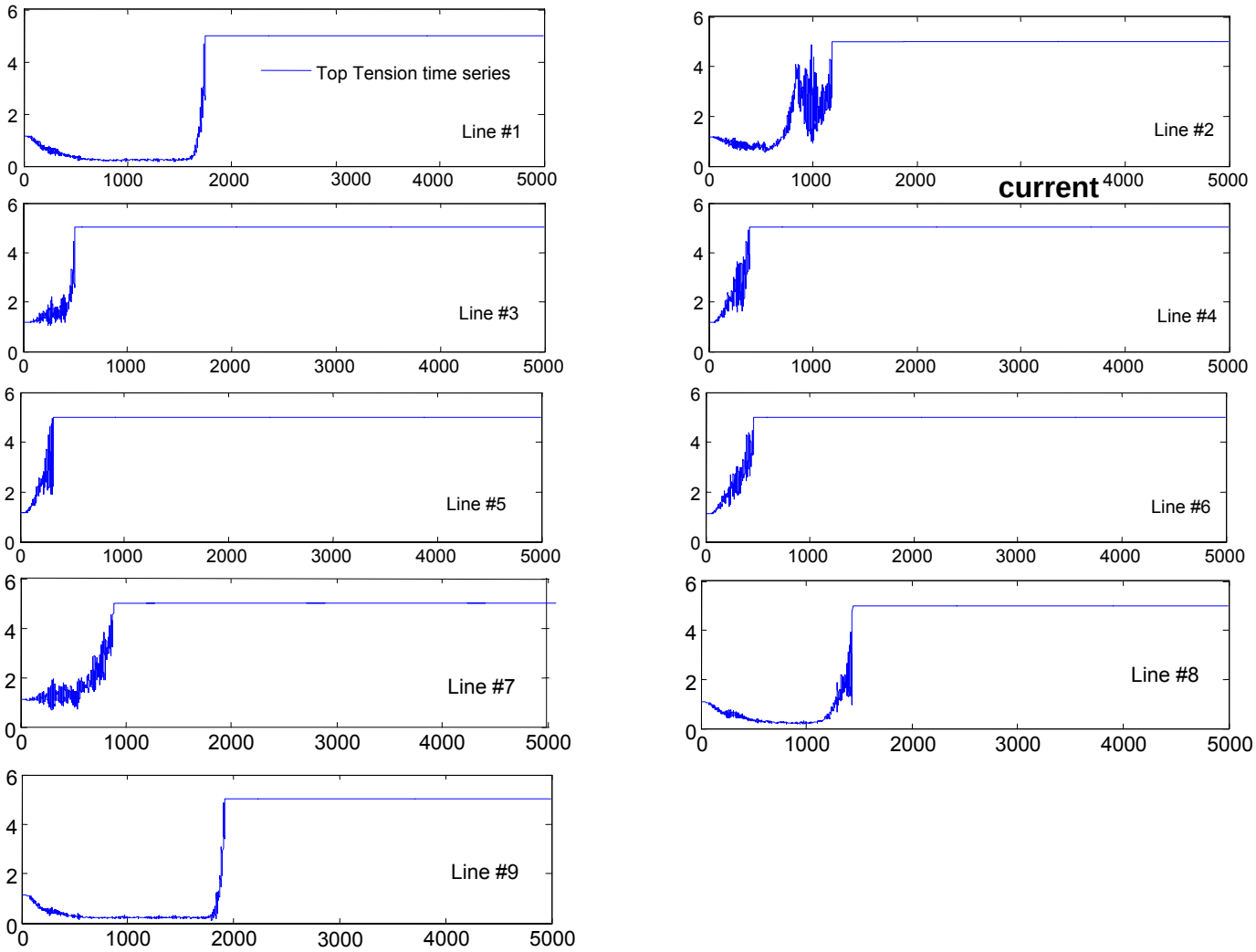

Figure 9. Line Tensions at the Fairlead during Progressive Failure of Mooring System for MODU I. MBL for rig wire is 5.0 MN (1124 kips).

The sequence of the failure pattern is also illustrated in Figure 10. The sequence of the line failures is repeated from Table 2 for convenience. The line positions shown connect the anchor points to the position of the MODU when the line failed. The pattern again agrees well with the reported forensic studies (Sharples 2006b, Delmar 2005a). Their study included the locations of the line remnants on the seafloor within the mooring spread. Lines that actually failed at the connection to the suction pile were carried away by the MODU. Those lines are indicated by a dashed line in the figure.

Figure 10. Mooring Line Failure Pattern for MODU I

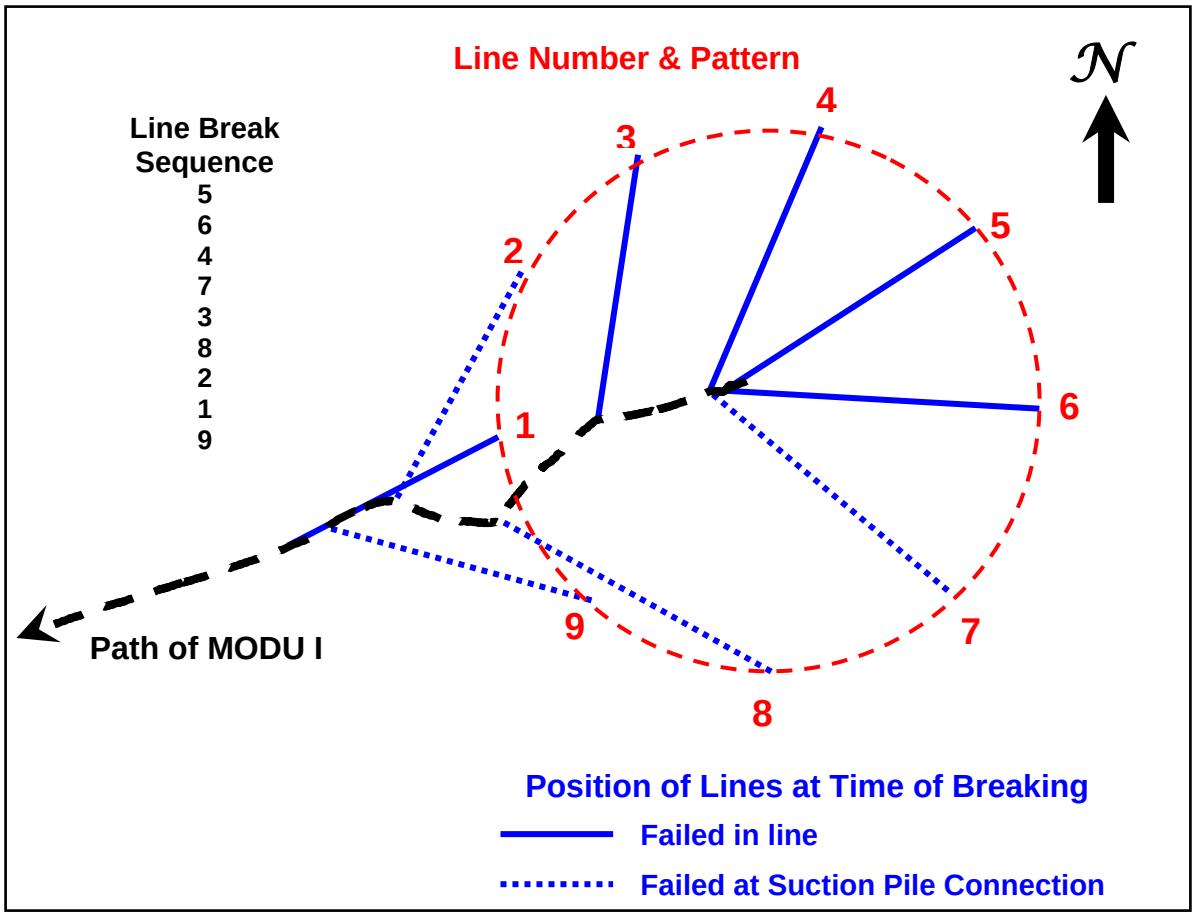

MODU I was also analyzed to with a taut-moor system consisting of wire rope - polyester rope-wire rope mooring system. The rig wire rope strength was the same as that used in the semi-taut moor chain wire system analysis reported above. The polyester system was also designed for a 10-year return period environmental criterion. When

analyzed in the same Ivan environment, no mooring line broke and the system did not fail. The maximum tensions in the rig wire at the fairlead were reduced by about 25 percent.

MODU II. MODU II was modeled as a rectangular hull with an 8 line omni-spread taut wire rope-polyester rope-wire rope mooring system in 9000 ft of water.

Ivan passed just to the west of the location. No information is available on when during the storm that the mooring system failed. Forensic studies of the pattern of the mooring line remnants suggested that the MODU drifted north during the progressive failure of the mooring system (Delmar 2005b).

A previous analysis (Loeb 2005) reported that the mooring system failed due to environmental forces caused by wind, wave, and current conditions that exceeded a 65-year return period per API standards. The wind, wave, and current values were

Table 4. API 65 RP Parameters

	Parameter	Loeb 2005	Hindcast
Wave	Sig. Wave Height	37.1 ft	39.1 ft
	Peak Period	13.9 sec	13.8 sec
Wind	30 min speed at 10 m	84 mph	83 mph
Current	Surface	2.8 kt	3.7 kt

This was based on an analysis that examined many combinations of plausible wind, wave, and current combinations that could have caused the initial mooring line failure (Delmar 2005b). The wind, wave, and current forces were assumed to be collinear. The values of environmental parameters will be referred to as “API 65 RP”.

The Ivan hindcast database (Oceanweather 2004) was reviewed to find a wind, wave, and current environment that most closely matched these conditions so as to determine viable directions for that environment. The value for the surface current was determined from API 2MET INT by matching the wind and wave values. The directions of the wave and currents relative to the wind were + 5 degrees and + 30 degrees to the right of the wind.

These values are also shown in Table 4 as “Hindcast “and were used to represent API 65 RP in the analyses reported below and listed in Table 5.

Based on the Ivan hindcast (Oceanweather 2004), maximum wave conditions occurred at the location while Ivan was still a bit south of the location and the wind, wave, and currents were generally to the northwest. A few hours later, the maximum wind speed occurred and the wind and waves had shifted and were northerly. Since the magnitudes of the wind speeds and wave heights at these times differed by less than 10 percent at these two times, we will simply use one set of parameters to describe this condition and refer to it as “Ivan Max”.

Since the hull form of MODU II suggested that there could be considerable directional sensitivity in the loads and responses, several environments were studied. We considered both collinear and non-collinear cases. The non-collinear directions were based on observations from hindcasts. Parameters for these cases are shown in Table 5, and the directional characteristics are shown in Figure 11.

Table 5. Environmental Parameters & Directions Used to Analyze MODU II

		Parameter	Value	Direction toward (0 deg N)	Case	Mooring System Result
API 65 RP North Collinear	**Wave**	Sig. Wave Height	39.1 ft	0	**A**	**Failed**
		Peak Period	13.8 sec	na		
	Wind	30 min peed at 10 m	83 mph	0		
	Current	Surface	3.7 kt	0		
API 65 RP North Non-collinear	**Wave**	Sig. Wave Height	39.1 ft	15	**B**	**Failed**
		Peak Period	13.8 sec	na		
	Wind	Speed at 10 m	83 mph	0		
	Current	Surface	3.7 kt	30		
API 65 RP Northwest Collinear	**Wave**	Sig. Wave Height	39.1 ft	295	**C**	**Survived**
		Peak Period	13.8 sec	na		
	Wind	Speed at 10 m	83 mph	295		
	Current	Surface	3.7 kt	295		
API 65 RP Northwest Non-collinear	**Wave**	Sig. Wave Height	39.1 ft	310	**D**	**Survived**
		Peak Period	13.8 sec	na		
	Wind	Speed at 10 m	83 mph	295		
	Current	Surface	3.7 kt	325		
Ivan Max Non-Collinear Northwest	**Wave**	Sig. Wave Height	51.5	281	**E**	**Failed**
		Peak Period	15.5	na		
	Wind	Speed at 10 m	98 mph	263		
	Current	Surface	3.5 kt	296		

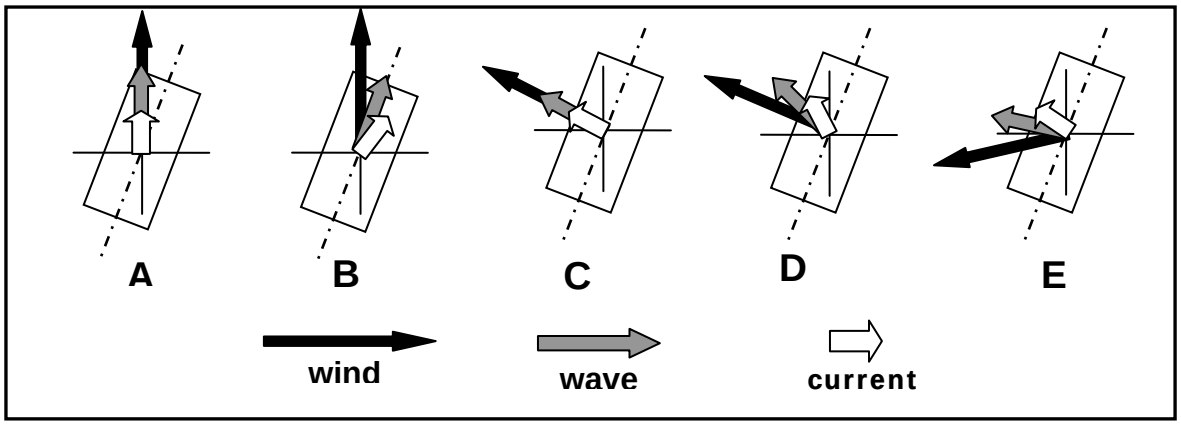

Figure 11. Directional Environments for Cases in Table 4

The mooring system failure in Case A API 65 RP Collinear agrees with the previous analysis (Loeb 2005, Delmar 2005b). The mooring line failure pattern found here was also similar to the results found in that analysis and the pattern found in the forensic study of the mooring failure. The results for B API 65 RP Non-Collinear also indicated that the mooring system would have failed.

Cases C and D investigated the response of the mooring system to the collinear and non-collinear versions of the same API 65 RP environment approaching MOSU II from a more broadside direction. Results indicate that the mooring system would not have failed. Further investigation indicated this resulted from lower wind forces on MODU II when the wind was from this direction.

Case E investigated the response of the mooring system to the Ivan Max Non-Collinear environments, and indicated that the moor5ing system would certainly have failed in this more severe environment.

Summary. These results show that the mathematical models used in this study can satisfactorily predict the progressive failure of a MODU mooring system and are adequate to assess mitigation options to prevent a total drift off.

Additionally, the comparison of the failure of the chain-wire system and the wire-polyester-wire system on MODU I illustrated the robustness of mooring system that include polyester inserts. And the analysis of MODU II illustrated the directional sensitivity of responses or a rectangular MODU and its mooring system to storm environments.

Anchor Performance & Geotechnical Considerations

While the primary focus of the project was on the behavior of the floating MODUs and mooring line failures, failures in foundation elements of the mooring system were also investigated.

Anchors are used to moor deepwater MODUs in the Gulf of Mexico include

- Drag Embedment Plate Anchors (DEAs),
- Near-normal or Vertically Loaded Plate Anchors (VLAs), and
- Suction Caissons.

Anchor Performance in hurricanes Ivan, Katrina, and Rita. As indicated in Table 1, there were a number of instances of anchor failures during hurricanes Ivan, Katrina, and Rita. The anchor failures included both in-plane and out-of-plane loadings.

In-Plane Failures - Anchors are pulled out on the most heavily loaded lines, initiating a failure sequence in which additional loads were shed to adjacent lines which then failed either from anchor pull-out or line breakage. In these cases, the anchor was loaded essentially in the plane it was intended to be loaded ("in-plane" loading). For a suction caisson, in-plane loading means that the line is pulling in the direction of the load-attachment padeye. For a plate anchor (DEA and VLA), in-plane loading means that the line is pulling in the plane of the shank.

Available information indicates that both drag embedment and vertically loaded plate anchors suffered in-plane failures during these hurricanes, while no suction caissons failed in this manner.

Out-of -Plane Failures - Failures in the most heavily loaded lines (the anchor capacity exceeds the line capacity) initiate a failure sequence that causes the vessel to move off station and shed additional loads to adjacent lines. An anchor can be loaded out of the plane it was intended to be loaded. Out-of-plane loading for a plate anchor (DEA and

VLA) means that the line is pulling out of the plane of the shank, and out-of-the-the plane of the padeye for suction caissons.

Under “out-of-plane” loading conditions, anchors can pull out or fail structurally. A plate anchor can be pulled over sideways, and a suction caisson can be twisted, which can reduce the capacity of the anchor compared to its in-plane capacity leading to the possibility that the anchor will pull out before its mooring line breaks. Anchor pull-out is a particularly significant issue for a MODU that has gone adrift because the anchor (weighing tens to several hundreds kips) can be dragged across the sea floor and damage wells, flowlines, pipelines, and other mooring systems. Cases where anchor drag occurred during MODU failures are summarized in Table 1.

Available information indicates that both plate anchors and suction caissons failed due to out-of-plane loading.

Appendix C includes a back-analysis of case studies two MODUs during hurricane Ivan. The cases were mooring systems with suction caisson anchors that failed in Hurricane Ivan. These case studies highlight the significance of out-of-plane loading. Possible alternatives to improve the capacity of anchors under out-of-plane loading are investigated. Some of the important results and conclusions are summarized here.

MODU I and II Foundation Failures. Information was available to this study for MODU I and MODU II (Delmar 2005a and 2005b). Both mooring systems utilized suction caisson anchors. The mooring system for the MODU II was taut with the line loading the caissons at about 40° to the horizontal under design loading conditions, while the mooring system for MODU I was semi-taut with the line loading the caisson at about 10° to the horizontal under design loading conditions.

The in-plane capacities of the suction caisson anchors were estimated using the model developed by Aubeny et al., 2003. Results are shown in Figure 12, in which the curve denotes combination of axial (vertical) and lateral (horizontal) loads that would cause the

anchor to move. The anchor capacity for the taut mooring system (MODU II) is essentially governed by the axial capacity of the suction caisson, while the capacity for the semi-taut mooring system (MODU I) is essentially governed by the lateral capacity.

Figure 12. Vertical & Horizontal Capacities for Suction Anchors for MODU I and MODU II

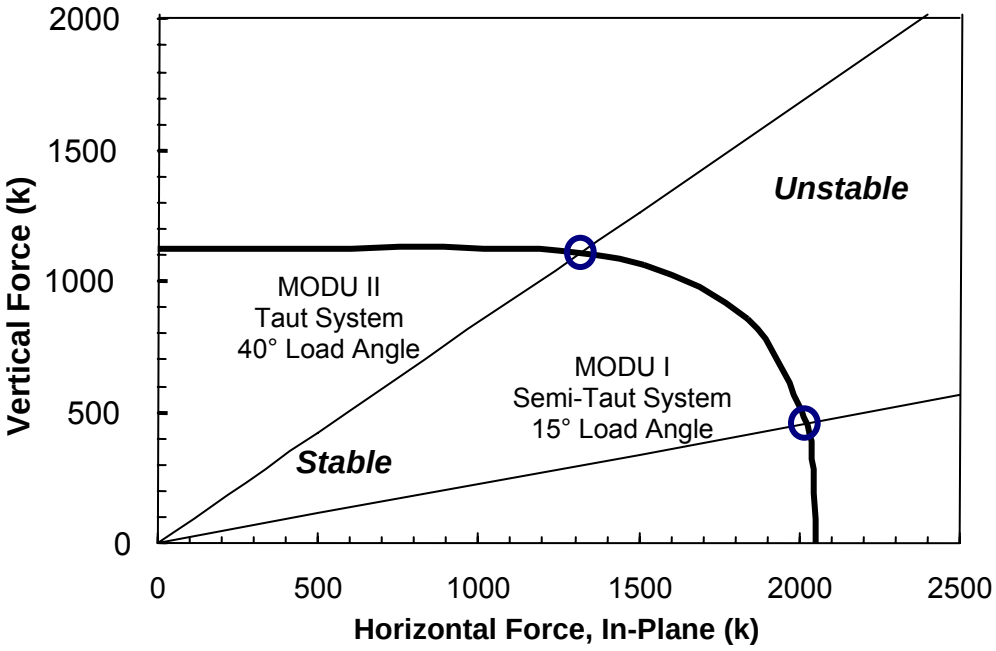

The total in-line loading capacity is summarized in Table 6 for the anchors in each of the two mooring configurations. For both configurations, the line is expected to break before the capacity of the anchor was reached in Ivan. This result is consistent with the actual performance of the anchors; the initial failures occurred in the lines and not at the anchors.

Table 6. Line Tension at Anchor Capacity for In-Line Loading

Condition	Line Tension at Anchor Capacity (kips)	Maximum Tension at Anchor in Ivan when Line Broke (kips)
Taut (MODU I)	1,700	1,200 to 1,500
Semi-taut (MODU II)	2,100	1,200

The out-of-plane loading on suction piles can twist the caisson as well as reduce the total axial and lateral capacity of the caisson. For MODU I, all lines broke in this taut system before any noticeable failure of the suction caisson anchors occurred, even though some caissons were apparently loaded out-of-plane angles by more than 90 degrees (Delmar 2005a). This result may suggest that simplistic estimates of the torsional capacity tend to be conservative, and that instability for suction anchors at high out-of-plane loading angles may indicate that the anchor will begin to rotate, not necessarily pull-out.

MODU II suffered damage to its foundation elements. Four padeyes broke due to out-of-plane loading (Delmar 2005b). The geotechnical performance of each suction anchor is described in Table 7. None of the anchors failed in a geotechnical sense of anchor pullout. However, evidence of soil yielding did occur in a number of instances, implying that a limit state had been reached.

Table 7. Summary-Suction Anchor Geotechnical Performance for MODU II

Geotechnical Performance Category	Suction Anchor Number	Maximum Applied Torsion (kip-ft)	Maximum Applied Tension (kips)	Anchor-Soil Condition
I: No Evidence of Significant Soil Yielding	3	6791	1207	Normal
	5	64	1501	Normal
	6	461	957	Normal
	7*	3659	1518	Normal
II: Anchor Rotation - rotational yield mechanism in soil	1	241	30	Rotation
	8*	3258	679	Rotation
	9*	4027	495	Rotation
III: Disturbance, likely lateral-axial yielding in soil	2*	4217	584	Disturbance
	4	725	1439	Depression

*Structural failure occurred at pad-eye.

Methods to reduce the impact of out-of-plane loads are discussed in Appendix C. Possible alternatives to reduce the effects of out-of-plane loading on anchor performance are:

- Put the padeye on a suction caisson on a swivel so that it can spin around the circumference;
- Put a constrained hinge between the shank and the fluke on a plate anchor to limit the overturning moment that is applied sideways under out-of-plane loading.

A torpedo pile configured with the load attachment at the top can provide more axial capacity and less lateral capacity under in-plane loading than a suction caisson of the same weight. It would provide a similar overall capacity for a taut mooring system but a smaller capacity for a semi-taut system. However, the advantage of this torpedo pile is that its capacity is not reduced under out-of-plane loading.

Summary

When MODU mooring systems are overloaded, the failure sequence may begin in the lines or the anchors. Increasing the capacity of anchors under these “in-plane” loading conditions will be effective at reducing the possibility of a station-keeping failure for a MODU if this failure mechanism is likely to begin with anchor pull out. For mooring systems designed with an approach similar to that used for permanent mooring systems, we expect that a failure initiating at the line is more likely than one initiating at the anchor. Once a MODU moves off station, the out-of-plane loading on the anchors can reduce the capacity of the anchors, and possibly lead to rotation, pull out, or a structural failure of the anchor.

Information was available to study suction anchor performance for a taut and semi-taut mooring systems that failed. Mooring failures in the taut system were due to mooring line failures. Mooring failures in the semi-taut system resulted both from mooring line failures and padeye failures due to out of plane loading. There was some evidence that some anchors might have reached their limit state.

No detailed information was available on failures of plate anchors.

Mitigation Ideas to Control Drifting MODUs or Intervene to Prevent Total Drift-Off

A preliminary list of ideas for technical solutions that could (1) prevent the total drift-off of a MODU by intervention during the progressive failure of a mooring system during a hurricane, and (2) control or reduce the drift of an unmoored MODU in a hurricane were developed. A Workshop with industry and MMS representatives was then held to get their views on these ideas and to collect other ideas. The workshop also included a session during which all ideas were ranked in order of anticipated technical applicability and probability of leading to a solution that could be applied offshore. The following sections describe the ideas and results from the Workshop.

We began with the following premises:

- Industry has studied ways to reconfigure conventional MODU mooring systems in order to maximize robustness against total loss of station-keeping ability
- Drilling companies have upgraded mooring capabilities on MODUs to the extent they feel is economically justifiable
- Industry has studied the risk/reliability issues associated with temporary mooring systems, and is developing new consequence-based procedures for establishing design criteria for temporary MODU moorings
- Industry and OTRC have the analytical tools that can model progressive failure and drift-off of semisubmersible MODUs
- Recent actions taken and measures considered to date will not lead to MODU moorings with the same level of reliability as for permanent mooring systems
- Even with recent improvements and increases in criteria, if hurricanes as severe as Ivan/Katrina/Rita strike the GoM again, there would still be a possibility of some MODUs losing their mooring systems and going adrift, possibly for > 100 miles
- Under certain conditions, MMS will not permit drilling on a particular lease during hurricane season

These premise provided guidance for developing strategies and ideas to prevent or mitigate drift-off and to control drifting MODUs. The strategies were categorized as follows:

- **P**revent Drift-Off (P)
- Drift-Off **M**itigation (M)
- Drift **C**ontrol Strategies (C)

Table 8 captures the Working Session discussions of different strategies and ideas. The strategies and ideas shown in *italics* were presented to the Workshop as "seeds". Workshop participants were formed into two Work groups and brainstormed these and other strategies and ideas and then discussed and assessed the merits of all ideas.

Finally, Table 9 presents the two Work Groups ranked mitigation ideas based on their discussions. This list and the discussion provide a number of ideas for further study that could lead to cost-effective technical options to mitigate MODU drift due to mooring failures in hurricanes and reduce the hazards and risks to the offshore infrastructure (e.g., floating and fixed production structures, pipelines and flowlines, subsea well systems).

Table 8. Discussion of Strategies & Ideas to Prevent or Mitigate Drift-Off & Control Drifting MODUs

Strategy		Idea	Workshop Discussion
Prevent Drift Off (P-x)			
P-1	*Timing Of Last Line Failure*	*Design mooring system to fail progressively such that the last line(s) would not fail before severe hurricane conditions had subsided after the hurricane had passed*	• No history of MODU mooring system surviving with less than 2-3 lines intact - unlikely could be designed • Current anchor design is emphasizing higher holding capacities & promoting line failure at the fairlead
P-2	*Auxiliary Mooring System*	*Design mooring system to fail in a controlled manner and engage an auxiliary mooring system with necessary elasticity to ride out remainder of storm*	• Other approaches likely more economical, e.g., o DP vessel o Design more robust mooring system that approaches capacity of permanent system
		Drill additional "well" to allow lowering an additional tension element through the moon pool & connect it to the "wellhead"	• Con - Connect time would drastically increase T-time
			• MMS would like an auxiliary system to prevent drifting. Issues o Needs to be engineered o Utilize a soft material o Clump weights or chain at piggy-back o Requires a weak link o Need to ensure that it will not cause extra damage if it fails
	Stronger Mooring Systems	Develop & use higher capacity mooring systems though design & material selection	• Allow for nylon mooring lines to take advantage of their high flexibility • Use Dyneema rope instead of wire rope as ground wires for suction piles

Table 8. Discussion of Strategies & Ideas to Prevent or Mitigate Drift-Off & Control Drifting MODUs (con't)

Strategy		Idea	Workshop Discussion
Drift-Off Mitigation Strategies (M-x)			
M-1	*Timing of First Inference with Nearest Infrastructure*	*Design mooring system to fail progressively such that the last line failure would occur after peak of storm when diminished hurricane metocean conditions would be insufficient to push drifting rig into neighboring infrastructure*	• Difficult if not impossible to engineer a system that would reliable perform in this manner
M-2	*Design to Drag*	*Design mooring system to fail in a controlled manner and engage an auxiliary drag anchor system with sufficient drag to keep MODU from drifting into neighboring infrastructure*	• Not a good idea if near subsea & pipeline infrastructure - may be useful if drill site a long way from infrastructure • Use anchors that are designed not to drag or damage pipelines and limit the chain at the anchor o e.g., Vryhof anchor used in Lake Maracaibo
	Design to fail at fairlead	Design mooring system for lines to disconnect remotely at fairlead <u>if you know that you are going adrift</u> to avoid dragging though pipeline & subsea infrastructure	• Disconnect remotely o at prescribed overload o via explosive charge o via mechanical cutting device (e.g., shears) • Disconnect anchor if anchor drags a prescribed distance
	Emergency deployed anchor(s) to prevent or control drift off		• Do not want
	Collision damage mitigation	Minimize damage to critical surface structures by placing retention system around structure to reduce MODU hull-to-structure impact load	• Cable system at - 30 ft • Inflatable bumper system

Table 8. Discussion of Strategies & Ideas to Prevent or Mitigate Drift-Off & Control Drifting MODUs (con't)

Strategy		Idea	Workshop Discussion
Drift Control Strategies(C-x)			

C-1	*Fly by Wireless*	*Outfit MODU with a DP (dynamic positioning) system consisting of thrusters and/or rudders, monitor MODU position via GPS, and remotely engage DP system to control drift track to avoid collision with infrastructure*	• Requires reliable functioning GPS capable of determining drift direction
			• Active system would require reliable shore-to-MODU control system
			• Requires electronic display of infrastructure
			• Issues for full blown thrusters include
			  o Power - 4 thrusters could require 4 MW
			  o Batteries
			• Success depends on available sea-room
			  o Most cases just a few miles
			• Could lower powered thrusters control drift direction?
			  o Lower powered systems might be useful in remote locations
			• Must know seastate heading
			OTRC comment - Wind is primary driver in determining drift direction in severe hurricane conditions
			• Would a rudder system be effective & feasible?

Table 8. Discussion of Strategies & Ideas to Prevent or Mitigate Drift-Off & Control Drifting MODUs (con't)

Strategy		Idea	Workshop Discussion
C-2	*Auto-Deploy Drogues*	*Outfit MODU with self- or remotely-deployable drogues, monitor MODU via GPS, deploy drogues to slow drift rate and avoid collision with infrastructure*	• Drogues probably not feasible since driving forces are currents *OTRC comment - Driving force is actually due to wind during severe part of storm. Afterwards, hurricane currents may dominate local winds, or MODU may get in a Loop Current*
C-3	*Early Capture*	*Outfit MODUs with "capture" lines attached to buoys, monitor position of drifting MODU via GPS, and mobilize anchor handling boats to intercept and tow MODUs headed for infrastructure*	• Combine drogues (sea anchors) with rudder? • Pre-or uncontrolled deployment could cause capture line to become fouled in MODU hull or ripped off • Better to create line system fixed to side of rig that could be deployed when the support vessel arrives. MODU would still be unmanned. • Note that AHVs & cutters not likely to operate in seas > 8-10 ft
	Overall consideration for drift prevention or control mitigation measures		In considering the weight penalties and costs of drift prevention or drift control mitigation methodologies, compare the additional weight and cost to simply upgrading the MODU's mooring system to that of a permanent mooring system

Table 9. Ranked Ideas to Prevent or Mitigate Drift-Off And to Control Drifting MODUs

Rank	Ideas
	Group 1

1	Avoid dragging anchors or chain on seafloor to avoid damage to pipelines and subsea facilities
	• Ensure line failure at fairlead
	  o By design
	  o By controlled explosives or shear rams
	• Allow no uplift on anchors
	• Continue development of better anchors
	• Continued utilization of additional storm lines
	• Use suction piles with Poly, HMPE , … lines

2	Construct barriers to protect critical infrastructure against collisions with drifting MODU hulls • Focus on top producers & hubs
3	Control drifting MODU to avoid collisions • Thrusters • Real time data to determine best drift path • Drill farther from critical risk infrastructure during hurricane season
	Group 2
1	Release rig and steer • After initial mooring line(s) fail, remotely cut remaining lines at fairlead to release rig to drift without lines dragging? • Steer remotely via thrusters or rudder?
2	Invest in stronger primary mooring system rather that mitigation measures
3	Utilize non-grabbing anchors and no chain to avoid pipeline damage by a drifting MODU

Conclusions & Recommendations

The mathematical models used in this study can satisfactorily predict the drift tracks of MODUs adrift in a hurricane and are adequate to assess mitigation options control drift.

The mathematical models used in this study can satisfactorily predict the progressive failure of a MODU mooring system and are adequate to assess mitigation options to prevent a total drift off.

A number of mitigation strategies and ideas were developed to (1) prevent the total drift-off of a MODU by intervention during the progressive failure of a mooring system during a hurricane, and (2) control or reduce the drift of an unmoored MODU in a hurricane were developed. These strategies and ideas were reviewed with industry representatives. A number of the strategies and ideas have merit and the potential to offer practical cost-effective technical solutions to mitigate MODU drift due to mooring failures in hurricanes and reduce the hazards and risks to the offshore infrastructure. The tools needed to assess these mitigation options to control drift or prevent a total drift are available and proven. Further studies are being planned.

Mooring foundation anchors including plate anchors (DEAs and VLAs) and suction caissons failed during hurricanes Ivan, Katrina, and Rita. Available information indicates that both drag embedment and vertically loaded plate anchors suffered in-plane failures, and both plate anchors and suction caissons failed due to out-of-plane loading. Further studies are needed to provide better understanding of the performance and failures of plate anchors and suction anchors to out-of-plane loadings. A study to develop a publicly available standardized database on the performance and failure of commercially available plate anchors and suction caissons would improve the reliability of deepwater mooring foundations.

Acknowledgments

Many people and organizations contributed to the success of this project.

We appreciate the MMS's interest in this project and the data that they provided.

We also acknowledge Evan Zimmerman (Delmar), David Petruska (BP), Hongbo Hsu (Shell), and Malcolm Sharples (Offshore Risk & Technology Consulting Inc.) for their willingness to serve on a Steering Team and the valuable guidance, counsel, and advise they provided throughout the project. Delmar, BP, and Shell provided information that added significant value to the project.

We appreciate the valuable discussions with John Stiff (ABSC) which helped us coordinate this project with the industry JIP on JIP on MODU Mooring Strength and Reliability.

The financial support of the Minerals Management Service and the OTRC Industry Consortia is gratefully acknowledged and appreciated.

References

Aubeny 2003, Inclined load capacity of suction caisson anchors, Aubeny, C.P., Han, S.W., and Murff, J.D. 2003, Intl. J. for Numerical and Analytical Methods in Geomechanics, Vol. 27, pp. 1235-1254.

Delmar Systems, Inc. 2005a, Noble Jim Thompson Kepler MC 383 in Hurricane Ivan

Delmar Systems, Inc. 2005b, Deepwater Nautilus Cheyenne Well D LR 399 Mooring Performance during Hurricane Ivan

Delmar Systems, Inc. 2006, personal communication

Kim 1999, Hull/Mooring/Riser Coupled Dynamic Analysis of a Truss Spar in Time Domain, Kim, M. H., Ran, Z., & Zheng, W., Proc. ISOPE'99, Brest, France

Kim 2001, Variability of TLP Motion Analysis Against Various Design/Methodology Parameters, Kim, M. H., Tahar, A., & Kim, Y.B., 11th Proc. ISOPE'01, Stavanger, Norway

Halkyard 2004, Full Scale Data Comparison for the Horn Mountain Spar, Halkyard, J., Liagre, P., and Tahar, A., Proc. OMAE 2004 #51629, Vancouver, Canada

MMS 2006, project communication

Oceanweather 2004, Hindcast Study of Hurricane Ivan (2004), Offshore Northern Gulf of Mexico, FINAL REPORT, Oceanweather Inc, Report to the MMS, December 2004

Oceanweather 2005, Hindcast Study of Hurricane Katrina Offshore Northern Gulf of Mexico, FINAL REPORT, Oceanweather Inc. Report to the MMS, September 2005

Oceanweather 2006, Hindcast Data on Winds, Waves, and Currents in Northern Gulf of Mexico in Hurricanes Katrina (2005), Oceanweather Inc Report to the MMS (Revised), September 2006

Sharples 2006a, personal communication

Sharples 2006b, Post Mortem Failure Assessment of MODUs during Hurricane Ivan, Report to MMS, MMS Project 548

Sharples 2006c, MODU Performance during Hurricane Ivan, 2006 Offshore Technology Conference, Paper OTC 18322

Ward et al 2005, Hurricane Readiness & Recovery Conference Report, Final Conference Summary Report prepared for the MMS by OTRC, MMS Project 559

Appendix A: Numerical Prediction of MODUs Drift during Hurricane Katrina

G. V. Tahchiev and J. Zhang
The Zachry Department of Civil Engineering, Texas A&M University
College Station, Texas 77843-3136, USA

Abstract

Severe hurricanes, such as Katrina, broke the mooring lines of a number of Mobile Offshore Drilling Units (MODU) deployed in the Gulf of Mexico and some of those MODUs went adrift. To avoid or mitigate the damage caused by a drifting MODU, it is desirable to understand the mechanics of the drift of a MODU under the impact of severe wind, wave and current and have the capability of predicting the trajectory of the drift. To explore the feasibility and accuracy of predicting the trajectory of a drifting MODU based on hindcast met-ocean conditions and limited knowledge of the condition of the drifting MODU, this study employed a simplified equation describing only the horizontal (surge, sway and yaw) motions of a MODU under the impact of steady wind, current and wave forces. The simplified hydrodynamic model neglects the first- and second-order oscillatory wave forces, unsteady wind forces (owing to wind gustiness), wave drift damping, and the effects of the body oscillation on the steady wind and current forces. It was assumed that the net effects of the oscillatory forces on the steady motion are insignificant. To verify the accuracy and feasibility of our simplified approach, the predicted drifting trajectories of two MODUs were compared with the corresponding measurements recorded by the Global Positioning System (GPS).

Introduction

Recently, strong hurricanes, such as Ivan, Katrina and Rita, tracked through a high-density corridor of the oil and gas infrastructures in the Gulf of Mexico (GOM). Extreme winds and

large waves exceeded 100-years design criteria during these hurricanes, causing mooring line failure to a number of Mobile Offshore Drilling Units (MODU) in the GOM. Five semi-submersible MODUs went adrift during hurricane Ivan (Sharples, 2004) and nineteen MODUs adrift or significantly damaged during hurricanes Katrina and Rita (Smith, 2006). In addition to the damage to MODUs, a drifting MODU imposes a great danger to other critical elements of the oil and gas industry. To avoid or mitigate the damage caused by a drifting MODU, it is desirable to understand the mechanics of the drift of a MODU under the impact of severe wind, wave and current and have the capability of predicting the trajectory of the drift.

To explore the feasibility and accuracy of predicting the trajectory of a drifting MODU given hindcast met-ocean conditions and limited (sometimes incomplete) knowledge of the condition of a drifting MODU, this study employed a simplified governing equation describing only the horizontal (surge, sway and yaw) motions of a MODU to develop a numerical program, known as ‘DRIFT’. To validate ‘DRIFT’, the predicted drift of a MODU was compared with its corresponding measured trajectory recorded by Global Positioning System (GPS). In addition to the benefit of being able to predict the trajectory of unmoored MODU for search and rescue missions in the aftermath of hurricanes (if GPS data is not available), ‘DRIFT’ may be used in future studies to explore innovative technical solutions and methods to control, reduce, or stop the motion of a MODU that has gone adrift during a hurricane.

Certain assumptions were made in previous studies for simplifying the computation of the drift of a floating body. Both Su (1986) and Hodgins and Mak (1995) excluded the vertical body oscillations and rotations (heave, pitch and roll) but retained the body motion in surge, sway and yaw directions. A thorough review of the related previous studies was given by Anderson et al. (1998). They also proposed generalized analysis of the force balance of a drifting object in the open ocean, which considered the body motion in surge and sway directions only. It seems that the previous studies overwhelmingly focused on the drifting of relatively small boats for the purposes of search and rescue. Following these studies, we

employed a similar approach, which suits our intention that it is as simple as possible initially. We considered the horizontal (surge, sway and yaw) motions of the body which were induced by steady wind, current and wave (mean drift) forces only. It is noted that our simplification neglected many other external forces applied on the body, such as oscillatory wave forces, unsteady wind forces (owing to wind gustiness), and wave drift damping. In addition, it also neglected the interaction between the body oscillation and wind and current forces. For example, the heave of the body may periodically increase and decrease the area of the body exposed to wind and current. All these simplifications were made based on the assumption that the net effects of oscillatory forces on the steady motion of the body are insignificant.

Two semi-submersible drilling units representing MODUs typically deployed in deep waters of the GOM were chosen for our simulation. In the following description, they are referred as ‘MODU I’ and ‘MODU II’, respectively. The coefficients for computing wind and current force in surge and sway directions as a function of the angle between their directions and the x-axis of the hull were given based on respective model tests. The coefficients for computing the steady wave forces were obtained as a function of wave period (or frequency) and wave direction using WAMIT (WAMIT, Inc., 1999). Met-ocean conditions (wind, current and wave) during the peak of Hurricane Katrina were made available by Oceanweather Inc (Oceanweather Inc., 2006). The trajectories of the two drifting MODUs recorded by the GPS during Hurricane Katrina were provided to us on the condition that no proprietary information is allowed in our publications. The predicted drifts of the two MODUs using ‘DRIFT’ are then compared with the corresponding measurements for examining the efficacy of our approach.

Hindcast Met-ocean Conditions

Two sets of hindcast data of Hurricane Katrina were provided for predicting the drift of the MODUs. The first one known as “Emergency Response Data” (ERD) was derived based upon a preliminary assessment of the impact of the hurricane and the second called “Revised

Data" (RD) was refined upon utilizing a large base of measured wind, wave, and current data. In deriving the latter, a large base of measured wind, wave, surge and current data is used, and a more advanced ocean current model is employed (Oceanweather Inc., 2006). The major differences between the two sets of data relevant to this study are: 1) the latter provides 3-point current velocity profile while the former only renders the depth-average current velocity; and 2) the wind velocity of RD is more towards the North and its magnitude is slightly smaller (about 10%) than those of ERD. The hindcast met-ocean data relevant to this study consists of wind and current speeds, wind and current directions, significant wave height, peak period and wave vector-mean direction updated for every 15 minutes. They are available on a set of rectangular grids of the size, $\Delta\varphi = 0.05°$ and $\Delta\lambda = 0.05°$, where φ is the degree of latitude and λ the degree of longitude. To obtain the related met-ocean data at the position of a drifting MODU, a quadratic interpolation FORTRAN subroutine, DQD2VL, was used for interpolation. More detailed information about the subroutine DQD2VL is given by Visual Numerics Inc. (1999).

Multidirectional wave spectra for every 15 minutes were available on a set of grids of much greater size, $\Delta\varphi = 0.2°$ and $\Delta\lambda = 0.2°$. A 3-D plot of a typical multidirectional wave spectrum is shown in Figure A1 and the portion at high frequencies is amplified in Figure A2, which shows the wave direction changes and wave spreading increases with the increase in frequency, especially at relatively high frequencies.

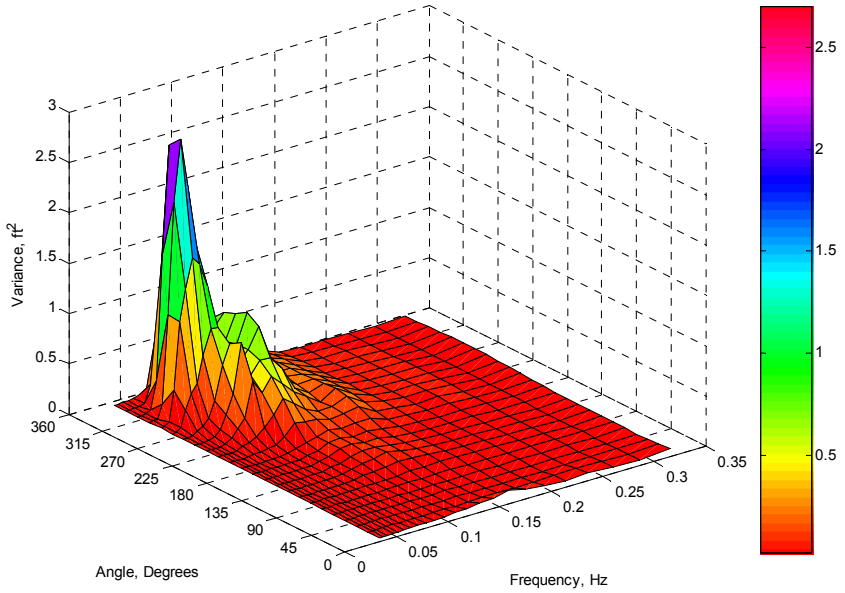

Figure A1. A typical multidirectional wave spectrum during Katrina

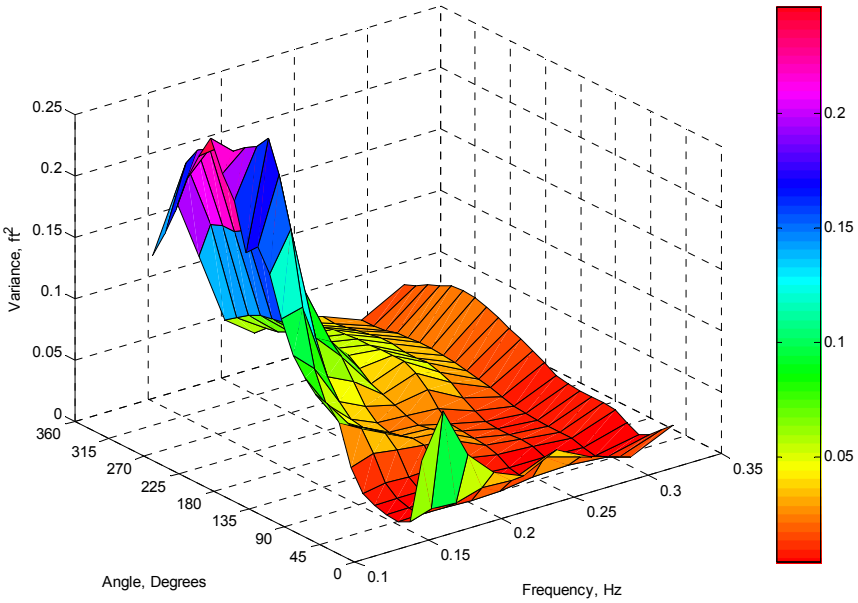

Figure A2. Portion of the multidirectional wave spectrum at relatively high frequency

Simplified Governing Equation and External Forces

The justification of developing a complicated and more accurate numerical model depends on the accuracy of the input data, in this case, the hindcast data. When the input data involved errors of certain magnitude (or uncertainty), it is appropriate to develop a simplified numerical model likely resulting in errors of the similar magnitude as the input. At this stage this study only considers the most important factors in the governing equation of describing

the drift of an unmoored MODU only. The equation describing the horizontal (surge, sway and yaw) motions of a floating body due to steady wind, current and wave (wave mean drift) forces is given below.

$$\left[\mathbf{M}_S + \mathbf{M}_{\text{add}}\right]\ddot{\mathbf{x}}(t) = \mathbf{F}_{\text{Wind}} + \mathbf{F}_{\text{Current}} + \mathbf{F}_{\text{WMDF}}, \tag{1}$$

where

$$\mathbf{x} = \begin{bmatrix} \text{Surge} \\ \text{Sway} \\ \text{Yaw} \end{bmatrix} = \begin{bmatrix} \xi_1 \\ \xi_2 \\ \alpha_3 \end{bmatrix},$$

and the overhead dot stands for the time derivative. The terms at the right-hand side of the equation represent the external forces (moments). $\mathbf{F}_{\text{WMDF}}$ stands for wave mean-drift force and yaw moment, $\mathbf{F}_{\text{Wind}}$ the wind force and $\mathbf{F}_{\text{Current}}$ the current force. At the left-hand side, $\mathbf{M}_S$ and $\mathbf{M}_{\text{add}}$ represent the body mass and added-mass matrix, respectively. The computation of steady wind, current and wave forces are briefly described below.

Wind Force

The *x*- and *y*-component of the steady wind force applied on the structure of a MODU above the sea surface at its center of pressure, z_{CP} is approximately calculated by:

$$\begin{aligned} \mathrm{F}_{\text{Windx}}(\theta_w) &= \frac{1}{2}\rho_a C_{dw} A_{pw} \cos(\theta_w) U_{W/B}^2 = C_{Wx}(\theta_W) U_{W/B}^2 \\ \mathrm{F}_{\text{Windy}}(\theta_w) &= \frac{1}{2}\rho_a C_{dw} A_{pw} \sin(\theta_w) U_{W/B}^2 = C_{Wy}(\theta_W) U_{W/B}^2 \end{aligned} \tag{2}$$

where ρ_a is the air density, C_{dw} the drag coefficient, A_{pw} the projected area of the structure above the sea surface in the direction of the wind. The relative velocity between wind and the body is denoted by $U_{W/B}$, which is equal to $U_W - \frac{dx}{dt}$, where U_W is the steady wind velocity at pressure center z_{CP}. It is related to the wind speed at 10 m above the sea level in the following equation (Wilson, 2003).

$$U_W\left(z_{CP}\right)=U_{10}\left(\frac{z_{CP}}{10}\right)^{0.125} \tag{3}$$

The angle between the wind direction and the *x*-axis fixed on the body is denoted by θ_w. The wind force coefficients, $C_{Wx}\left(\theta_W\right)$ and $C_{Wy}\left(\theta_W\right)$, for MODU I and II were obtained based on the related tests in a wind tunnel. They together with the total wind force coefficient are plotted in Figures A3a and A3b, respectively.

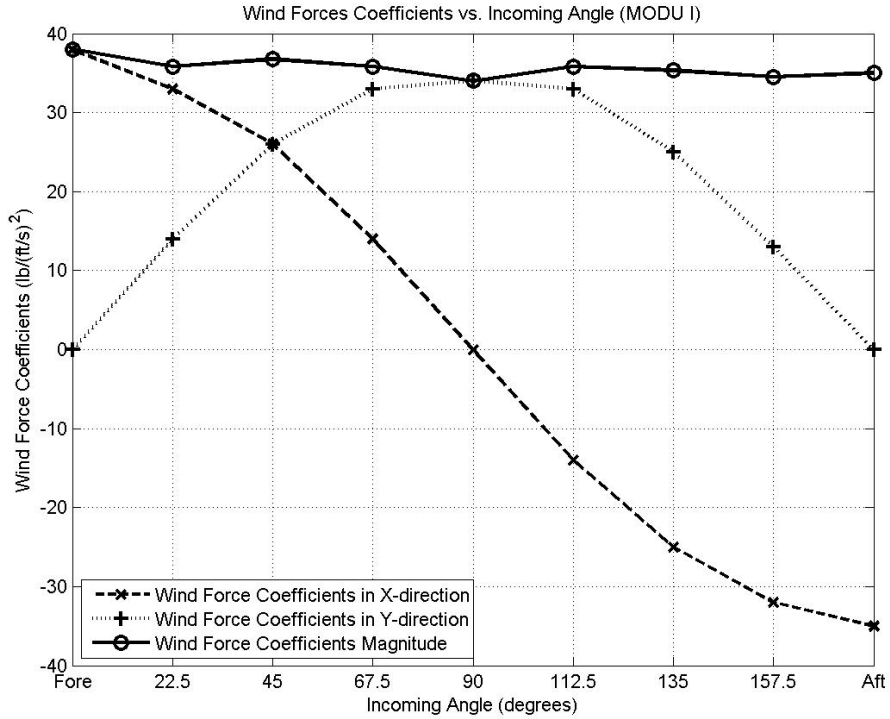

Figure A3a. Wind forces coefficients of MODU I.

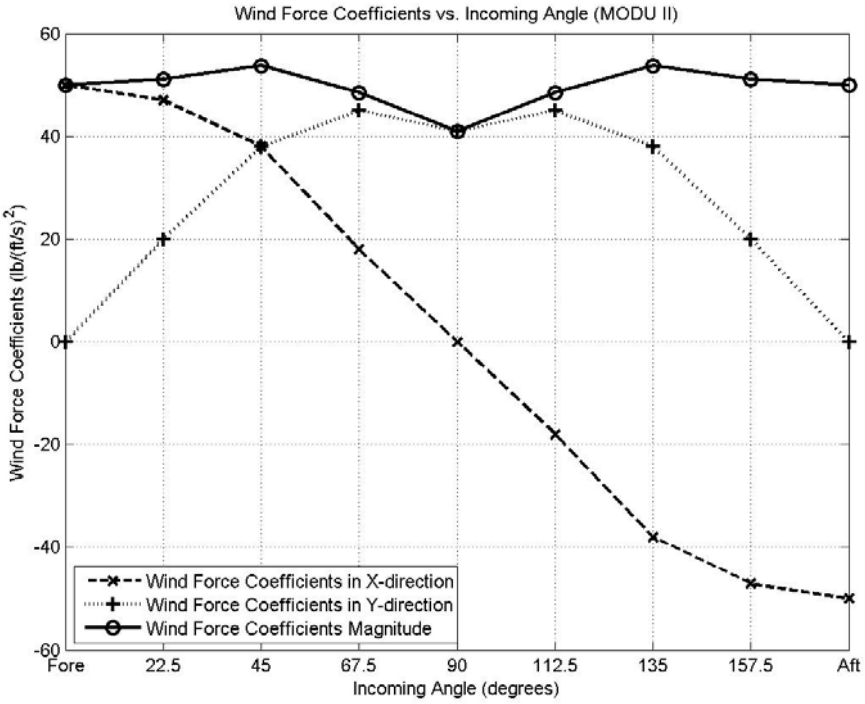

Figure A3b. Wind forces coefficients of MODU II.

Current Force

Similar to the wind force, the *x*- and *y*-component of the steady current force is approximately calculated by

$$\begin{aligned} \mathrm{F}_{Currentx}(\theta_C) &= \frac{1}{2}\rho C_{dc} A_{pc} \cos(\theta_C)\left[\bar{U}_c - \frac{dx}{dt}\right]^2 = C_{Cx}(\theta_C)\left[\bar{U}_c - \frac{dx}{dt}\right]^2, \\ \mathrm{F}_{Currenty}(\theta_C) &= \frac{1}{2}\rho C_{dc} A_{pc} \sin(\theta_C)\left[\bar{U}_c - \frac{dx}{dt}\right]^2 = C_{Cy}(\theta_C)\left[\bar{U}_c - \frac{dx}{dt}\right]^2, \end{aligned} \tag{4}$$

where ρ is the water density, C_{dc} the drag coefficient, A_{pc} the projected area of the structure below the sea surface, $\bar{U}_c - \frac{dx}{dt}$, the relative velocity between the current and horizontal velocity of the body, and θ_C is the angle between the current direction and the x-axis fixed on the body. Similar to the wind force coefficients, the current force coefficients, $C_{Cx}(\theta_C)$ and $C_{Cy}(\theta_C)$, of MODU I and II, were obtained based on the related model tests. Together with the total current coefficient, they are plotted in Figures A4a and A4b, respectively.

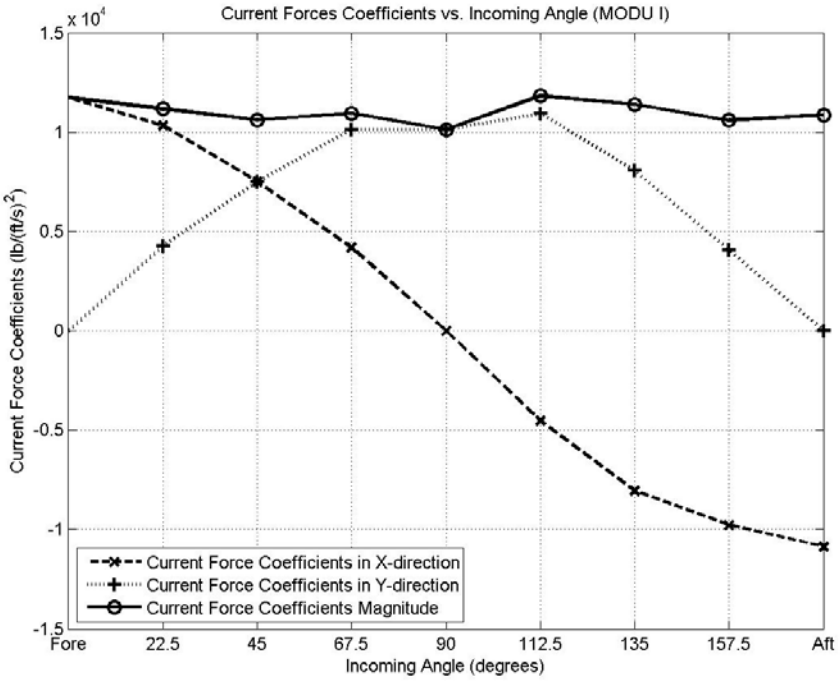

Figure A4a. Current forces coefficients of MODU I.

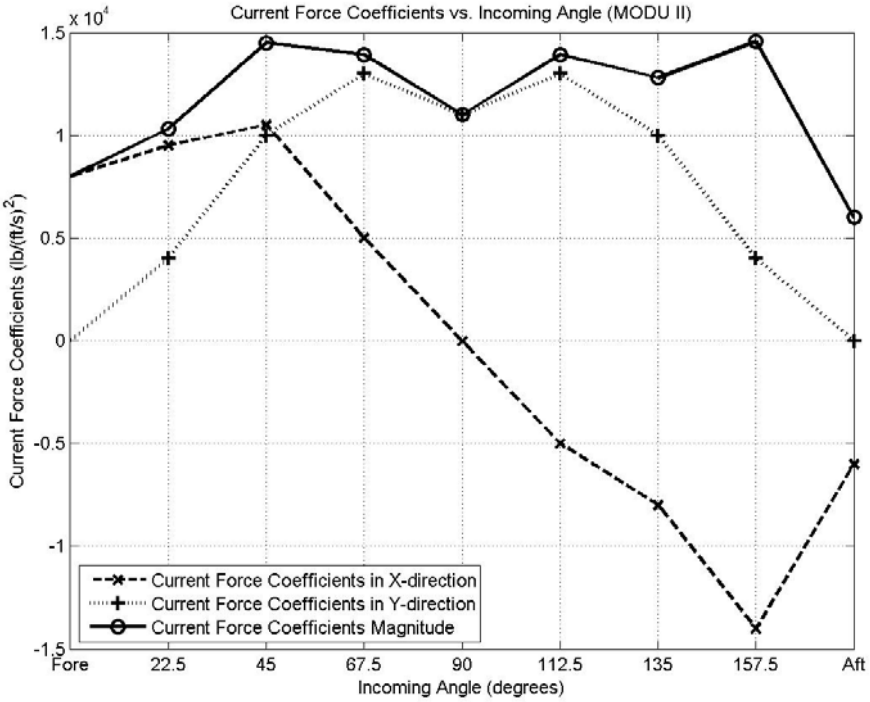

Figure 4b. Current forces coefficients of MODU II.

Wave Mean-Drift Force

As mentioned earlier, the distance between the two neighboring grids giving multi-directional wave spectra is much greater than that giving the significant wave height, peak period, and (vector) mean direction. Therefore, the computation of the wave mean force was based on the significant wave height, peak period and mean wave direction. That is, the wave mean force was calculated based on an energy density spectrum, such as a Pierson-Moskowitz (P-M) or JONSWAP spectrum which can be determined based on given significant wave height and peak period (Goda 1990). However, it was found that wave spreading may significantly reduce the magnitude of the resultant wave force and the direction of the resultant wave mean-drift force may be different from the wave (vector) mean direction. Hence, the corresponding corrections were made to the wave force computed based on an energy density spectrum. The reasons for and how to make the corrections are elucidated below.

The wave mean-drift force coefficients of the two MODUs, defined as the force per unit square wave amplitude (or energy density) at a discrete frequency, were calculated using WAMIT. As an example shown in Figure A5, they depend on the wave frequency and are much greater at relative high frequencies (0.15 – 0.33 Hz) than near the spectral peak (~0.08 Hz). Although wave energy is much greater near the spectral peak than at relatively high frequencies, the contribution to the resultant mean force from waves at relatively high frequencies is nevertheless significant. As shown in Figures A1 and A2 the directions of waves at high frequencies are noticeably different from those near the spectral peak. The latter virtually dictates the mean wave direction because of its dominantly large energy but may not do so in determining the direction of the resultant mean-drift force. Consequently, the direction of the resultant wave mean-drift force can be different from the mean wave direction. Furthermore, wave spreading reduces the magnitude of wave force, especially at high frequencies where the spreading is in general greater. Therefore, the reduction in the wave force due to wave spreading must be accounted accordingly. By comparing the directions and magnitudes of the wave mean-drift force computed respectively using a multi-directional spectrum and the corresponding energy density spectrum at the same grid, it was

found that the direction of the wave mean force in general differs from the mean wave direction in the range from 5 to 30 degrees and that the magnitude of mean force computed based on a multi-directional spectrum is smaller than that computed based on the corresponding energy density spectrum in the range from 20 - 40 %.

In our study, an energy-density spectrum is described by a P-M instead of a JONSWAP spectrum. It is because the shape of an energy density spectrum derived by summing up the energy density in all directions at the same frequency of a multi-directional spectrum is closer to the corresponding P-M instead of a JONSWAP spectrum. A comparison of these three spectra is shown in Figure A6, which represent the typical trend of storm waves during Hurricane Katrina. It should be noted that three spectra compared in the figure have the same significant wave height and peak period and are located at the same grid.

In summary, the resultant mean-drift force was initially calculated based on a transfer function calculated using WAMIT and a P-M spectrum described by the significant wave height and peak period at the location of a MODU. The initial direction of the force was set as the same direction of the mean wave direction. To make the corrections on the direction and magnitude of the resultant force, the mean-drift forces at the nearest four grids surrounding the location of a MODU were also computed, respectively, based on a directional energy-density spectrum and the corresponding P-M spectrum. The differences in the direction and magnitude of the corresponding mean-drift forces indicated the correction on the mean-drift force at each grid. A linear interpolation of the corrections at these four grids led to the correction on the direction and magnitude of the mean-drift forces initially computed using a P-M spectrum. The mean-drift force after the correction was used in computing the drift of a MODU.

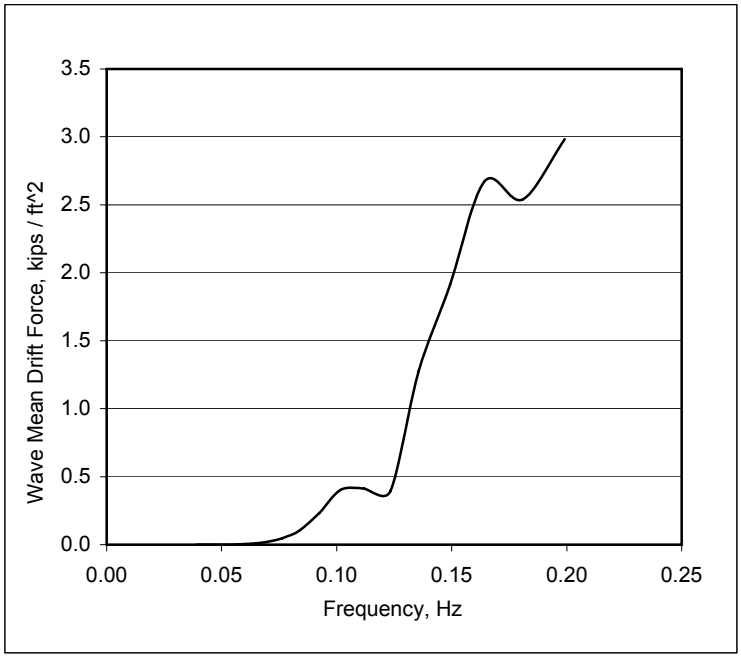

Figure A5. Wave surge force coefficients of MODU I for the incident angle = 0.

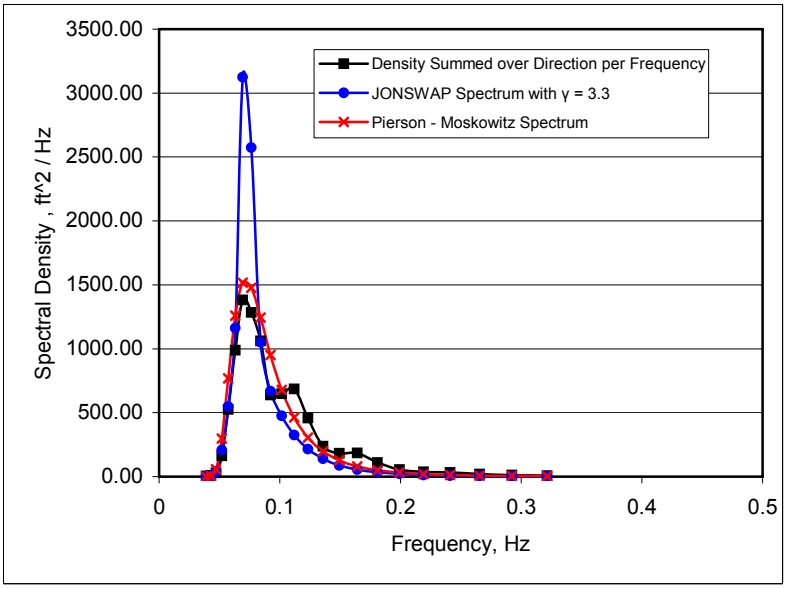

Figure A6. Comparison among three wave energy spectra located at the same grid.

Numerical Scheme

An ordinary differential equation of the following general form describes the 3-Degree-Of – Freedom (DOF) motion of a MODU,

$$\tilde{\mathbf{A}}\ddot{\mathbf{x}}(t) + \tilde{\mathbf{B}}\dot{\mathbf{x}}(t) + \mathbf{C}\mathbf{x}(t) = \tilde{\mathbf{F}}(t), \qquad (5)$$

where $\tilde{\mathbf{A}}$ is the combined added- and body-mass matrix, $\tilde{\mathbf{B}}$ the damping matrix, **C** the hydrostatic stiffness matrix, and $\tilde{\mathbf{F}}(t)$ the total external force. In our simulation, the drag (damping) term was moved to the right-hand side of the equation. Since it involves unknown velocity, it is solved using an iterative procedure. In addition, the stiffness term is set to zero, when it is assumed all mooring lines were broken and the weight of a MODU is balanced by its buoyancy. The differential equation was then solved using a Newmark-β method of $\gamma = 1/2$ and $\beta = 1/4$ (Wood, 1990). A cosine-shape ramp function of time duration 20 s was employed at the beginning of every 15 min when the met-ocean condition was up-dated to ensure a smooth transition. In all simulations, the time step $\Delta t = 0.1$ s was adopted, which was adequate to reach convergent solutions.

Properties of MODUs

Both MODU I and II are semi-submersible rigs. MODU I has a hull of a triangular shape with three vertical columns while MODU II has two pontoons and two vertical columns on each pontoon. Their characteristics are summarized in Tables A1 and A2, respectively. It is noted that MODU II is more than twice in displacement than MODU I.

Table A1. Main Characteristics of MODU I

Properties	***Values***	***Units***
Total Displacement	59376.0	kips
Volume	927369.5	ft^3
Transverse Metacentric Height (GMT)	12.5	ft
Longitudinal Metacentric Height (GML)	12.5	ft
Vertical Center of Buoyancy (VCB)	-42.9	ft
Vertical Center of Gravity (VCG)	21.0	ft
Waterplane Area	5769.0	ft^2
Mean Draft	58.5	ft
Radius of Gyration (Roll)	105.0	ft
Radius of Gyration (Pitch)	110.0	ft
Radius of Gyration (Yaw)	120.0	ft
Wind Pressure Center Height (*Zp*)	117	ft

Table A2. Main Characteristics of MODU II

Properties	***Values***	***Units***
Total Displacement	121585.9	kips
Volume	1899000.0	ft^3
Transverse Metacentric Height (GMT)	31.2	ft
Longitudinal Metacentric Height (GML)	92.6	ft
Vertical Center of Buoyancy (VCB)	-37.0	ft
Vertical Center of Gravity (VCG)	-9.0	ft
Waterplane Area	16800.0	ft^2
Mean Draft	60.0	ft
Radius of Gyration (Roll)	100.0	ft
Radius of Gyration (Pitch)	110.0	ft
Radius of Gyration (Yaw)	120.0	ft
Wind Pressure Center Height	82	ft

Comparison between Predicted and Measured Trajectory of MODU I

Drift of MODU I

The drift trajectory of MODU I during Katrina recorded by the GPS for every 30 min together with the position of the eye of Katrina from 0:00 to 12:00 UT are plotted in Figure A7. In this figure and the following description and figures, all time is referred in Universal Time (UT) on August 29, 2005. It is noted that to conceal the proprietary information, the real longitude and latitude of the trajectory were not revealed in this and the following related figures. Because no information of the yaw angle of the MODU was available, 30-min simulations of the drift of the MODU for different initial yaw angles were performed to examine whether or not the predicted drifting is sensitive to the initial yaw angle. It was found that the prediction for MODU I is not sensitive to the initial yaw angle, which is expected because MODU I has a nearly equilateral triangular hull and the resultant current and wind force coefficients are insensitive to the yaw angle as shown in Figures A3a and A4a.

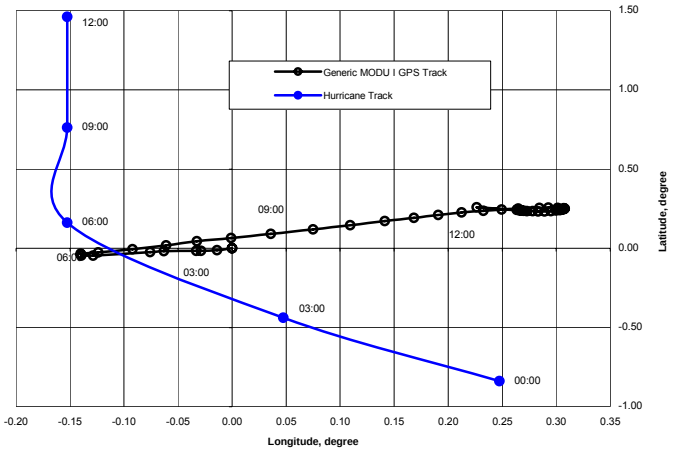

Figure A7. The position of MODU I with respect to that of Katrina's eye

Predicted drift based on ERD

The simulated drift of MODU I based on the met-conditions of ERD is compared with the corresponding measurement from 06:30 to 12:00 in Figure A8. For every 30-min, the simulation of the drift started at the corresponding measured location and the drifting velocity at the end of the previous 30-min prediction was used as the initial velocity input for the next 30-min simulation. Satisfactory agreement is observed in the figure. The distance between the measured and predicted drifting position of the MODU at the end of each simulation is less than 1 km. The predicted drift is slightly southern to the measured one from 06:30 to 08:00 and then moves northern to the measurement from 08:00 to 12:00.

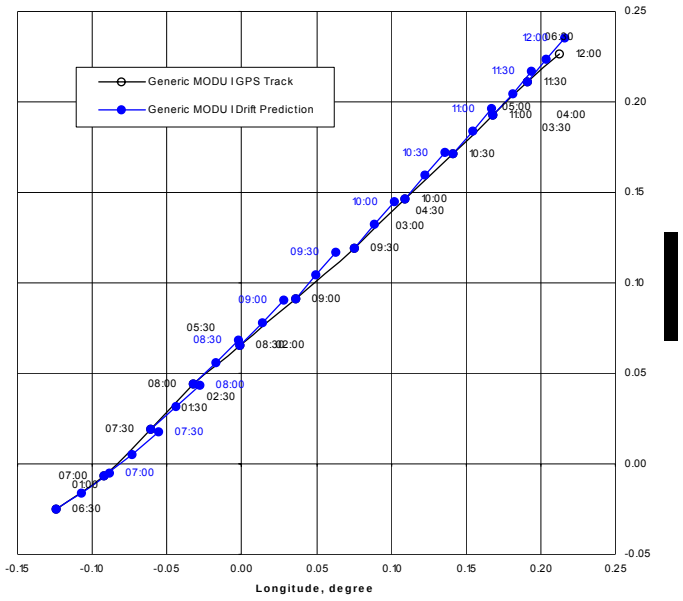

Figure A8. Comparison between predicted based on ERD and measured drifts of MODU I with every 30-min corrected initial position.

Predictions of the drift starting at 04:00 and ending at 12:00 (continuously without any corrections on the drift) are compared with the corresponding measurement in Figure A9. Overall agreement between the prediction and measurement is satisfactory, showing the distance between the predicted and measured position of the MODU I at the end of the simulation is about 2 km. From 4:00 – 5:00 and 6:00 – 12:00, the predicted and measured

trends of drifting are in satisfactory agreement. The orientation of the drift in these two durations was expected based on the location of the MODU I with respect to that of hurricane's eye. It is known that a low pressure storm system, such as a hurricane, rotates counter clockwise in the northern hemisphere. The MODU was located to the North of the Katrina's eye at 4:00. Following the counter clockwise wind, both prediction and measurement show the MODU drifting toward the Southwest. After 6:00, the eye of Katrina moved to the North of the MODU, both prediction and measurement indicate the MODU drifting toward the Northeast. From 5:00 – 6:00, when the eye of Katrina was very close to the location of MODU I, it was drifting very slowly because the wind velocity close to the center of the hurricane eye was small. However, there is a qualitative difference though small between the predicted and measured drifts. The measurement indicated the MODU drifting to the North while the simulation predicted it drifting to the South. The discrepancy probably results from inaccurate hindcast met-ocean conditions near the hurricane eye, which is not surprising considering that the uncertainty about the hindcast met-ocean condition near the hurricane eye is very high.

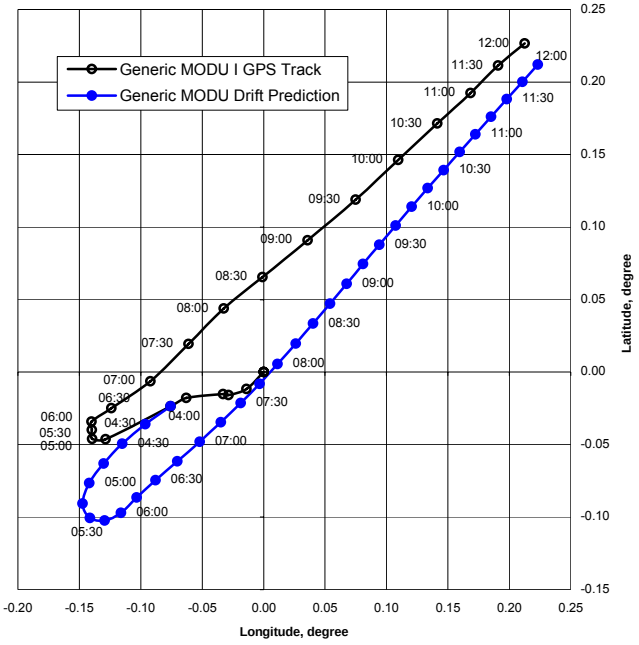

Figure A9. Comparison of the continuous predicted based on ERD and measured drift of MODU I from 04:00 - 12:00 UT

Predicted drift based on RD and considering loop currents and dragging anchors

The RD of Katrina was provided to us after the predicted drift based on ERD was made. Meanwhile, it was found that strong loop currents were present in the area of drifting MODUs during Katrina (AOML/NOAA 2005). Furthermore, more information about the condition of drifting MODU I was later provided to us after our industrial partners did more thorough forensic investigations on drifting MODUs. It was told that MODU I might drag one or two anchors during its drift, which is different from our previous assumption made in Section 6.1.1 that all mooring lines of MODU were broken during its drift. Hence, we included the velocity induced by the loop currents (3.048 ft/s and direction of 350 degree) in addition to the current velocity induced by Katrina (AOML/NOAA 2005). In computing the drift, the resistance resulted from one or two dragging anchors was set to be 311.25 kips from 6:30 to 7:30 and 543.75 kips from 07:30 to 12:00, which was assumed to be opposite in the direction to the drifting MODU. It should be noted that the above magnitude and direction of the resistance resulting from dragging anchors were determined empirically and provided from our industry partners (Zimmerman, 2007). More accurate estimate of the steady dragging-anchor resistance should be made based on the couple analysis of the interaction between a drifting MODU and its dragging mooring lines and anchors, which needs significant additional efforts and should be included in our future research project. Based on the loop current velocity, the resistance from dragging anchors, and the met-ocean condition provided by the RD, we conducted the simulation of the drift of MODU I again. The simulated drift is compared with the corresponding measurement from 06:30 to 12:00 in Figure A10. Similar to the procedure stated in Section 6.2, the simulation started at the corresponding measured location for every 30-min and the drifting velocity at the end of the previous 30-min prediction was used as the initial velocity input for the next 30-min simulation. Satisfactory agreement is observed in the figure, showing that the distance between the measured and predicted drifting position the end of each 30-min simulation is less than 2 km. The predicted drift is always to the North of the measurement from 06:30 to 12:00.

Predictions of the drift starting at 6:30 and ending at 12:00 (continuously without any corrections on the drift) are compared with the corresponding measurement in Figure A11. Overall agreement between the prediction and measurement is satisfactory, showing the distance between the predicted and measured position of the MODU I at the end of the simulation is about 10 km north to the measurement, which is greater than the discrepancy observed in Figure A9 and is consistent with the trend showing in Figure A10.

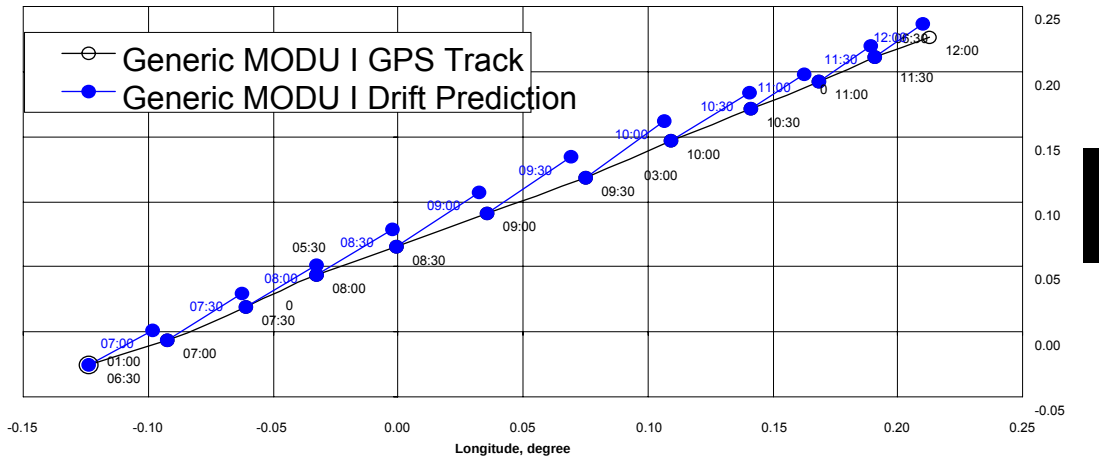

Figure A10. Comparison between predicted based on RD and measured drifts of MODU I with every 30-min corrected initial position.

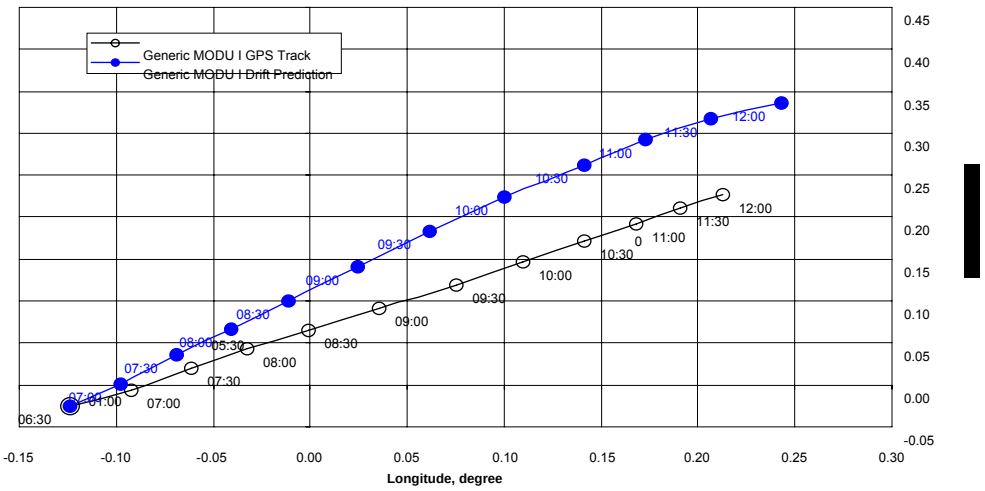

Figure A11. Comparison of the continuous predicted based on RD and measured drift of MODU I from 06:30 - 12:00 UT

Drift of MODU II

The recorded position of MODU II during the hurricane and the trajectory of the hurricane's eye are depicted in Figure A12. It shows that MODU II started to drift after the eye of Katrina moved to its North. Hence, it is expected to drift to the East due to the counter clockwise wind, which is confirmed by its recorded trajectory. Similar to the simulations conducted in the case of MODU I, we explored the sensitivity of the drift of MODU II to the initial yaw angle. The predictions of the drift of MODU II using different initial yaw angles for the duration from 06:00 to 06:30 were made. The comparison between these predictions and the corresponding measurement shows the predicted drifts using the initial yaw angle set at 0° and 45° are virtually the same. However, the drift predicted with initial yaw angle at 90° is more toward South while that at 135° is the closest to the measured trajectory of the MODU. For that reason, the initial angle of 135° was chosen in our simulation of the drift of MODU II. The dependence of the drifting prediction on the initial yaw angle in this case is significant in comparison with that of MODU I. This is probably due to the shape of the hull of MODU II, which is quite different from the equilateral hull of MODU I.

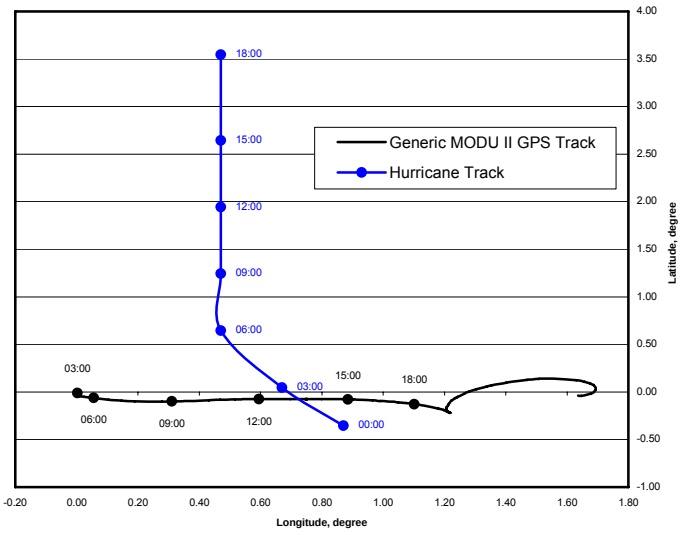

Figure A12. GPS of MODU II and hurricane eye trajectory

Predicted Drift Based on ERD

Based on the met-condition of ERD, the simulated drift of MODU II from 06:00 to 10:30 was made with the correction of its initial position for every 30 min and is compared with the recorded drift in Figure A13. The starting position of the simulation is chosen to be 06:00 when MODU II began to drift significantly (see Figure A12). Similar to the simulation made for MODU I, the data for wind, wave and current was updated for every 15 min. The comparison shows satisfactory agreement between the prediction and measurement. The distance between the measured and predicted position of MODU II at the end of each 30 minute simulation is less than 1.5 km. The predicted drift is toward the South of the measured trajectory at the beginning of the simulation and gradually shifts toward the North of the measured position, especially from 9:00 – 10:30. This trend is similar to that observed in the case of MODU I when the prediction was made based on ERD.

The continuous simulation of the drift from 6:00 – 10:30 based on ERD was made and compared with the measurement in Figure A14. The predicted drift of the MODU deviates to the South with respect to its measured trajectory from 6:00 to 8:00 and then to the North from 08:30 to 10:30. This trend of the predicted drift is consistent with the one observed from the prediction with every 30-minute correction. After four and a half hour drift, the distance between the measured and predicted position of MODU II is about 4 km.

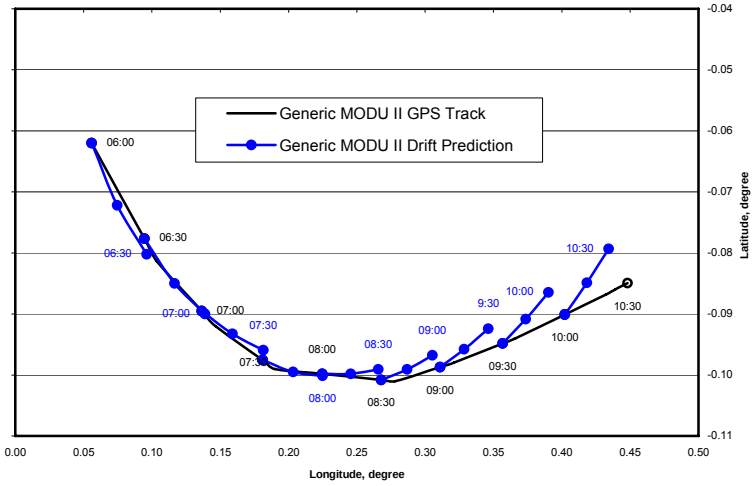

Figure A13. Comparison of 30-min simulated drift based on ERD with the measurement of MODU II.

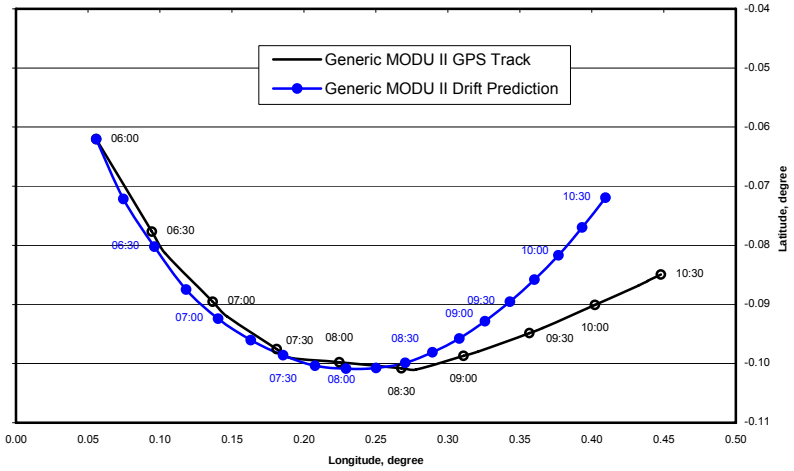

Figure A14. Comparison of continuous simulation based on ERD from 6:00 -10:30 with the measurement of MODU II.

Predicted drift based on RD and considering loop currents

The velocity induced by the loop currents in the vicinity of the drifting MODU II during Katrina was found to be 3.937 ft/s in magnitude and 0 degree in direction (AOML/NOAA 2005). The forensic investigation on MODU II confirmed that it did not drag any anchor during Katrina. Hence, the loop current velocity was included in the simulation in addition to the current velocity induced by Katrina. Based on the met-condition of RD and considering the effects of loop current, the simulated drift of MODU II from 06:00 to 10:30 was made with the correction of its initial position at the related measured position for every 30 min. The comparison with the corresponding recorded drift is given in Figure A15. Similar to that stated in Section 6.1.2, the data for wind, wave and current based on RD was updated for every 15 min. The comparison shows satisfactory agreement between the prediction and measurement. The distance between the measured and predicted position of MODU II at the end of each 30 minute simulation is about 1.5 km. Different from the trend observed in the corresponding predicted drift based on ERD and without considering the effects of loop currents, the predicted drift based on RD is always in the North of the measured trajectory.

The continuous simulation of the drift from 6:00 – 10:30 was made and compared with the measurement in Figure A16. The predicted drift of the MODU deviates to the North with respect to its measured trajectory. This trend of the predicted drift is consistent with the one observed in Figure A15. After four and a half hour drift, the distance between the measured and predicted position of MODU II is about 4 km.

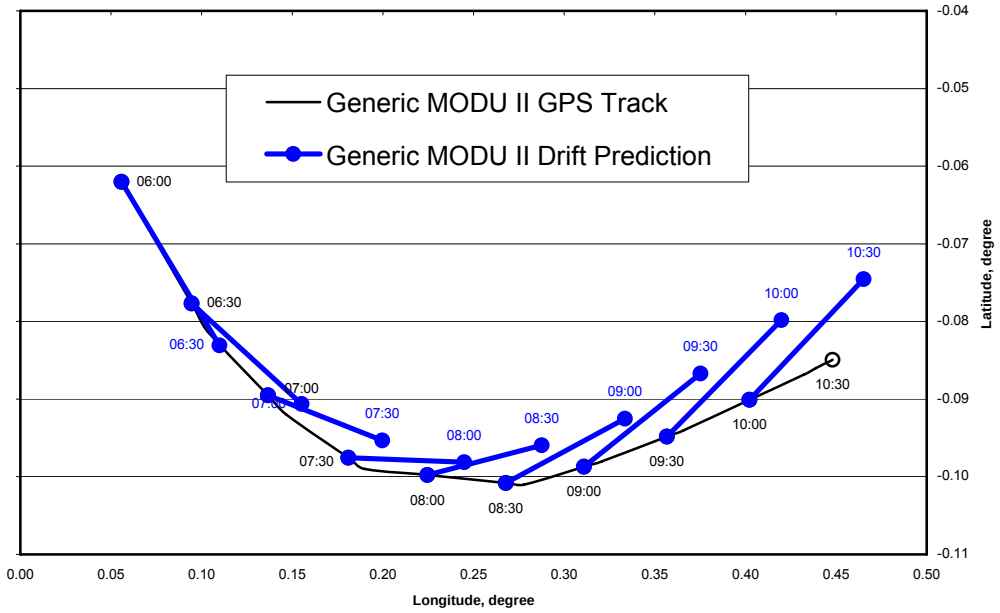

Figure A15. Comparison of 30-min simulated drift based on RD with the measurement of MODU II.

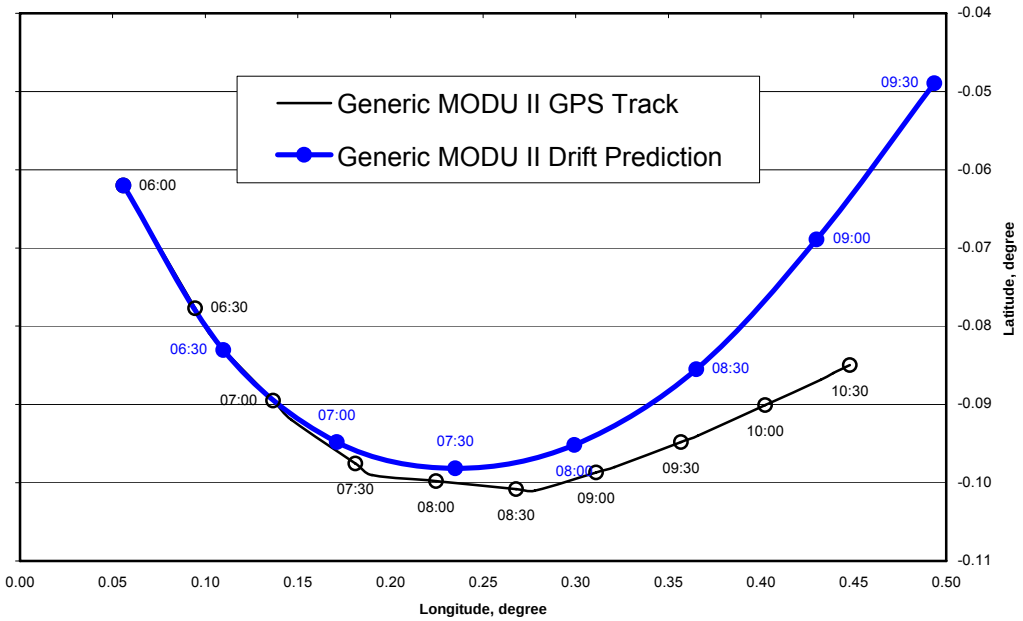

Figure A16. Comparison of continuous simulation based on RD and the measurement of MODU II.

Summary and Future Work

Numerical program ‘DRIFT’ was developed and used for predicting the trajectory of two typical semi-submersible MODUs which drifted during hurricane Katrina. To explore the feasibility and accuracy of predicting the trajectory of a drifting MODU given hindcast met-ocean conditions and limited knowledge of the condition of the drifting MODU, this study employed a simplified equation of motion describing only the horizontal (surge, sway and yaw) motions of a MODU under the impact of steady wind, current, loop currents and wave forces. The predicted drifts of the two MODUs were compared with the corresponding trajectories recorded by the GPS. Satisfactory agreements were observed between the recorded trajectories of MODU I and II and the corresponding predictions made based on the met-ocean condition of ERD and RD, respectively. In the case of MODU I, the resistance to the drift resulted from dragging anchors was empirically included in the prediction based on RD. The knowledge drawn from this study is summarized below.

1. The numerical program, ‘DRIFT’, based on a relatively simplified hydrodynamic model, is capable of predicting the trajectory of a drifting MODU.
2. Accurate prediction depends on the accuracy of input met-ocean conditions (wind, wave and current data) and the condition of the MODU and its damaged mooring system. If the input met-ocean conditions are inaccurate, the prediction will be inaccurate or even qualitatively different from the corresponding measurement.
3. At present stage, hindcast met-ocean conditions during a hurricane can be predicted with certain accuracy or uncertainty. Considering this factor, the simplified hydrodynamic model used in this study seems to be adequate.
4. Wave directions, spreading and energy of wave components at relatively high frequency range are crucial, especially at late stage of hurricane when the wind force is no longer dominant.
5. The resistance resulting from dragging anchors to the drifting of a MODU was determined empirically in this study. Accurate estimate of the steady resistance

resulting dragging anchor or anchors can be made based on the couple analysis of the interaction between a drifting MODU and its dragging mooring lines and anchors, which may result in better prediction on the drifting of a MODU in the future.

It should be noticed that the above summary is based on the comparison with the recorded trajectories of two drifting MODUs during Hurricane Katrina. More studies are required for the drifting of different MODUs in different hurricanes before drawing the final conclusion that we have the capability of predicting the trajectory of a MODU which completely or partially loses the positioning capability during hurricanes.

Acknowledgments

The authors would like to thank Offshore Technology Research Center (OTRC) of Texas A&M University and Minerals Management Service (MMS) for their financial support of this project. During the course of this work, the authors had the benefit of constructive discussions with Mr. Zimmerman of Delmar System, Inc. and Dr. Ward of OTRC.

References

Anderson, E., Odulo, A., Spaudling, M., 1998. Modeling of Leeway Drift. U.S. Coast Guard Research and Development Center, Report No. CG-D-06-99.

Goda, Y., 1990. Random Waves and Spectra. Handbook of Coastal and Ocean Engineering, Gulf Publishing Company, Houston, Vol.1, pp. 175-213.

AOML/NOAA, 2005 GOM Surface Dynamics Reports (08/29/2005 Report), http://www.aoml.noaa.gov/phod/altimetry/katrina1.pdf

Hodgins, D.O., Mak R.Y., 1995. Leeway Dynamic Study Phase I: Development and Verification of a Mathematical Drift Model for Four-person Liferafts. Transportation Development Center, Transport Canada, Report No. TP 12309E.

Oceanweather Inc., 2006. Hindcast Data on Winds, Waves, and Currents in Northern Gulf of Mexico in Hurricanes Katrina and Rita. www.mms.gov/tarprojects/580.htm.

Sharples, M., 2004. Post Mortem Failure Assessment of MODUs during Hurricane Ivan. www.mms.gov/tarprojects/548/Ivan_FinalReport.pdf.

Smith, E., 2006. Recovery and Rebuilding Following Hurricanes Katrina and Rita. www.trb.org/webmedia/2006am/553Smith.pdf.

Su, T.C., 1986. On Predicting the Boat's Drift for Search and Rescue. U.S. Department of Transportation, Report No. DOT/OST/P-34/87/059.

Visual Numerics Inc., 1999. IMSL FORTRAN Library User's Guide Math/Library Volume 2 of 3. www.vni.com/products/imsl/documentation/index.html#fort.

WAMIT, Inc., 1999. WAMIT User Manual Versions 5.4, 5.4PC, 5.3S. Massachusetts Institute of Technology, Cambridge.

Wilson, J.F. 2003. Dynamics of Offshore Structures. John Wiley & Sons Inc., Hoboken.

Wood, W.L., 1990. Practical Time-stepping Schemes. Clarendon Press, Oxford.

Zimmerman, E., 2007. Private Communication.

Appendix B: Progressive Failures of MODU Mooring Systems During Hurricanes

M.H. Kim, Z. Zhang, E.G. Ward, and S. Ma

Introduction

During 2004-2005, three consecutive category-5 hurricanes (Ivan, Katrina, and Rita) struck the central region of Gulf of Mexico (GOM) and damaged numerous drilling and production platforms. Since then, a number of forensic studies have been conducted to better understand the failure cause and mechanism and develop reasonable strategy for future design. This study focused on the failures of the mooring systems of two semisubmersible MODUs - the Noble Jim Thompson and the Deepwater Nautilus. The Noble Jim Thompson was located in Mississippi Canyon Block 383 in 5800 feet of water and Ivan's track passed close by to the east. The Deepwater Nautilus was located in Lloyd Ridge Block 399 in 90000 feet of water and Ivan's track passed close by to the west.

The progressive failure of mooring lines of a floating platform can be simulated by a vessel-mooring-riser coupled dynamic analysis program, TAMU-WINPOST, in time domain (Kim et al, 1999, 2001). This numerical tool has been extensively verified through comparisons against various experimental and field reports (Kim 1999, Halkyard 2004).

The vessel motions and mooring line tensions are simulated for a specified hurricane wind, wave, and current environment. When the tension in a mooring line exceeds the mean break strength, the mooring line is considered to have failed. That line can no longer apply any tension to the floating platform, and the stiffness of the mooring system is suddenly changed. When a line fails, the surface platform may experience a possibly large transient response, which may in turn result in a sudden increase of tension on neighboring lines.

The progressive mooring-line failures for the two generic MODUs - MODU I whose hull-shape is similar to the Noble Jim Thomson and MODU II whose hull shape and particulars are similar to the Deepwater Nautilus, were simulated for wind, wave, and current environments in hurricane Ivan these MODUs experience during hurricane Ivan. Results were compared to forensic data available from Sharples (2006), Loeb (2005), Petruska (2005), and Delmar (2005a, 2005b).

Hydrodynamic Modeling and Analysis

The hydrodynamic coefficients (6DOF added mass and radiation damping) and wave forces are calculated based on potential theory and 3D diffraction/radiation panel program WAMIT (Lee et al, 1991). The total number of panel elements on the wet hull surface is 804. The calculated RAOs (Response Amplitude Operator: 6DOF platform responses for unit-amplitude incident waves) are checked against the independent calculation by Delmar. For the calculation of the slowly-varying wave forces and the corresponding slow drift motions of the moored platform in irregular waves, the so-called Newman's approximation method (the second-order wave-force difference-frequency quadratic transfer functions (QTF) at slightly off-diagonal positions are approximated by diagonal values) was used. For the given platform type, wave-drift damping is expected to be small compared to other damping sources, such as radiation and viscous damping, so it is not considered. The viscous forces and the damping on the respective elements of the hull are calculated through modified Morison's formula.

Delmar (2006) provided estimates for : (1) the particulars of the hulls and mooring systems for MODUs I and II; (2) the viscous drag coefficients on various elements of the hull; and (3) wind-force coefficients for the platform elements above MWL at various heading angles.

MODU I

The hull form of MODU I is shown in Figure B1. The damping of the platform hull is modeled by using 3 truss and 27 plate members, and the drag coefficients for each component are estimated following API-2SK (Recommended Practice for Design and Analysis of Station-keeping Systems for Floating Structures, second edition, 1996) and further calibrated

against the wind-tunnel test data. The resulting drag coefficients for each of the MODU I component are also shown in Figure B1.

The damping of the platform hull is modeled by using 3 truss and 27 plate members, and the drag coefficients for each component are estimated following API-2SK (Recommended Practice for Design and Analysis of Station-keeping Systems for Floating Structures, second edition, 1996) and further calibrated against the wind-tunnel test data. The resulting drag coefficients for each of the MODU I component are also shown in Figure B1:

Figure B1. MODU I Hull and Drag Coefficients

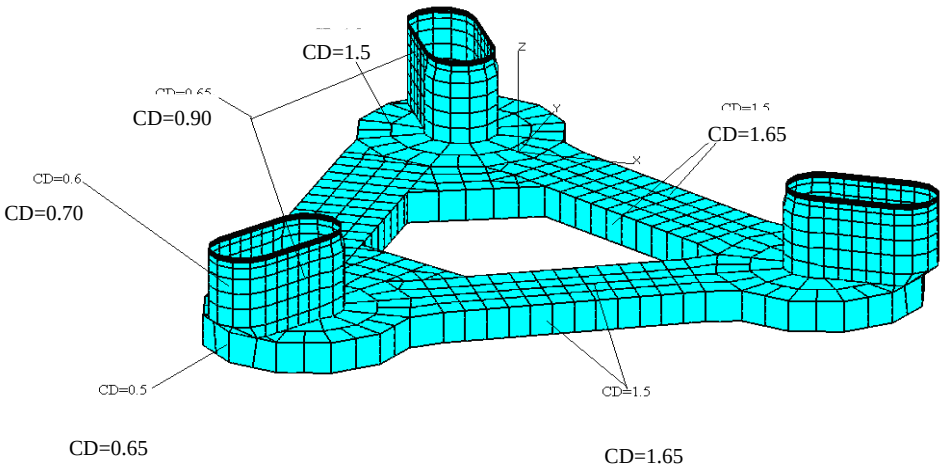

For further verification, the viscous drag force on the entire wet surface of the platform is numerically simulated by sending uniform current from various incident angles. The numerically simulated results agree well as shown in Table B1.

Table B1. Comparison of Numerically Simulated Coefficients with Delmar's Data

The current heading	Current force Fx (N)		Current force Fy (N)		Current force Mx (N.m)		Current force My (N.m)	
	Viscous model	Given data	Viscous model	Given data	Viscous model	Given data	Viscous model	Given data
0	0.5157E+06	0.5618E6	0	0	-0.1913E-02	0	-0.6001E+07	-0.6625E7
22.5	0.4775E+06	0.4941E6	0.2024E+06	0.2040E6	0.2407E+07	0.2414E7	-0.5585E+07	-0.5827E7
45	0.3693E+06	0.3589E6	0.3590E+06	0.3589E6	0.4147E+07	0.4232E7	-0.4359E+07	-0.4232E7
67.5	0.1970E+06	0.2005E6	0.4698E+06	0.4842E6	0.5463E+07	0.5708E7	-0.2262E+07	-0.2364E7

Environmental Loading

The Ivan maximum environment at the NJT's location was hindcast by Oceanweather Inc. (OWI). It is non-collinear environment with winds, waves, and currents approaching from different angles. The incident angle is measured with respect to the rig-heading axis. Their main characteristics are summarized in Table B2 and Table B3:

Table B2. Environmental Data for Wave and Wind (MODU I)

Wave	Significant wave height:	15.2 m
	Peak Period:	16.2 s
	Min/Max Cut-off Frequencies:	0.2094-1.2566
	Incident Angle:	60 deg
Wind	Mean speed at 10m height:	38.906 m/s
	Min/Max Cut-off Periods:	5 – 3600
	Peak coefficient:	0.025
	Incident Angle:	91 deg

Table B3. Environmental Data for Current (MODU I)

Water Depth (m)	Current Velocity (m/s)	Incident Angle (deg)
0	2.31648	45
48.4632	1.73736	45
96.9264	0.0	N/A

The wind force was calculated by using the measured wind-force coefficients obtained from a series of wind-tunnel tests. The wind-velocity time series are generated from API wind spectra.

Mooring Systems Analyzed for MODU I

The performances of two mooring systems were simulated for MODU I - a traditional chain-wire system and a taut wire-polyester-wire system. The chain-wire system is similar to the mooring system that failed on the Noble Jim Thompson during Ivan. The polyester system was analyzed to compare its behavior and performance in extreme storm conditions with the traditional chain-wire system.

Traditional Mooring System Configuration

The traditional mooring system for MODU I was a omni-spread 9 traditional semi-taut chain-wire lines as shown in Figure B2. The chain is at the bottom and the wire above it. The angle between each line is 40 degrees. The standard top pre-tension is set to be 1112 KN (250 kips). The material properties for each component of the traditional mooring system are shown in Table B4 below.

Table B4. Material property for the components of the C-W system

	3 3/4" Wire Rope	3 5/16" Chain	3 9/16" Chain	3 1/8" Rig Wire
Diameter	0.0953 m	0.1582 m	0.1788 m	0.08 m
EA	4.7E+5 KN	4.5E+5 KN	5.2E+5 KN	3.31E+5 KN
EI	0 KN-m^2	0 KN-m^2	0 KN-m^2	0 KN-m^2
Dry Weight	38.3 kg/m	155 kg/m	198 kg/m	27.0 kg/m
Wet Weight	33.3 kg/m	134.85 kg/m	172.26 kg/m	23.5 kg/m
Ci	2	3	3	2
Cd	1	2.45	2.45	1
Break Strength	7063 KN	5681.9 KN	7095.9 KN	5003 KN

Figure B2. MODU I C-W Mooring Pattern 3D View (Generated by HARP)

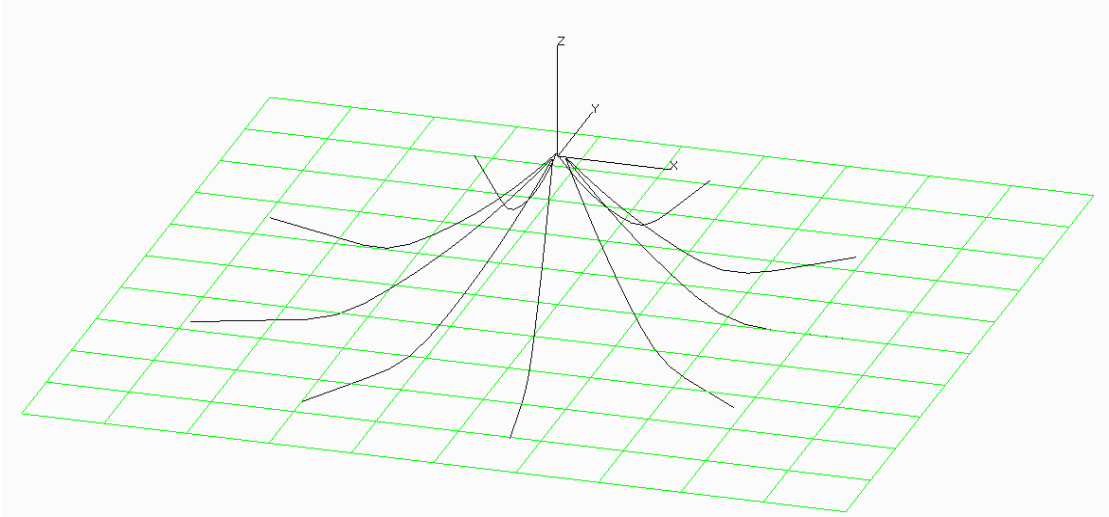

Polyester Mooring System Configuration

The alternative polyester mooring system for the MODU I also consists of 9 lines as shown in Figure B3. Each line has three mooring components: the bottom part is 100ft 3-3/4 inch wire rope; the long (1.5 times water depth) middle part polyester; and the top 300 ft 3-1/8 inch rig wire. The mooring is taut and there is no element touching the seafloor. The angle between each line is the same as the traditional mooring system i.e. 40 degrees. In general, the initial top tension of polyester lines is smaller compared to traditional steel mooring system, so 70%

of the traditional system (778.4 KN) is used here. The material properties for each component of the polyester mooring system are shown in Table B5 below.

Table B5. The material properties for polyester mooring system (W-P-W system)

	3 3/4" Wire Rope	7" Polyester	3 1/8" Rig Wire
Diameter	0.0953 m	0.178 m	0.08 m
EA	4.7E+5 KN	2.197E+5 KN	3.31E+5 KN
EI	0 KN-m^2	0 KN-m^2	0 KN-m^2
Dry Weight	38.3 kg/m	20.2 kg/m	27.0 kg/m
Wet Weight	33.3 kg/m	5.1 kg/m	23.5 kg/m
Ci	2	2	2
Cd	1	1	1
Break Strength	7063 KN	7848 KN	5003 KN

Figure B3. MODU I Polyester Mooring System Pattern

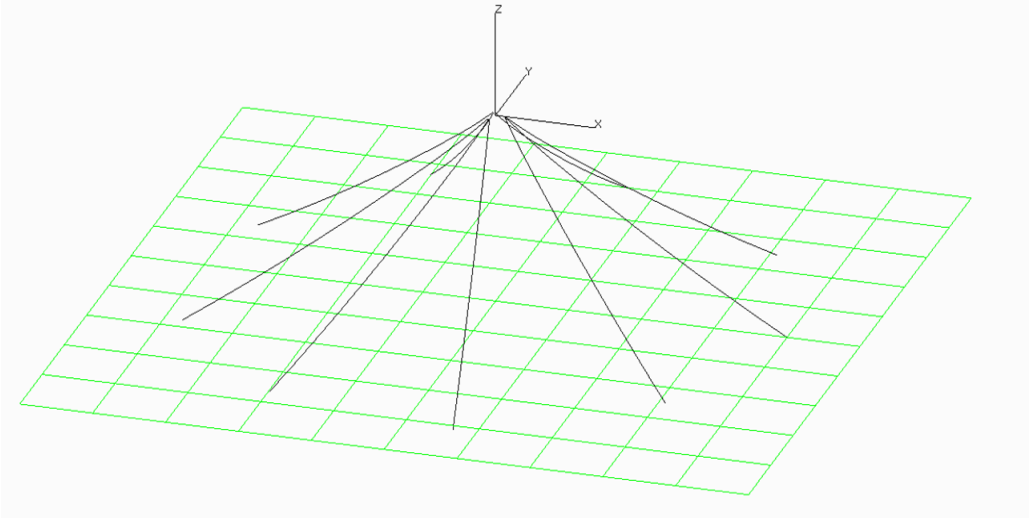

Compared to traditional steel mooring system, the lines in the polyester system have a greater minimum break load (MBL), smaller tension due to its lighter weight, and smaller horizontal displacement that is beneficial to riser design. The stiffer polyester mooring system tends to provide a smaller watch circle, allows bigger deck loads, and better chance of survivability in harsh environment. It also allows a smaller foot-print on the seabed, which is very crucial in deep- and ultra-deepwater developments.

In the present numerical simulations with polyester lines, linear and constant axial stiffness EA is assumed for simplicity neglecting the possible creep/hysteresis behavior (Lee et al., 2000). Since maximum tension is of primary importance for the present study, the storm stiffness is used instead of post-installation stiffness. More sophisticated polyester-mooring analysis including nonlinear stress-strain relationship have been reported, e.g., Arcandra 2004.

Simulation Results & Discussion for MODU I

The total simulation time is 5000 seconds. To suppress the transient responses as much as possible, the environmental force was gradually applied from zero to actual value during the ramping period 250s. We assumed that mooring lines break when tension reaches 100% of the MBL (minimum breaking load).

We did not model any weak links/connectors at anchors or in the middle of lines, so lines are to break at the fairlead, where the maximum tension occurs. It should be noted that both traditional and polyester lines used the same steel rig wire at its top for fair comparison.

The simulated platform displacement time series for the traditional mooring system is shown in Figure B4. The traditional mooring system failed and the polyester lines survived in the same environment. When the first line breaks (~ 250 sec), the platform tilts and experiences large transient motions, especially in rotational modes. Such a large transient response may also cause unexpectedly large inertia loading on high-altitude topside structures on deck. After the first line breaks, the other lines also fail, first in taut side, and later in slack side.

The progressive failure of the traditional mooring system is shown in Figure B5 and the sequence and time are summarized in Table B6. The numerical prediction of the failure pattern and sequence is in good agreement with Sharples (2006).

The simulated platform displacement time series for the polyester mooring system is shown in Figure B6. The polyester mooring system did not fail. The tension time series for the lines

in both mooring systems are given in Figure B7 and Figure B8. Note that the topmost element in both systems is the same rig wire with an MBL of 5007 KN. In Figure B7, the top tensions reach a maximum value equal to the MBL of 5007 KN (displayed as 5.007 $(10)^6$ N in the plots) and are shown as constant indicating a line break. Note that the tension of a broken line is set to zero after breaking in the continuing dynamic analysis of the mooring system. In Figure B8, the maximum top tension only reaches about 3.8 $(10)^6$ N in line 5, the heaviest loaded line [note that the plots for the individual lines are auto-scaled and vary between $(10)^5$ N and $(10)^6$ N]. Thus the maximum tensions in the rig wires (the weakest link in our analyses) for the polyester system never reach the MBL of 5007 KN. The major reason for the lower tensions in the polyester system is that both mean and dynamic tensions are reduced due to its lighter weight and more favorable dynamic characteristics. Also, the taut mooring system behaves in a quasi-static manner and the wave-frequency component of the line tension is significantly reduced, which can also be seen in the comparison of the top tension spectra for the rig wires for both systems in Figure B9.

To better understand the overall platform dynamics and physics, the magnitudes of constituent force components on the MODU I are summarized in Table B7. The diffraction force means the first-order wave-frequency loading and the viscous force includes current loading as well as contributions from wave- and body-motion induced velocities. The viscous forces contribute to both external and damping forces. It is seen that the wave loading is one order greater than wind and current forces. The wind and current forces are important for the mean offset and mean tension, while wave-frequency forces and motions are primary factors for the dynamic tension.

The traditional mooring system failed (dynamic failure) in this environment, while the polyester system unexpectedly survived.

Figure B4. Platform Displacement and Rotation Time Series for MODU I with Traditional Mooring System (Failed)

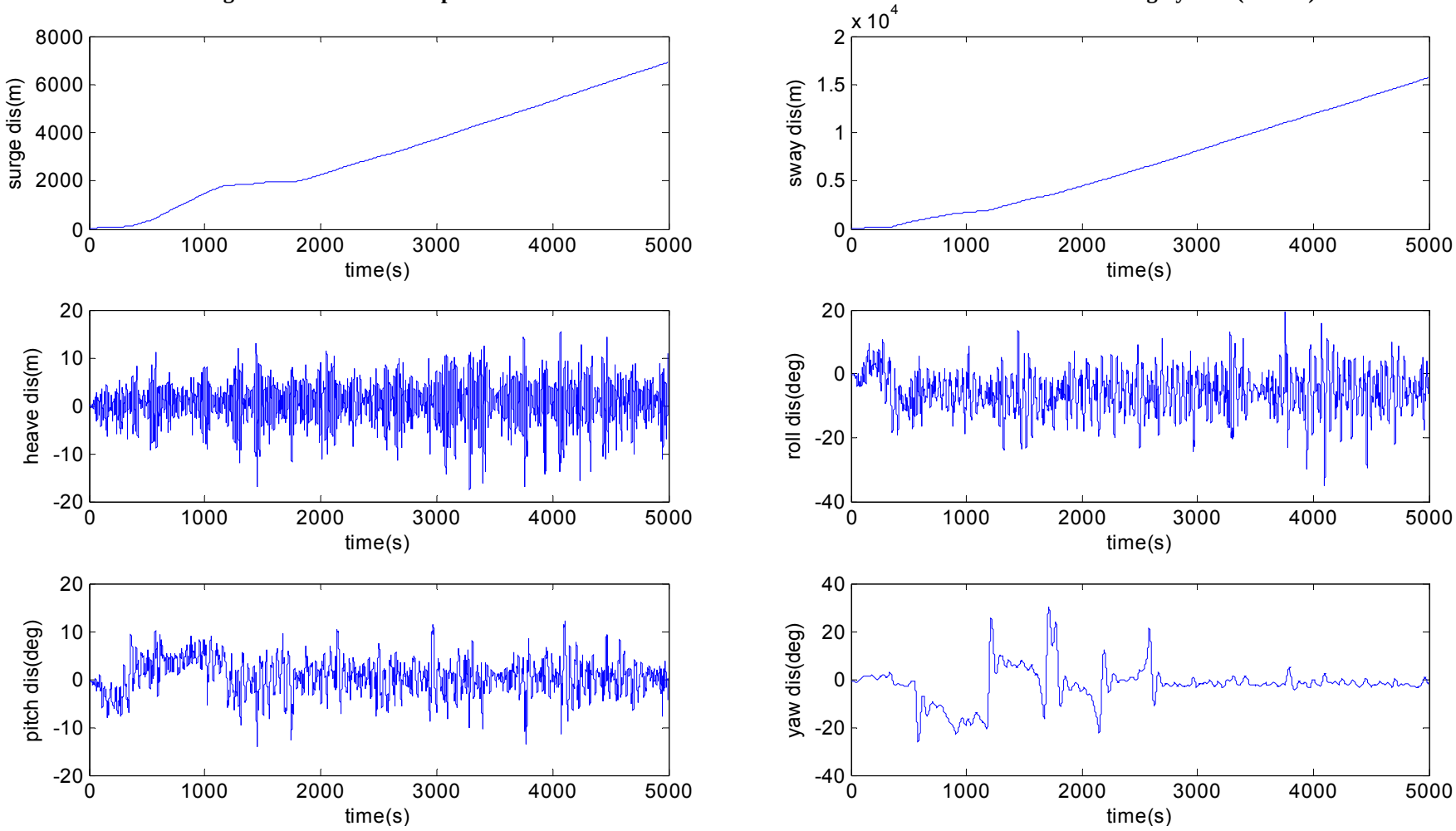

Figure B5. Progressive Failure of MODU I Traditional System

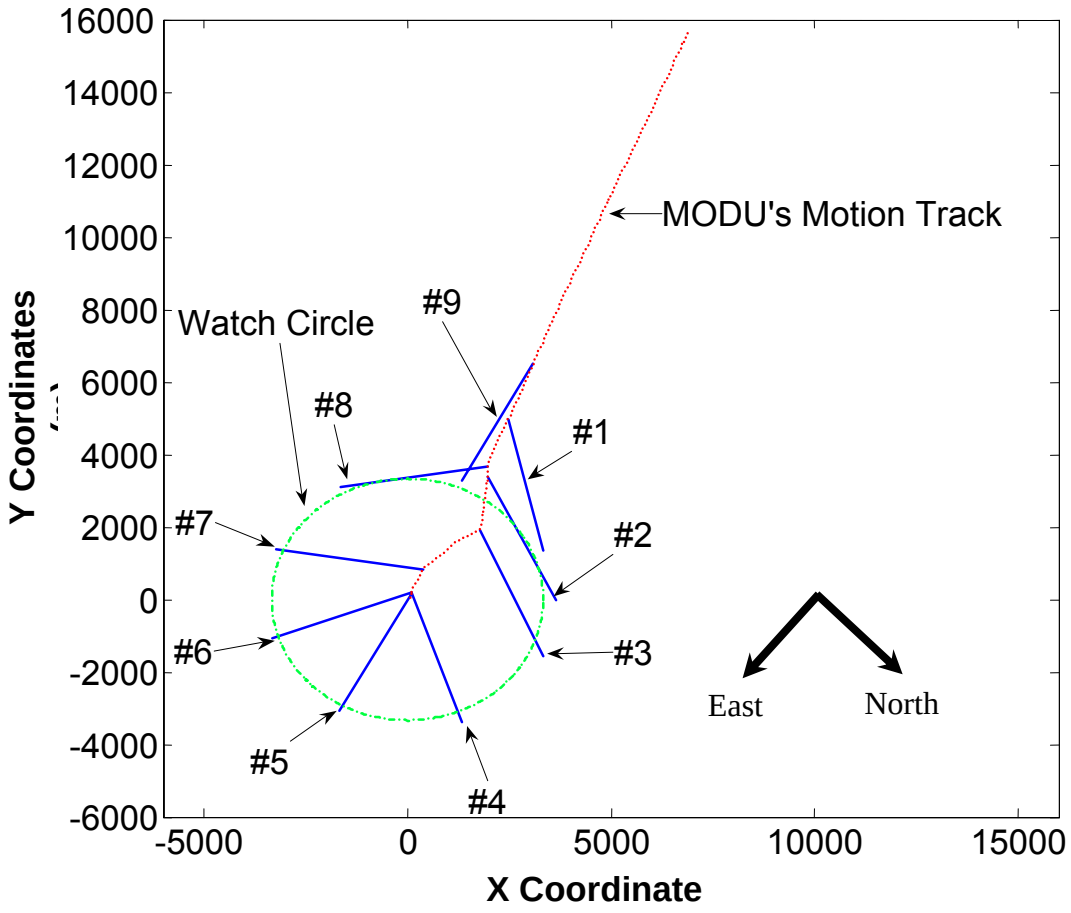

Table B6. Line Break Sequence for MODU I with Traditional Mooring System

Line #	Break Time (sec)	Break Node	Break Top Tension (N)	Sharples Prediction
5	276.6	36 (top)	0.5003447E+07	5
4	337.1	40 (top)	0.5003940E+07	4
6	338.7	36 (top)	0.5004967E+07	6
7	552.6	36 (top)	0.5004856E+07	7
3	1177.1	36 (top)	0.5003209E+07	8
2	1673.8	36 (top)	0.5006252E+07	3
8	1772.2	36 (top)	0.5004340E+07	2
1	2143.2	36 (top)	0.5010014E+07	9
9	2572.9	36 (top)	0.5006260E+07	1

Figure B6. Platform Displacement and Rotation Time Series for MODU I with Polyester Mooring System (Survived)

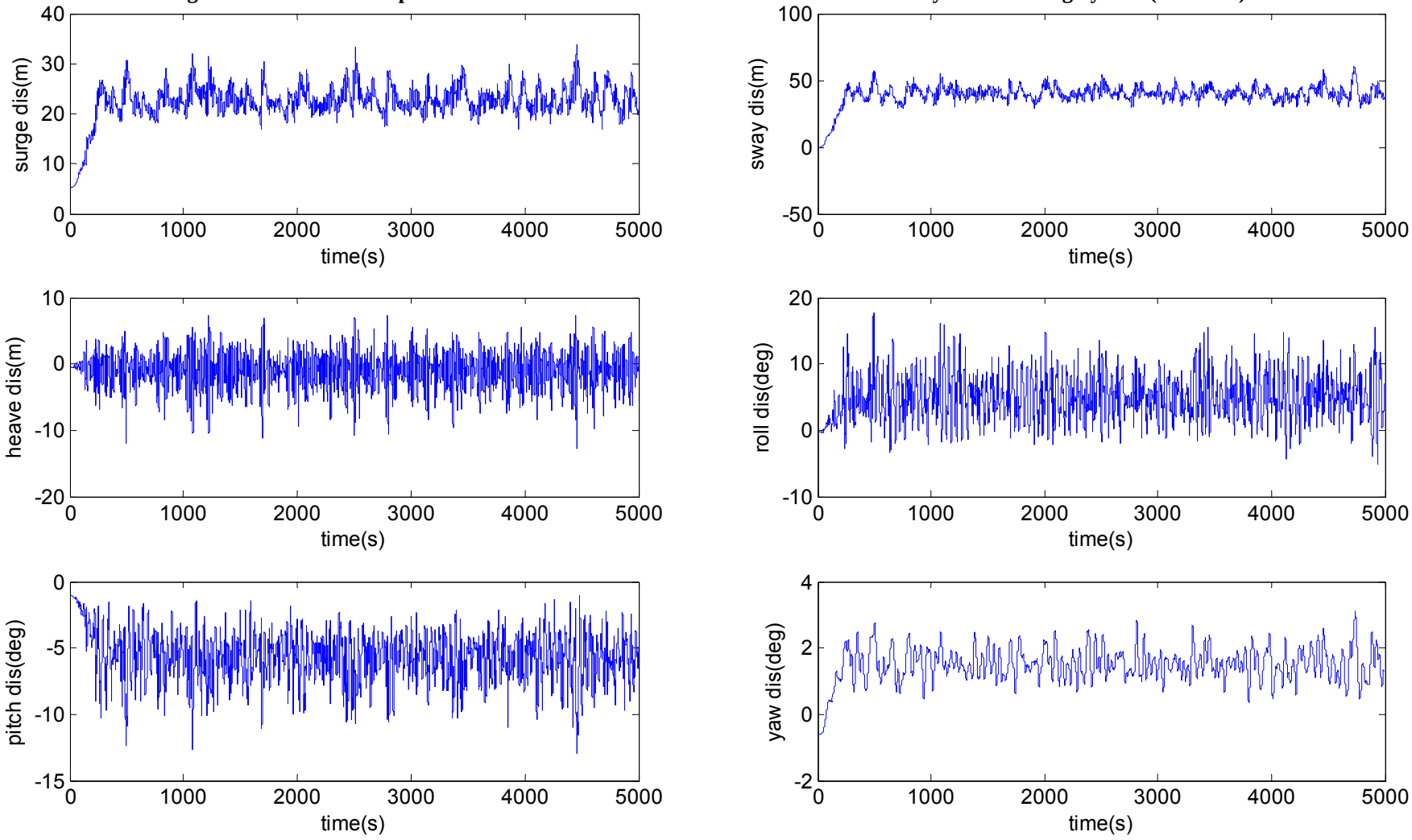

Figure B7. Line Top Tension Time Series of the Original System (Fail)

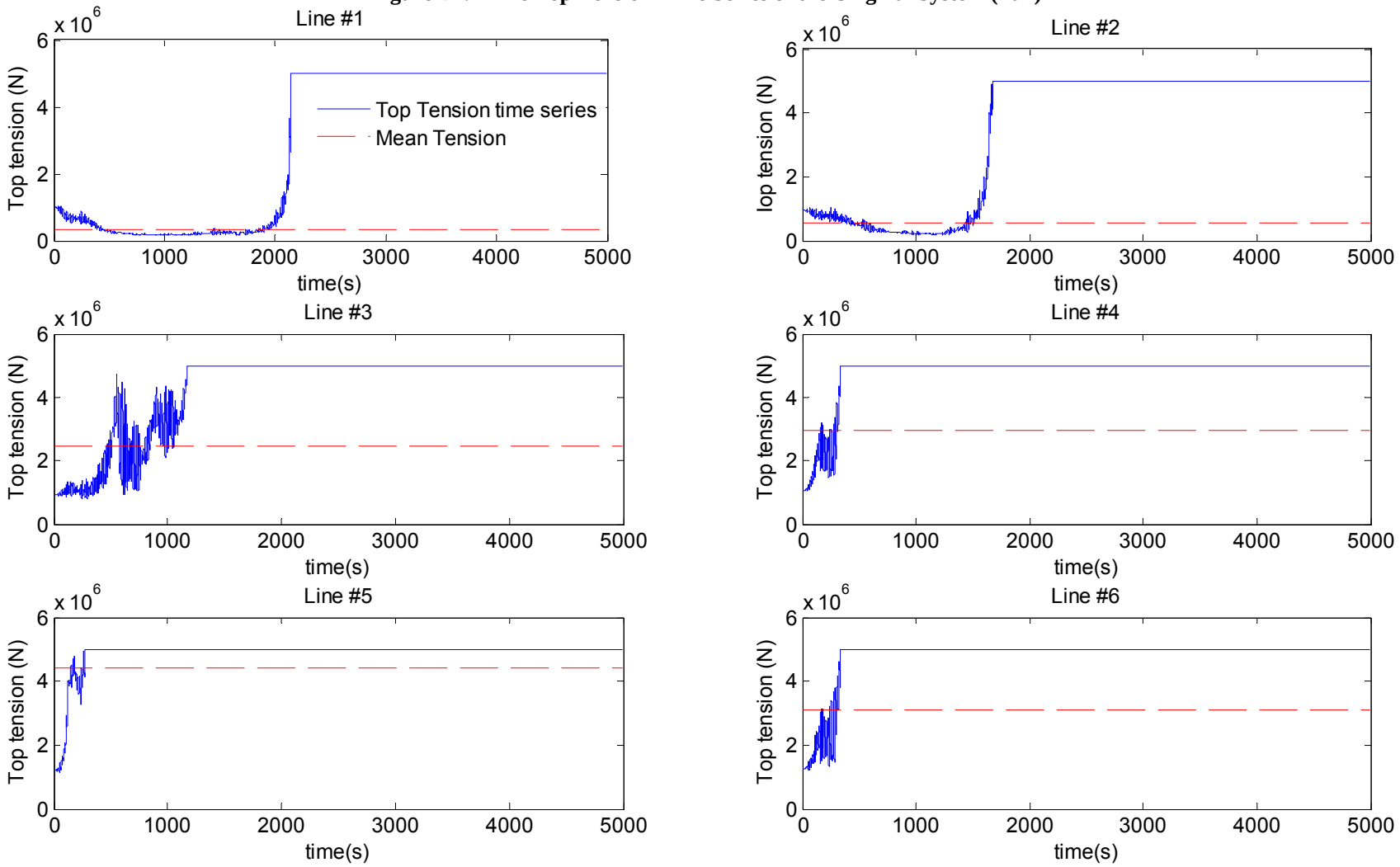

Figure B7. Line Top Tension Time Series of the Original System (Fail) cont'

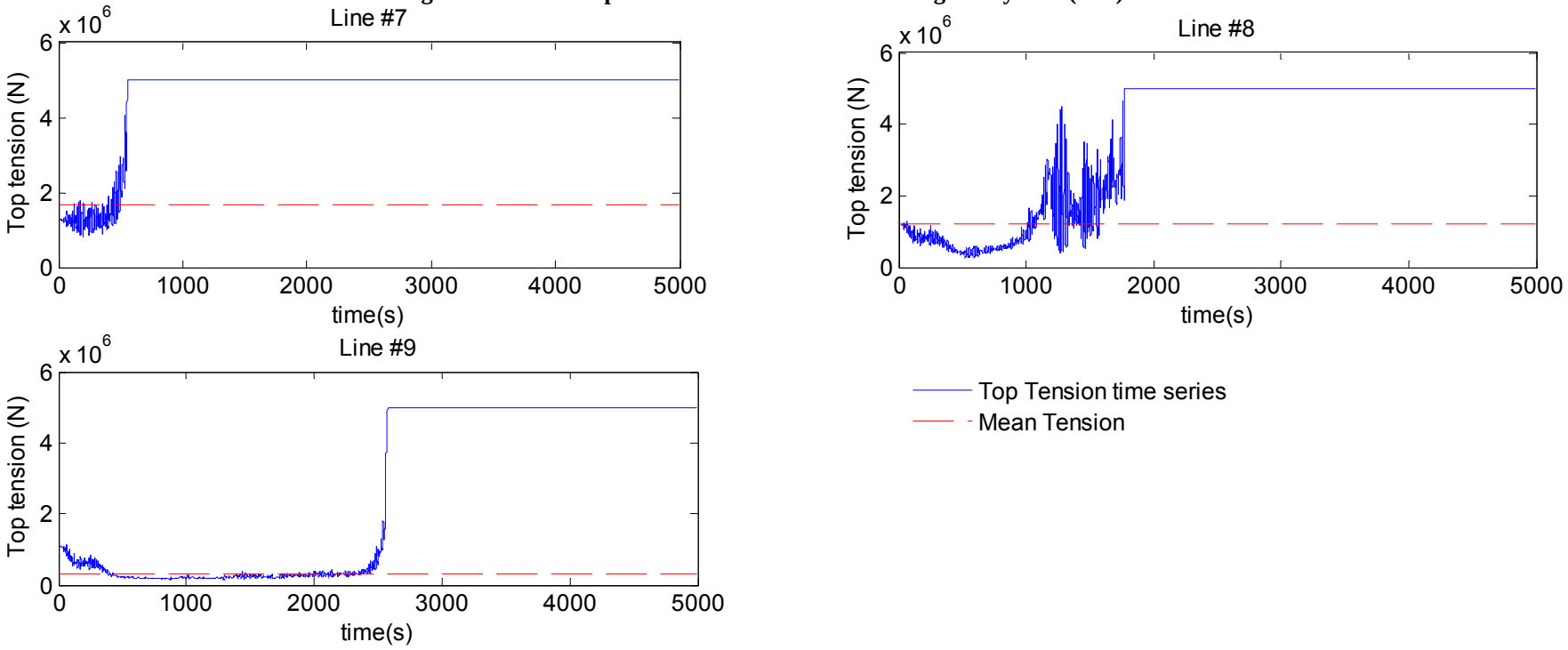

Figure B8. Line Top Tension Time Series of the Polyester System

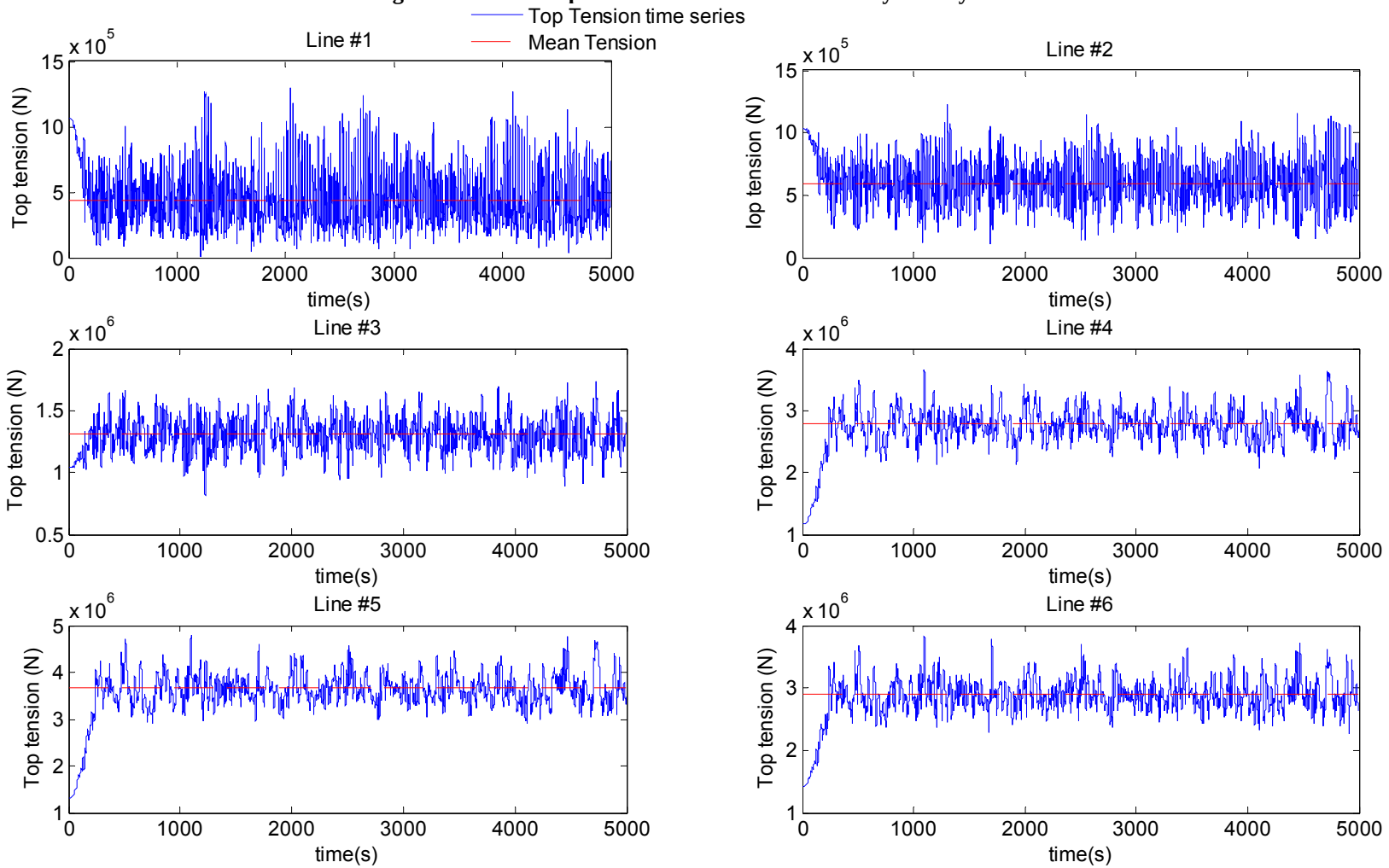

Figure B8. Line Top Tension Time Series of the Polyester System (cont')

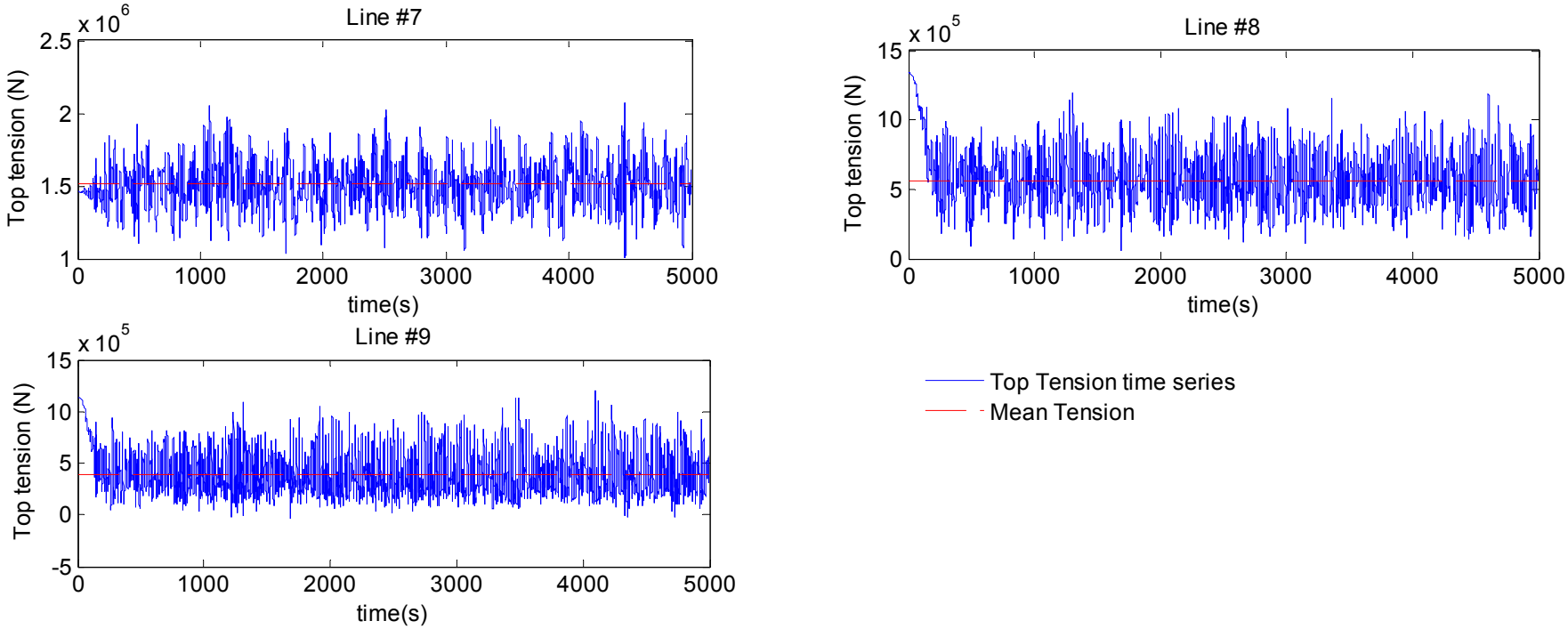

Figure B9. Comparison of Top Tension Spectra for the Traditional and Polyester Mooring Systems

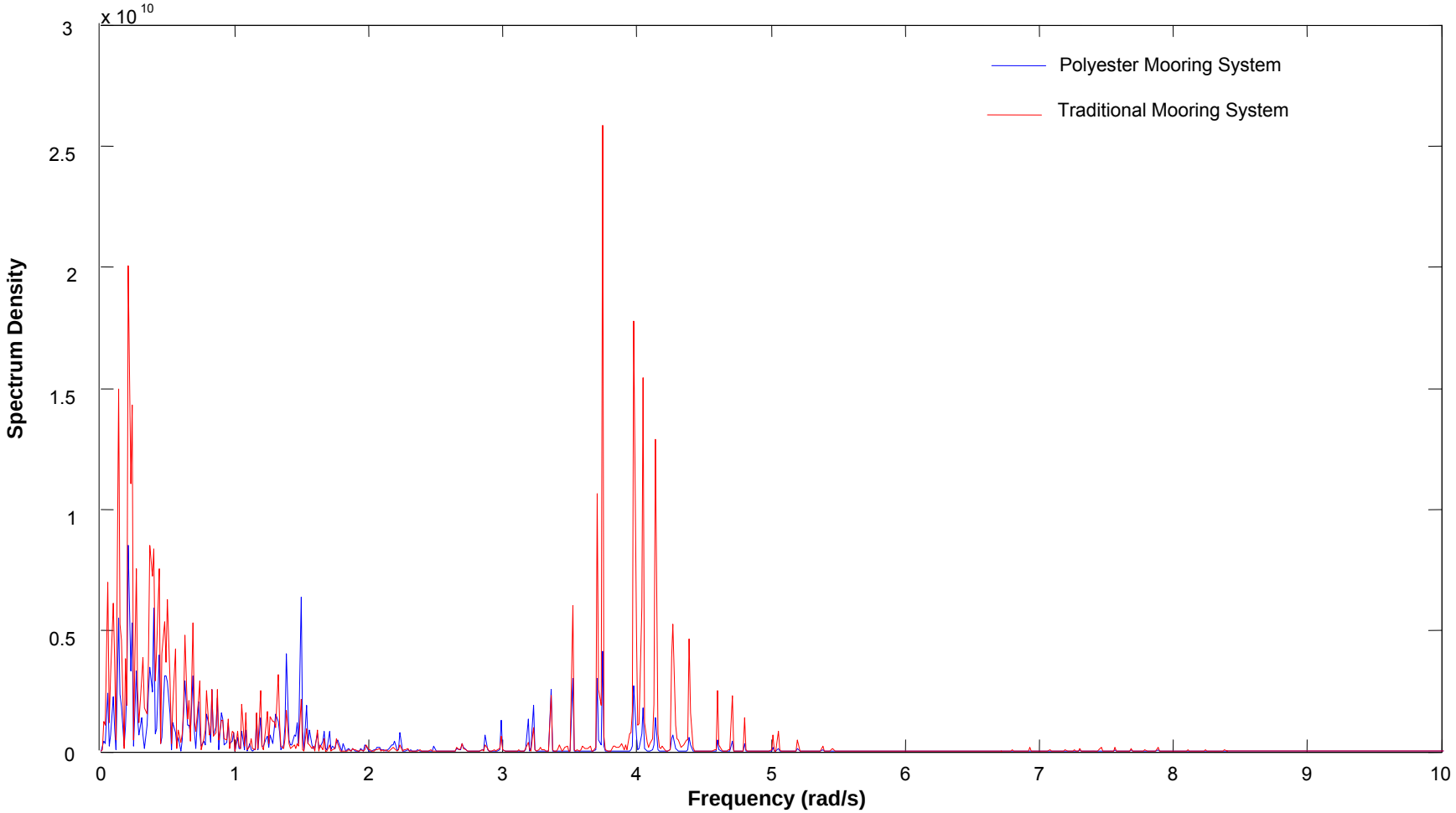

Table B7. Comparison of the Statistics of the Forces on MODU I for the Two Mooring Systems

Units (meter, deg, N)		Traditional						Polyester					
		Surge	Sway	Heave	Roll	Pitch	Yaw	Surge	Sway	Heave	Roll	Pitch	Yaw
Displacement	Mean	54.3559	130.3436	-0.4614	3.4016	-2.6079	-1.8633	14.9499	29.6636	-0.9259	6.2996	-5.1974	-2.1879
	Std. Dev.	3.5796	6.3176	2.6177	3.2547	1.8497	0.4156	2.4811	4.3382	2.7410	3.1831	1.6429	0.4847
	Max	70.1991	157.674	-13.3813	15.3123	-9.9223	-3.7508	25.3356	46.9472	-12.7893	19.2579	-13.2094	-3.7123
Diffraction Force	Mean	1.8536e+5	3.0277e+5	-7.0310e+5	-1.1766e+7	1.6220e+6	1.4281e+6	1.9466e+5	3.1954e+5	-8.0595e+5	-1.0593e+7	5.8358e+5	1.4246e+6
	Std. Dev.	1.1025e+7	1.9272e+7	4.1158e+7	5.6617e+8	3.4308e+8	2.9916e+7	1.1059e+7	1.9335e+7	4.1135e+7	5.6288e+8	3.4091e+8	2.9781e+7
	Max	-4.664e+7	-8.061e+7	1.384e+8	1.943e+9	1.124e+9	-1.175e+8	3.875e+7	6.733e+7	1.392e+8	1.909e+9	-1.117e+9	-1.058e+8
Viscous Force	Mean	2.0807e+6	2.2054e+6	-9.7140e+4	2.8097e+7	-2.4322e+7	-7.4940e+6	2.0720e+6	2.1772e+6	-2.5454e+5	2.9821e+7	-2.3757e+7	-9.3998e+6
	Std. Dev.	3.7871e+5	5.9529e+5	6.1830e+5	1.7310e+7	1.4204e+7	6.8576e+6	4.4093e+5	6.4636e+5	8.2568e+5	2.0863e+7	1.6198e+7	8.3714e+6
	Max	4378000	5683000	4842000	-135500000	-114300000	-57210000	5166000	7456000	-6360000	187800000	-104000000	-55650000
Wind Force	Mean	4.2715e+4	2.4471e+6	0	-7.2504e+7	-1.2656e+6	0	4.2715e+4	2.4471e+6	0	-7.2504e+7	-1.2656e+6	0
	Std. Dev.	1.0127e+4	5.8018e+5	0	1.7189e+7	3.0004e+5	0	1.0127e+4	5.8018e+5	0	1.7189e+7	3.0004e+5	0
	Max	-81260	4656000	0	-137900000	-2408000	0	-81260	4656000	0	-137900000	-2408000	0
Total Force	Mean	2.2233e+6	4.9553e+6	-8.0024e+5	-5.6173e+7	-2.3966e+7	-6.3658e+6	2.2240e+6	4.9439e+6	-1.0605e+6	-5.3276e+7	-2.4439e+7	-7.9752e+6
	Std. Dev.	1.0938e+7	1.9143e+7	4.0959e+7	5.7683e+8	3.5281e+8	3.0329e+7	1.0921e+7	1.9129e+7	4.0831e+7	5.7561e+8	3.5205e+8	3.1186e+7
	Max	-4.5349e+7	-7.6282e+7	1.3727e+8	-1.9388e+9	-1.2258e+9	-1.2444e+8	4.0444e+7	7.1419e+7	1.3687e+8	-1.9314e+9	-1.1666e+9	-1.0966e+8

MODU II

The same analysis approach as described above for MODU I was also used to analyze MODU II. MODU II was modeled as a rectangular hull, as shown in Figure B10, with an 8 line omni-spread taut wire rope-polyester rope-wire rope mooring system in 9000 ft of water. The hydrodynamic model had 3156 panels and 38 viscous plates

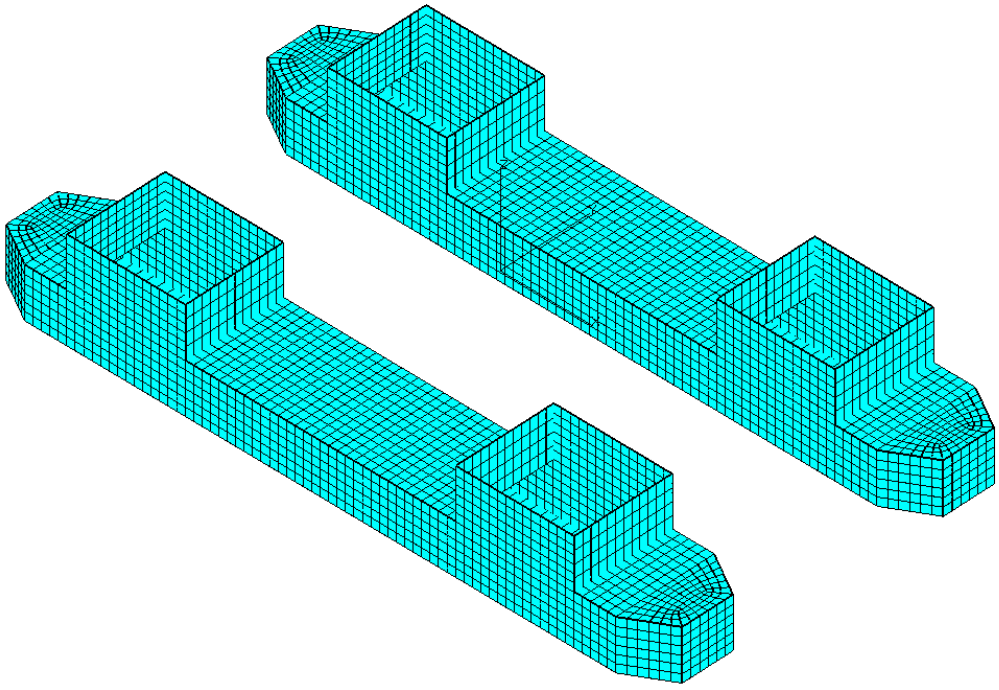

Figure B10. MODU II Hull Model

Mooring System for MODU II

The mooring system for MODU II was modeled as indicated in Table B8 and Figures B11 and B12.

Table B8. Mooring system Components for MODU II

3 5/8'' Rig Wire (2500ft)	EA:	438000 KN	Cm:	2
	Dry Weight:	35.7 kg/m	CD::	1
	Wet Weight:	31 kg/m	Break Strength:	6582 KN
7" Polyester Line (7500ft)	EA:	211900 KN	Cm:	2
	Dry Weight:	20.2 kg/m	CD::	1
	Wet Weight:	5.1 kg/m	Break Strength:	7848 KN
3 3/4" Wire Rope (3500ft)	EA:	470000 KN	Cm:	2
	Dry Weight:	38.3 kg/m	CD::	1
	Wet Weight:	33.3 kg/m	Break Strength:	7063 KN

The mean water depth is 2743m (8997ft). Anchor depth actually increases from southwest to northwest. Each line is divided into 19 high-order elements. The ramping period was 250s.

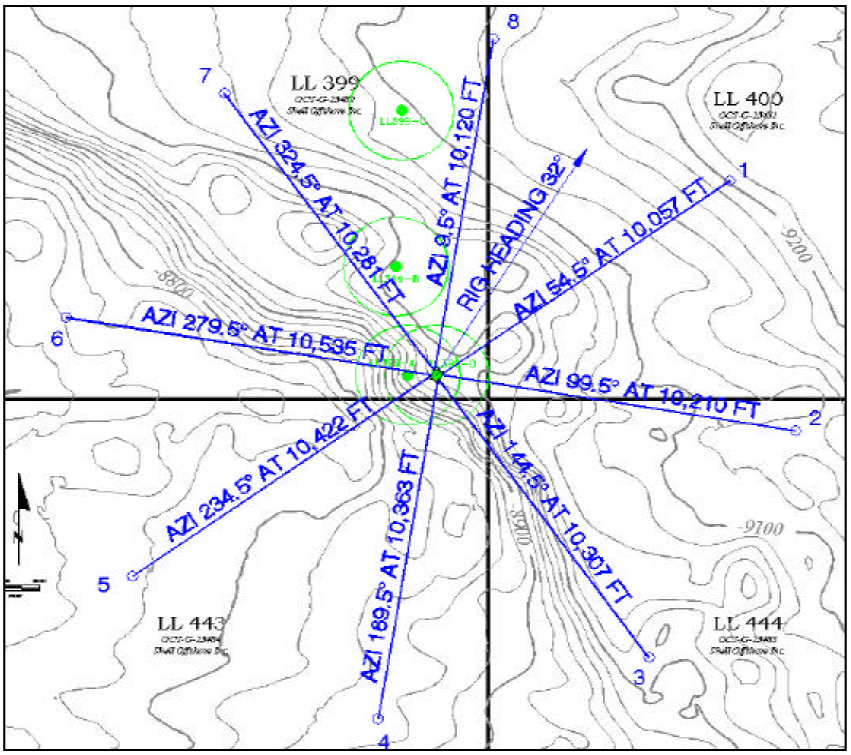

Figure B11. Mooring Layout for MODU II

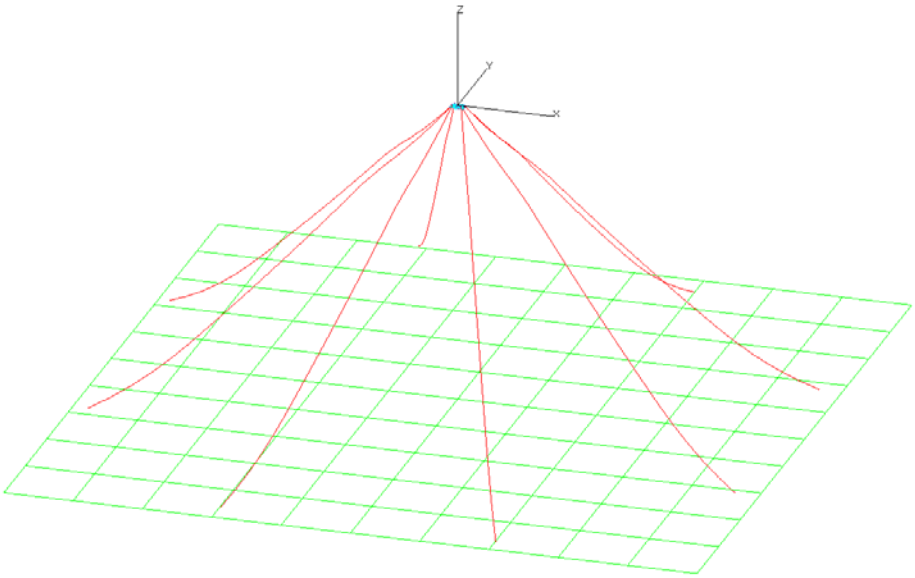

Figure B12. 3-D View of Mooring System for MODU II

Environmental Loading

Ivan passed just to the west of the location. No information is available on when during the storm that the mooring system failed. Forensic studies of the pattern of the mooring line remnants suggested that the MODU drifted north during the progressive failure of the mooring system (Delmar 2005b).

A previous analysis (Loeb 2005) reported that the mooring system failed due to environmental forces caused by wind, wave, and current conditions that exceeded a 65-year return period per API standards. The wind, wave, and current values are shown in Table B9.

Table B9. API 65 RP Parameters

	Parameter	Loeb 2005	Hindcast
Wave	Sig. Wave Height	37.1 ft	39.1 ft
	Peak Period	13.9 sec	13.8 sec
Wind	30 min speed at 10 m	84 mph	83 mph
Current	Surface	2.8 kt	3.7 kt

This was based on an analysis that examined many combinations of plausible wind, wave, and current combinations that could have caused the initial mooring line failure (Delmar 2005b). The wind, wave, and current forces were assumed to be collinear. The values of environmental parameters will be referred to as "API 65 RP".

The Ivan hindcast database (Oceanweather 2004) was reviewed to find a wind, wave, and current environment that most closely matched these conditions so as to determine viable directions for that environment. The value for the surface current was determined from API 2MET INT by matching the wind and wave values. The directions of the wave and currents relative to the wind were + 5 degrees and + 30 degrees to the right of the wind. These values are also shown in Table B9 as "Hindcast" and were used to represent API 65 RP in the analyses reported below and listed in Table B10.

Based on the Ivan hindcast (Oceanweather 2004), maximum wave conditions occurred at the location while Ivan was still a bit south of the location and the wind, wave, and currents were generally to the northwest. A few hours later, the maximum wind speed occurred and the wind and waves had shifted and were northerly. Since the magnitudes of the wind speeds and wave heights at these times differed by less than 10 percent at these two times, we will simply use one set of parameters to describe this condition and refer to it as "Ivan Max".

Since the hull form of MODU II suggested that there could be considerable directional sensitivity in the loads and responses, several environments were studied. We considered both collinear and non-collinear cases. The non-collinear directions were based on observations from hindcasts. Parameters for these cases are shown in Table B10, and the directional characteristics are shown in Figure B13.

Table B10. Environmental Parameters & Directions Used to Analyze MODU II

		Parameter	Value	Direction toward (0 deg N)	Case	Mooring System Result
API 65 RP North Collinear	**Wave**	Sig. Wave Height	39.1 ft	0	**A**	**Failed**
		Peak Period	13.8 sec	na		
	Wind	30 min peed at 10 m	83 mph	0		
	Current	Surface	3.7 kt	0		
API 65 RP North Non-collinear	**Wave**	Sig. Wave Height	39.1 ft	15	**B**	**Failed**
		Peak Period	13.8 sec	na		
	Wind	Speed at 10 m	83 mph	0		
	Current	Surface	3.7 kt	30		
API 65 RP Northwest Collinear	**Wave**	Sig. Wave Height	39.1 ft	295	**C**	**Survived**
		Peak Period	13.8 sec	na		
	Wind	Speed at 10 m	83 mph	295		
	Current	Surface	3.7 kt	295		
API 65 RP Northwest Non-collinear	**Wave**	Sig. Wave Height	39.1 ft	310	**D**	**Survived**
		Peak Period	13.8 sec	na		
	Wind	Speed at 10 m	83 mph	295		
	Current	Surface	3.7 kt	325		
Ivan Max Non-Collinear Northwest	**Wave**	Sig. Wave Height	51.5	281	**E**	**Failed**
		Peak Period	15.5	na		
	Wind	Speed at 10 m	98 mph	263		
	Current	Surface	3.5 kt	296		

Figure B13. Directional Environments for Cases in Table B10

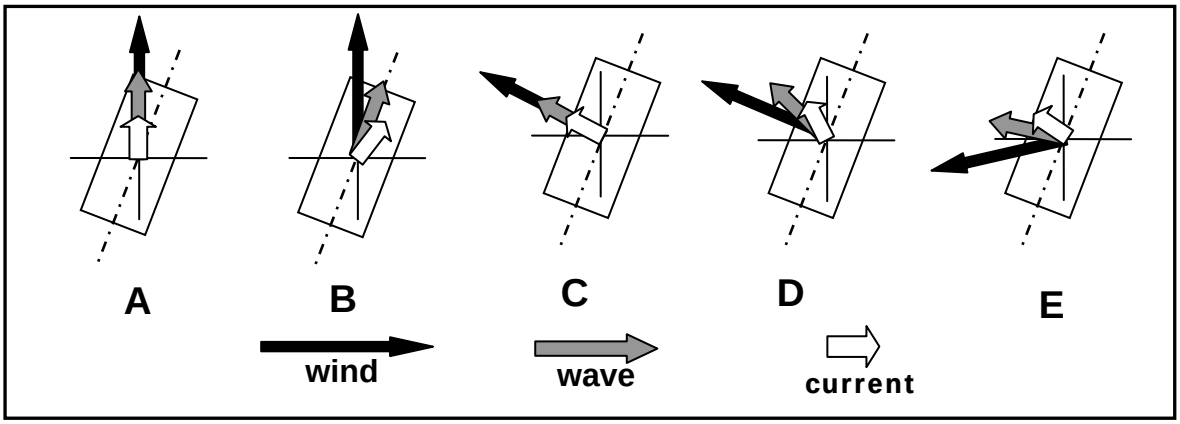

Simulation Results and Discussion for MODU II

For each of the five cases, Table 10 indicated whether the simulation indicated that the mooring system survived or failed. Simulation time series results for Cases A-D are shown in Figures B14 - B17 at the end of this section. Simulation results are not presented for Case E.

The mooring system failure in Case A API 65 RP Collinear agrees with the previous analysis (Loeb 2005, Delmar 2005b). The mooring line failure pattern found here was also similar to the results found in that analysis and the pattern found in the forensic study of the mooring failure. The results for Case B API 65 RP Non-Collinear also indicated that the mooring system would have failed in the same environment had been collinear.

Cases C and D investigated the response of the mooring system to the collinear and non-collinear versions of the same API 65 RP environment approaching MOSU II from a more broadside direction. Results indicate that the mooring system would not have failed. Further investigation indicated this survival resulted from lower wind forces on MODU II when the wind was from this more broadside direction.

Case E investigated the response of the mooring system to the Ivan Max Non-Collinear environments, and indicated that the mooring system would certainly have failed in this more severe environment.

Summary

These results show that the mathematical models used in this study can satisfactorily predict the progressive failure of a MODU mooring system and are adequate to assess mitigation options to prevent a total drift off.

Additionally, the comparison of the failure of the chain-wire system and the wire-polyester-wire system on MODU I illustrated the robustness of mooring system that include polyester inserts. And the analysis of MODU II illustrated the directional sensitivity of responses or a rectangular MODU and its mooring system to storm environments.

Further study is planned on the following topics:

1. In all the case studies, the lines break at the top, where maximum tension occurs. However, according to the forensic data, many lines fail at the anchor mainly due to the breakage at the pad-eye of suction piles by out-of-plane loading. In principle, this can be realized by the present time-domain analysis program.
2. The simulation was done assuming that the direction of wind, wave, and current do not change during the period of progressive line failure. However, in principle, the time-domain analysis can be extended to include time-varying environment similar to the passage of real hurricane.
3. When the first line starts to fail, the rest of lines are to be broken unless some temporary remedy, such as auxiliary lines with torpedo anchor, is provided. This kind of scenario can be well realized with the present time-domain analysis program.
4. The axial stiffness of the polyester line is in general not constant but varies with tension magnitude, which can approximately be modeled by adopting tension-dependent values of EA in time domain simulation.

References

Delmar Systems, Inc. 2005a, Noble Jim Thompson Kepler MC 383 in Hurricane Ivan

Delmar Systems, Inc. 2005b, Deepwater Nautilus Cheyenne Well D LR 399 Mooring Performance during Hurricane Ivan

Delmar Systems, Inc. 2006, personal communication

Kim 1999, Hull/Mooring/Riser Coupled Dynamic Analysis of a Truss Spar in Time Domain, Kim, M. H., Ran, Z., & Zheng, W., Proc. ISOPE'99, Brest, France

Kim 2001, Variability of TLP Motion Analysis Against Various Design/Methodology Parameters, Kim, M. H., Tahar, A., & Kim, Y.B., 11th Proc. ISOPE'01, Stavanger, Norway

Halkyard 2004, Full Scale Data Comparison for the Horn Mountain Spar, Halkyard, J., Liagre, P., and Tahar, A., Proc. OMAE 2004 #51629, Vancouver, Canada
Sharples 2006b, Post Mortem Failure Assessment of MODUs during Hurricane Ivan, Report to MMS, MMS Project 548

Sharples 2006b, Post Mortem Failure Assessment of MODUs during Hurricane Ivan, Report to MMS, MMS Project 548

Sharples 2006c, MODU Performance during Hurricane Ivan, 2006 Offshore Technology Conference, Paper OTC 18322

Oceanweather 2004, Hindcast Study of Hurricane Ivan (2004), Offshore Northern Gulf of Mexico, FINAL REPORT, Oceanweather Inc, Report to the MMS, December 2004

Lee et al., 2000, Development of API RP 2SM for Synthetic Fiber Rope Moorings, Lee, M.Y. & Devlin, P. 2000, Proc. Offshore Technology Conference, OTC 12178, Houston, Texas.

Arcandra 2001, Hull-Mooring-Riser Coupled Dynamics with Polyester Lines, Texas A&M Univ. Ph.D. Thesis

Sharples 2006b, Post Mortem Failure Assessment of MODUs during Hurricane Ivan, Report to MMS, MMS Project 548

Loeb, David (2005) Presentation “Deepwater Nautilus Mooring Incident” made at Hurricane Readiness & Recovery Conference, see Ward et al 2005, Hurricane Readiness & Recovery Conference Report, Final Conference Summary Report prepared for the MMS by OTRC, MMS Project 559

Petruska, David (2005), Presentation “Mississippi Canyon 383 Rig mooring Failure” made at Hurricane Readiness & Recovery Conference, see Ward et al 2005, Hurricane Readiness & Recovery Conference Report, Final Conference Summary Report prepared for the MMS by OTRC, MMS Project 559

Figure B14. Case A: Collinear: Incident Angle = 0 deg. Mooring Failed

Displacement:

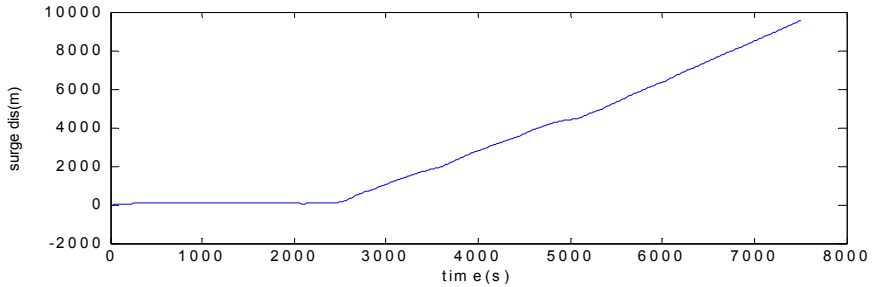

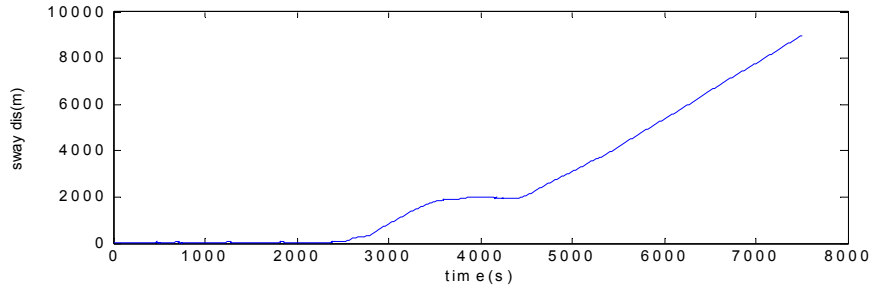

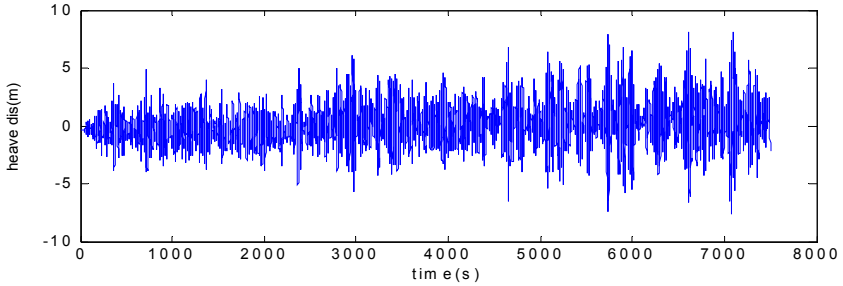

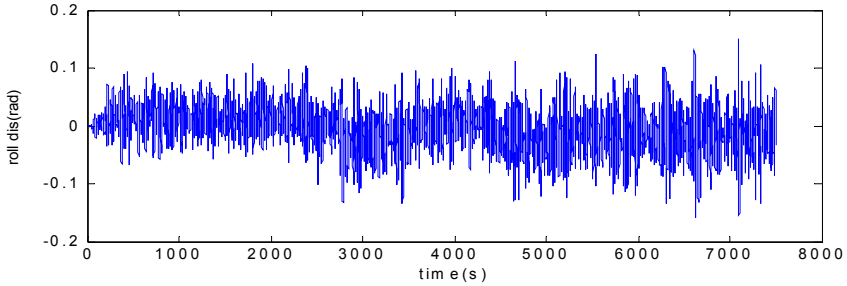

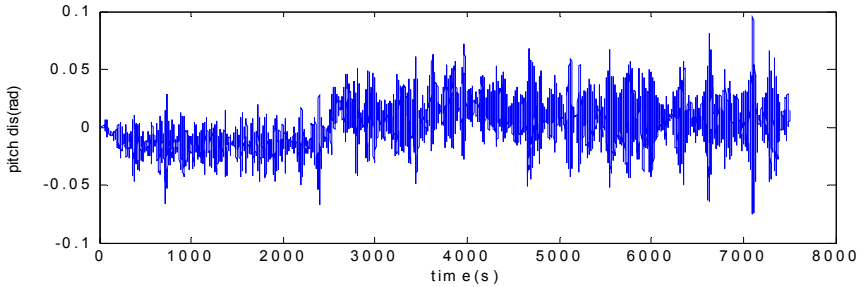

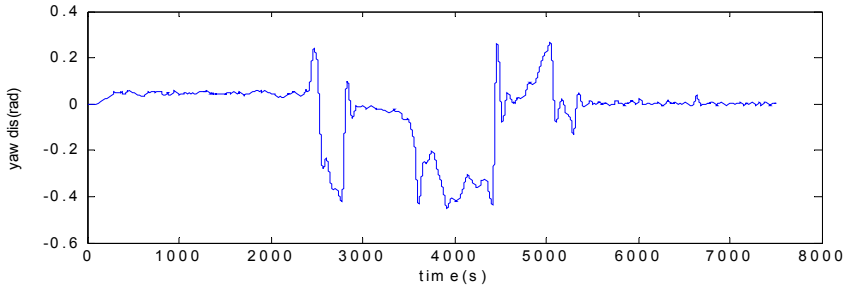

Diffraction Force:

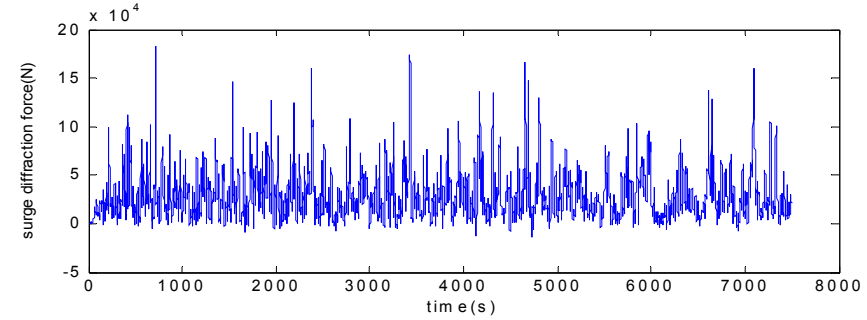

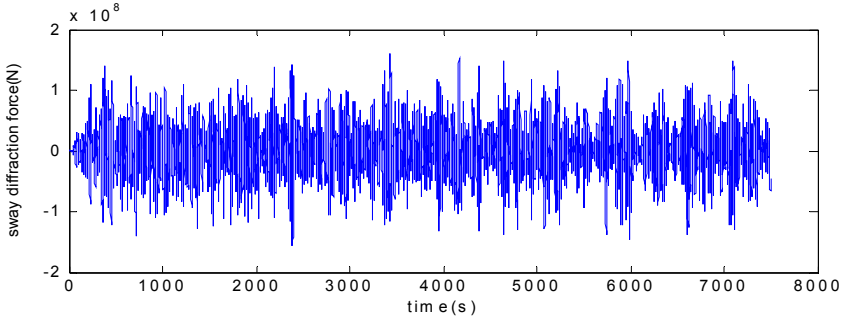

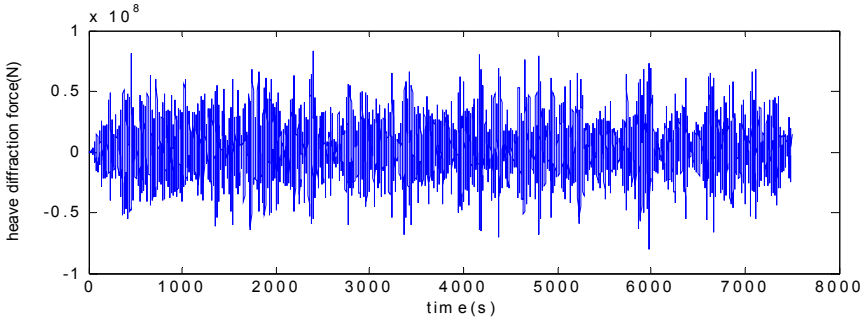

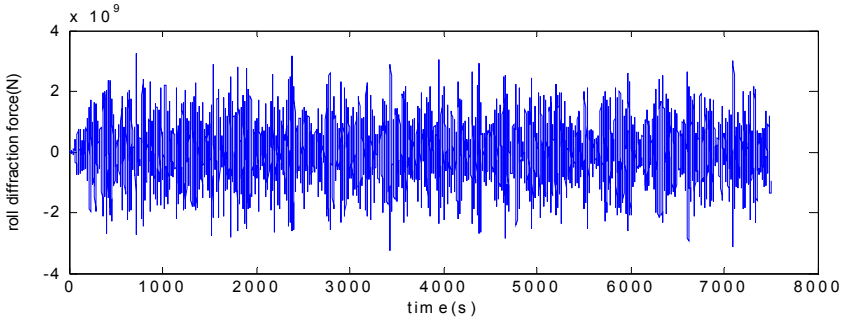

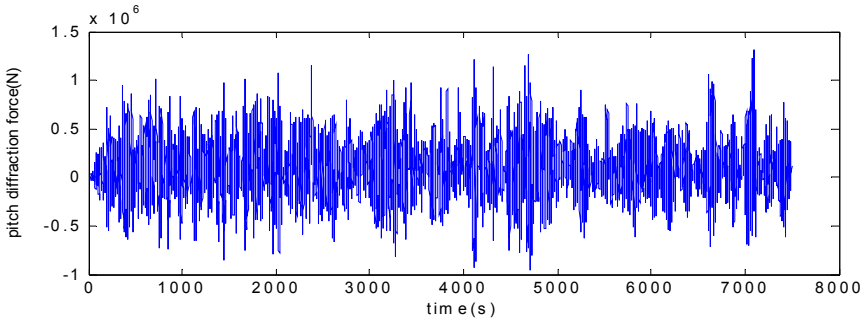

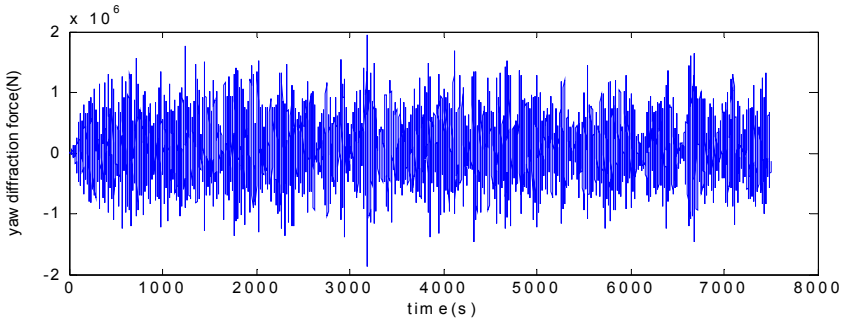

Viscous Force:

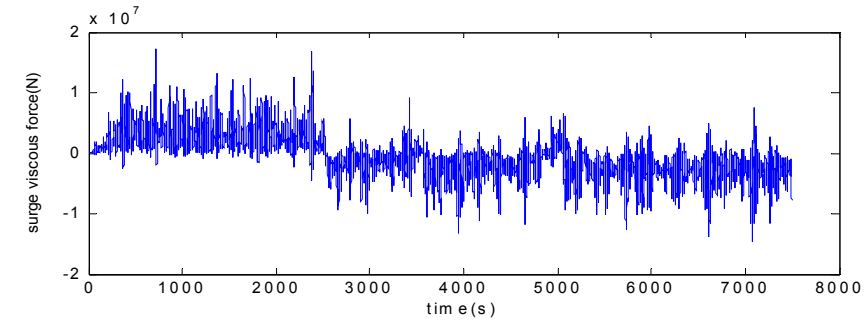

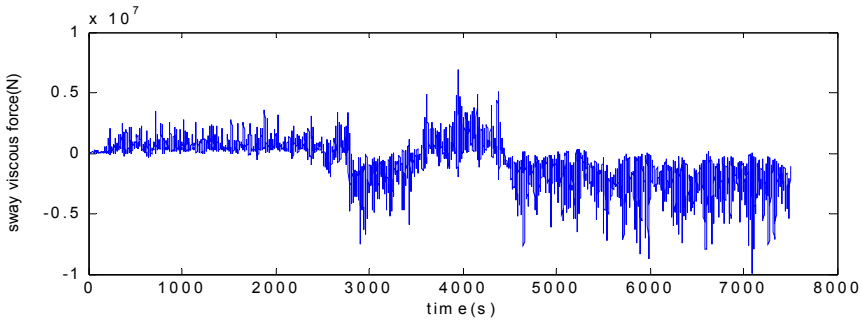

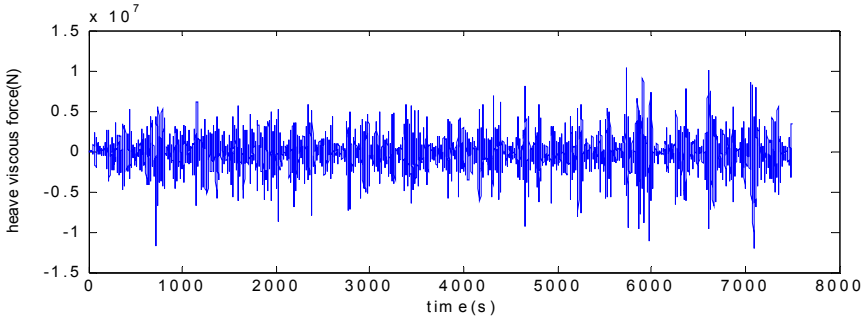

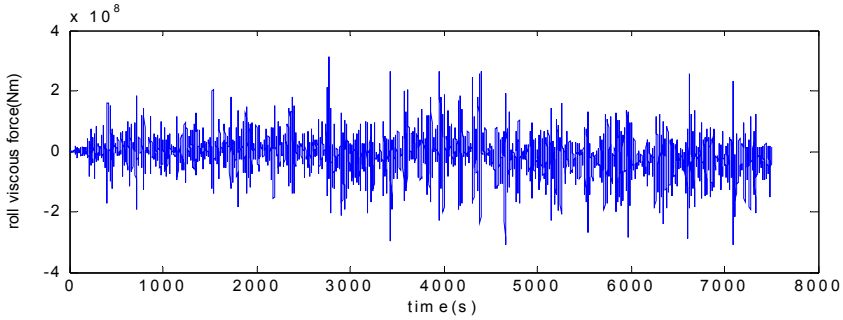

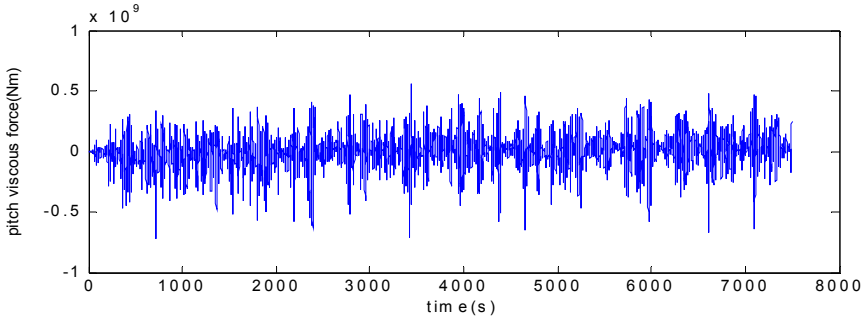

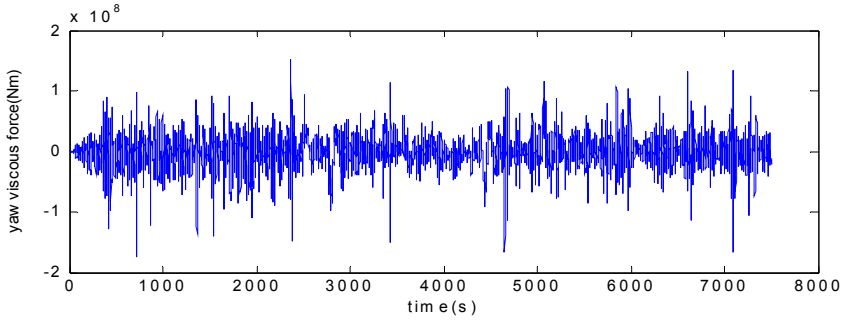

Wind Force:

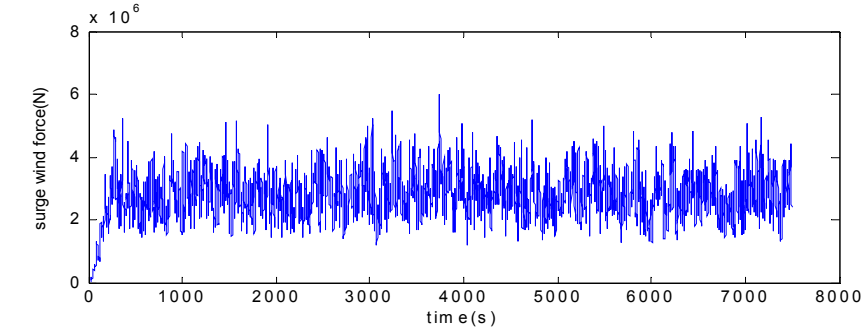
x 10^6
surge wind force(N)
time(s)

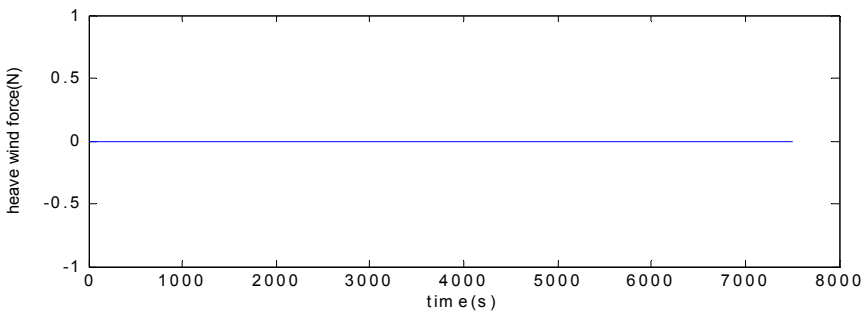
heave wind force(N)
time(s)

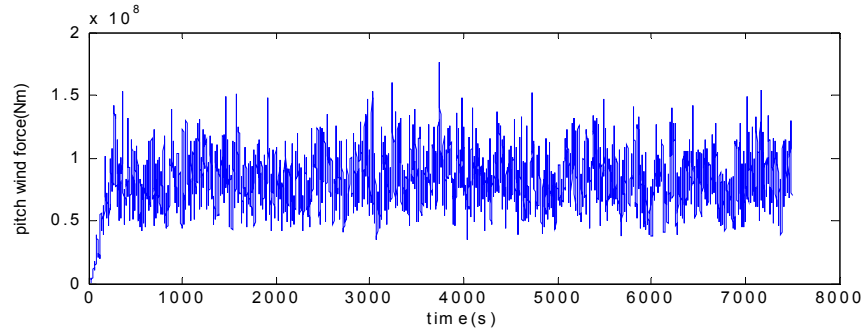
x 10^8
pitch wind force(Nm)
time(s)

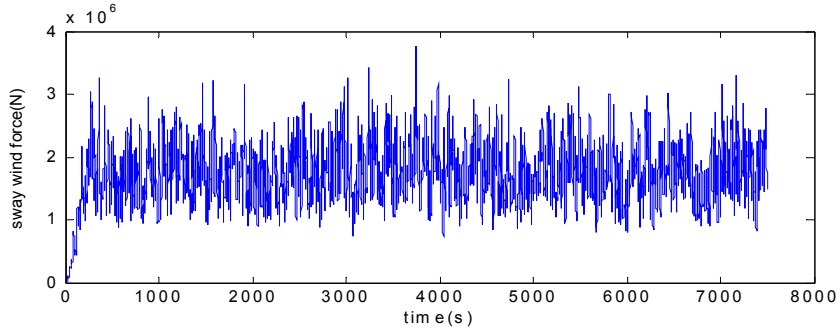
x 10^6
sway wind force(N)
time(s)

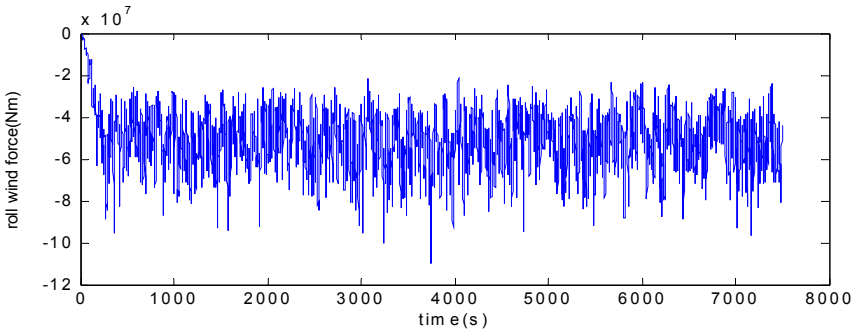
x 10^7
roll wind force(Nm)
time(s)

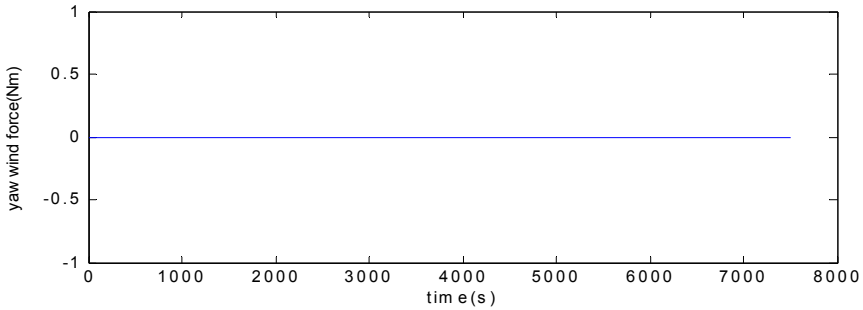
yaw wind force(Nm)
time(s)

Total Force:

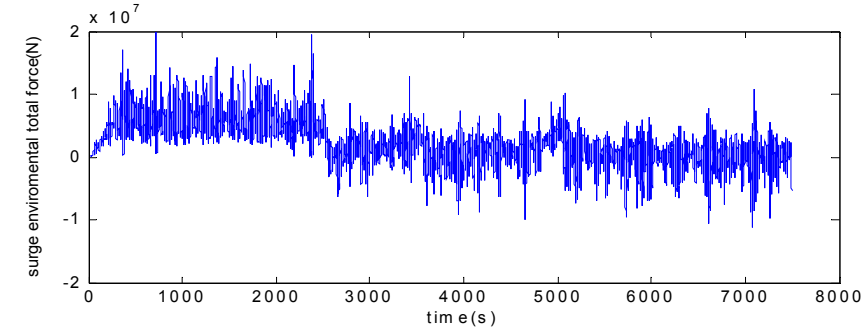
x 10^7
surge enviromental total force(N)
time(s)

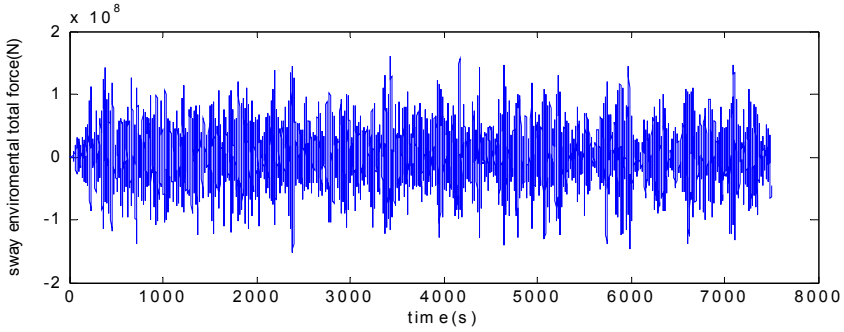
x 10^8
sway enviromental total force(N)
time(s)

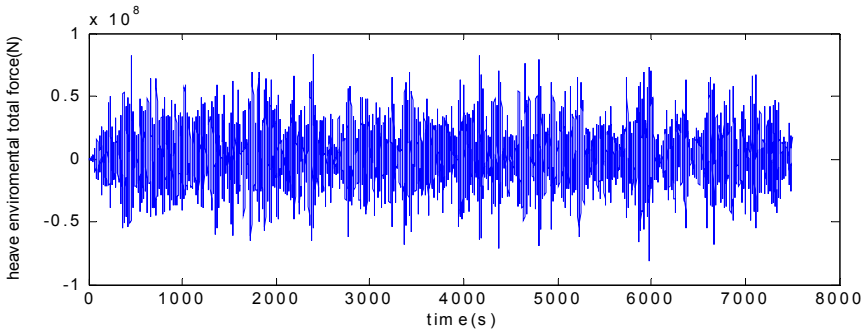
x 10^8
heave enviromental total force(N)
time(s)

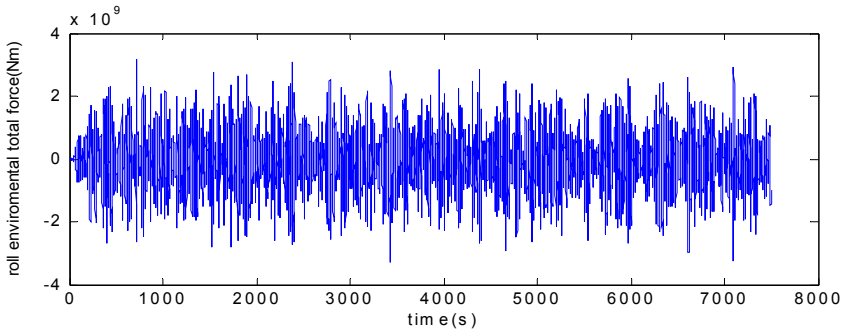
x 10^9
roll enviromental total force(Nm)
time(s)

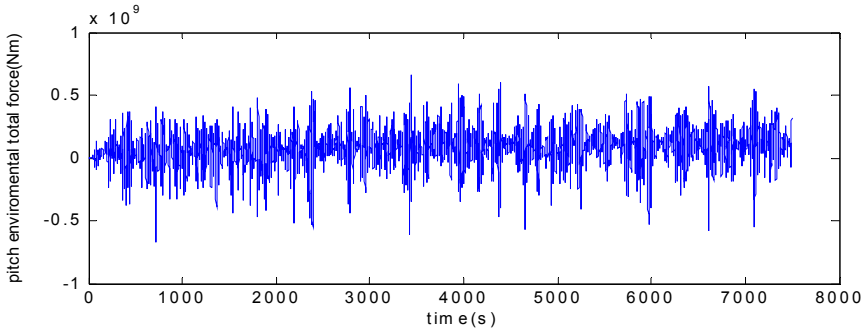
x 10^9
pitch enviromental total force(Nm)
time(s)

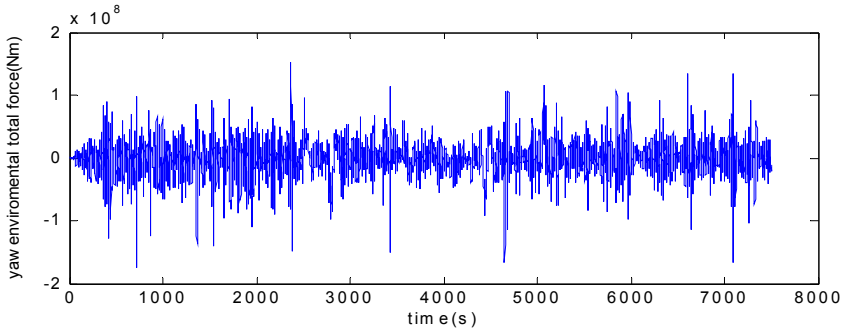
x 10^8
yaw enviromental total force(Nm)
time(s)

Top Tension:

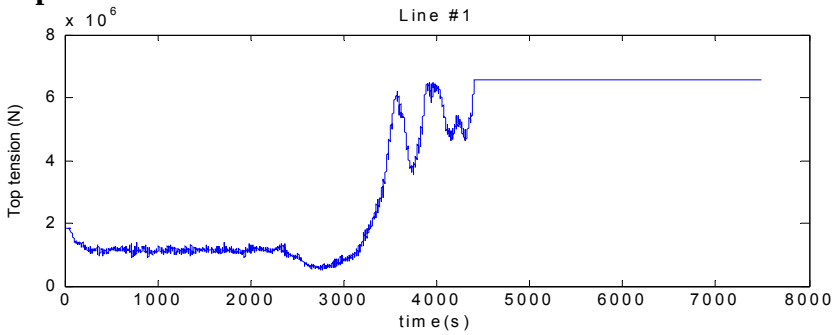
Line #1
x 10^6
Top tension (N)
time(s)

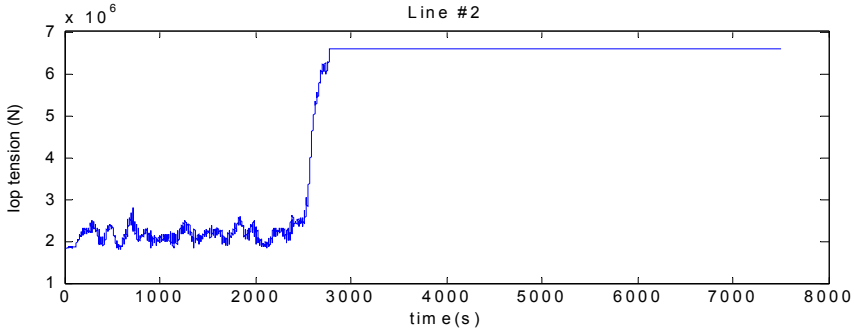
Line #2
x 10^6
lop tension (N)
time(s)

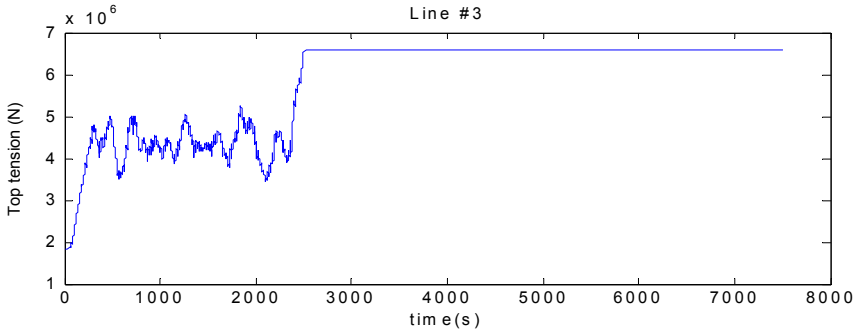
Line #3
x 10^6
Top tension (N)
time(s)

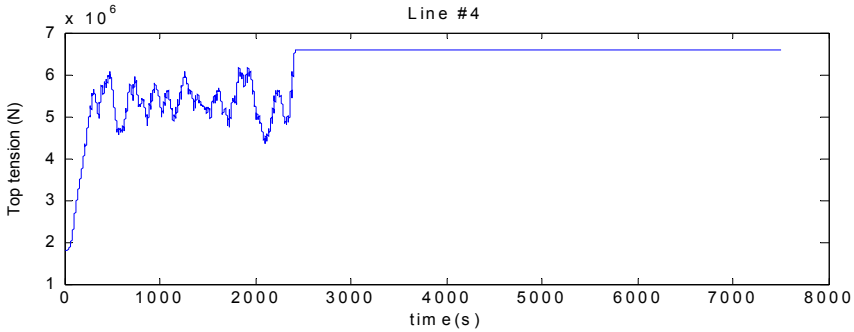
Line #4
x 10^6
Top tension (N)
time(s)

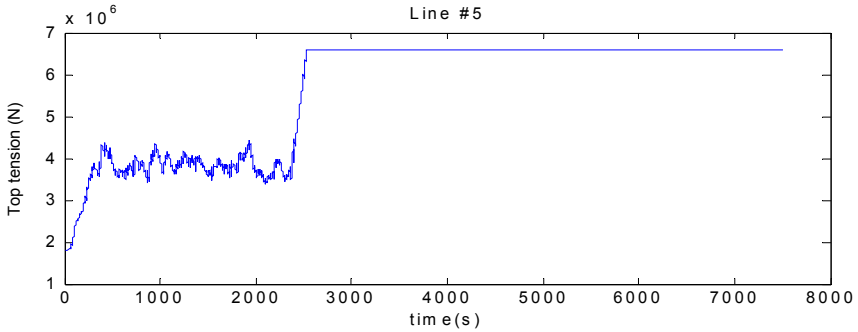
Line #5
x 10^6
Top tension (N)
time(s)

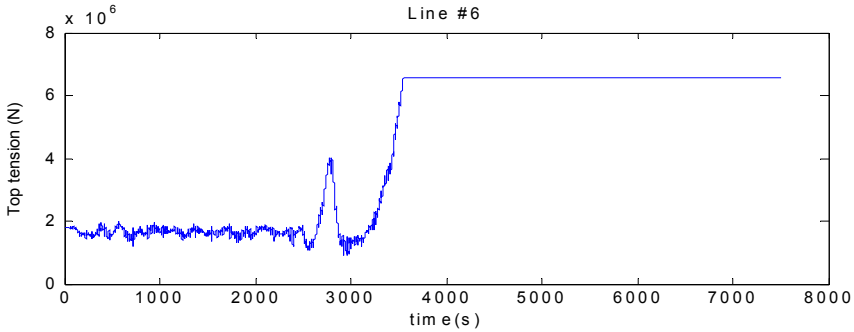
Line #6
x 10^6
Top tension (N)
time(s)

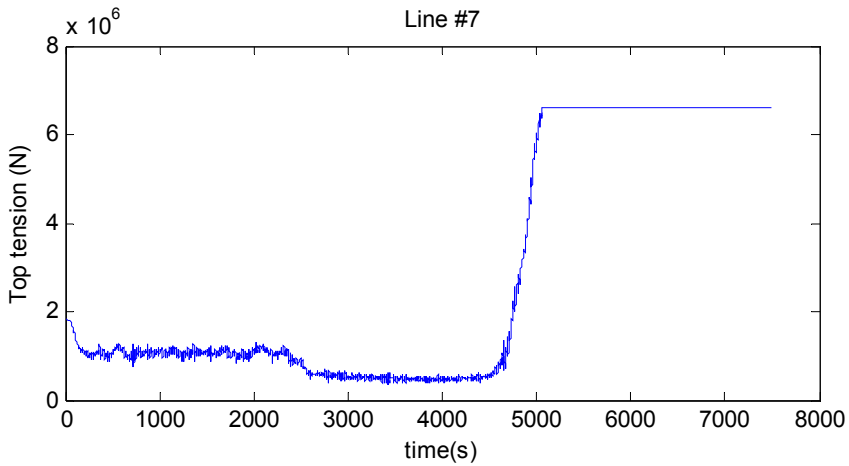

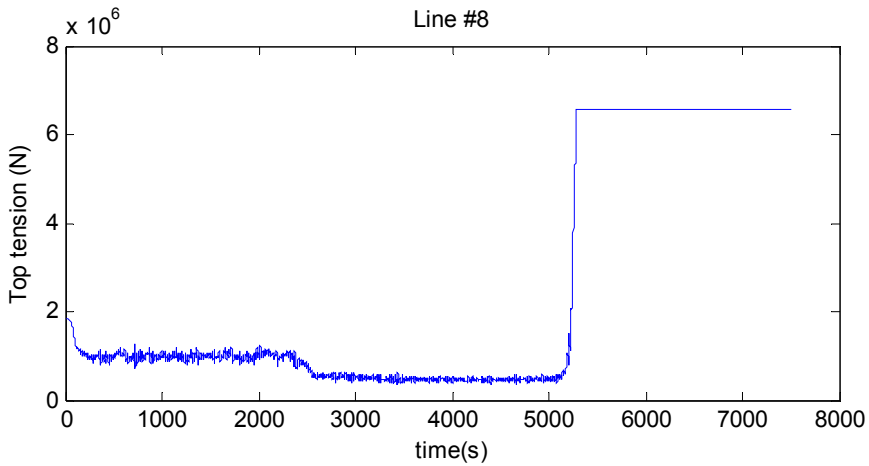

Case A Result: Mooring Failed

Line Break Sequence

#4	#3	#5	#2	#6	#1	#7	#8
2413.3 SEC	2499.9 SEC	2526.6 SEC	2775.2 SEC	3559.1 SEC	4411.9 SEC	5049.9 SEC	5288.0 SEC

Figure B15. Case B: Non-Collinear: Wind Incident Angle= 0 deg. Mooring Failed

Displacement:

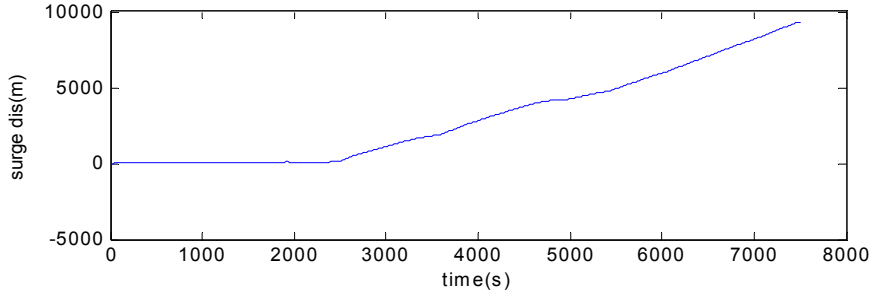

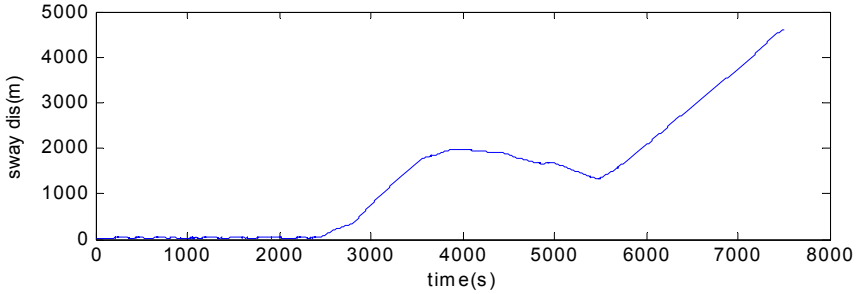

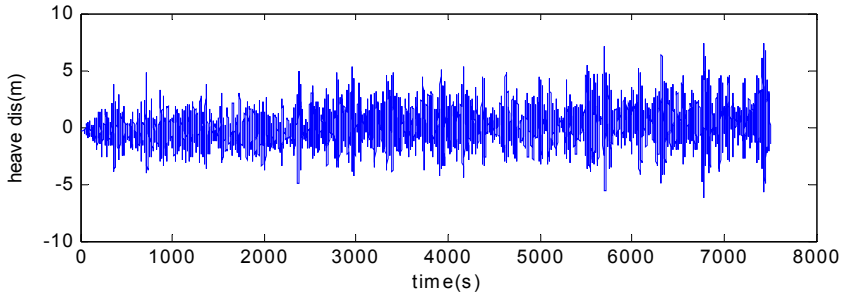

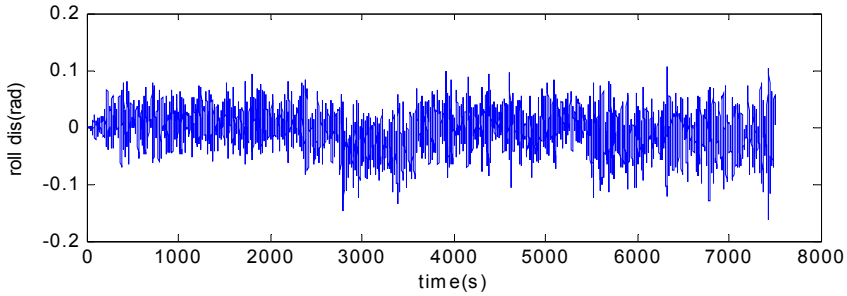

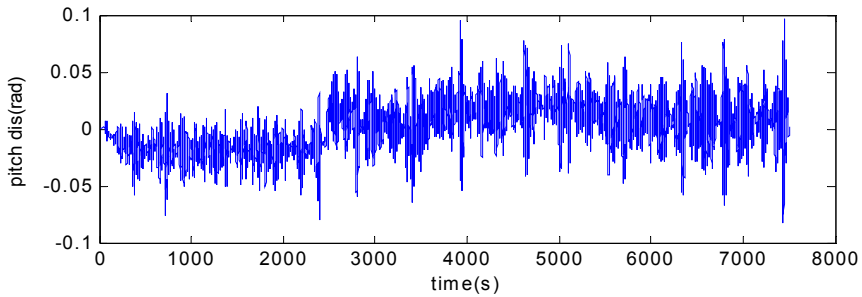

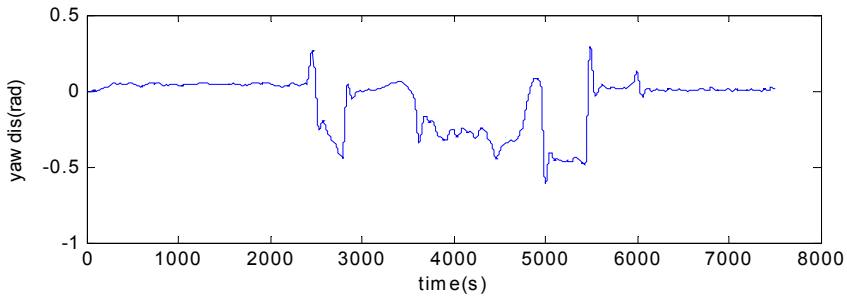

Diffraction Force:

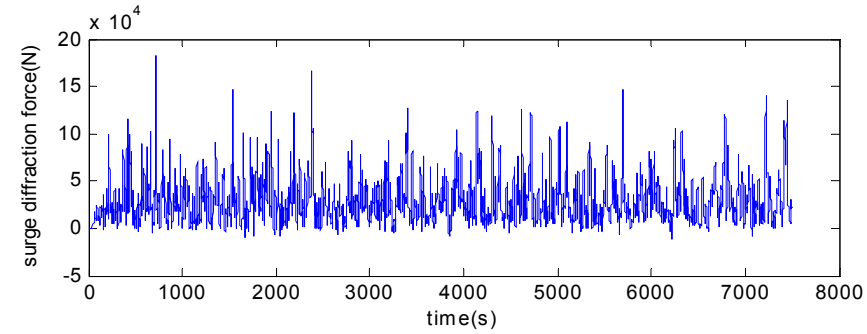

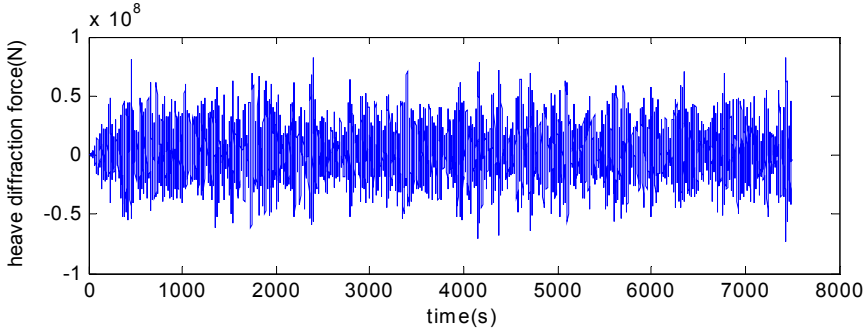

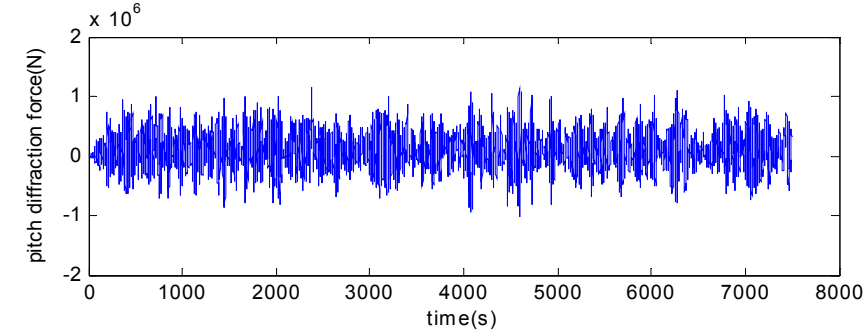

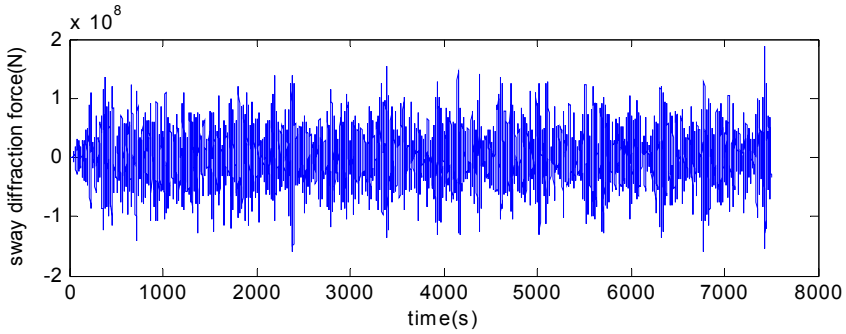

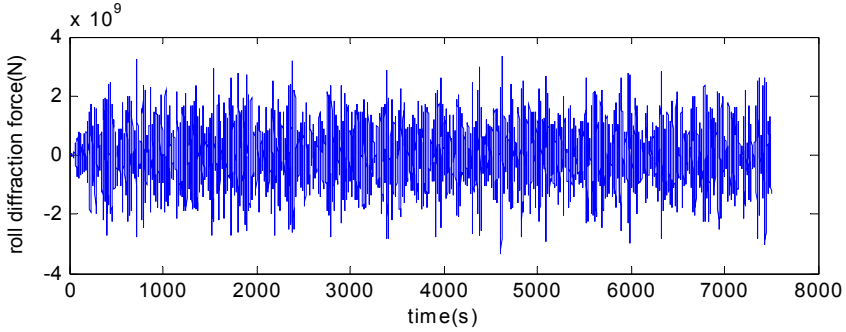

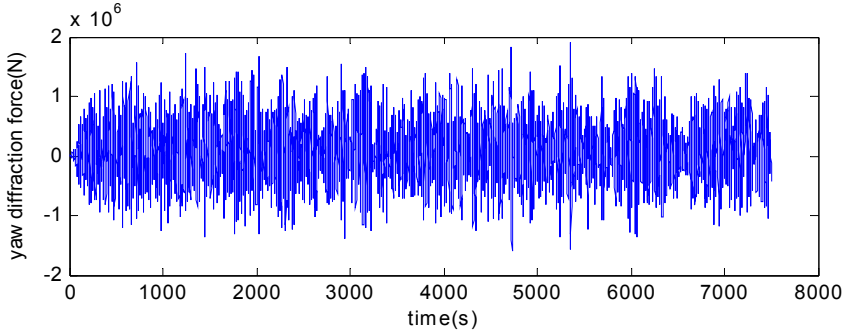

Viscous Force:

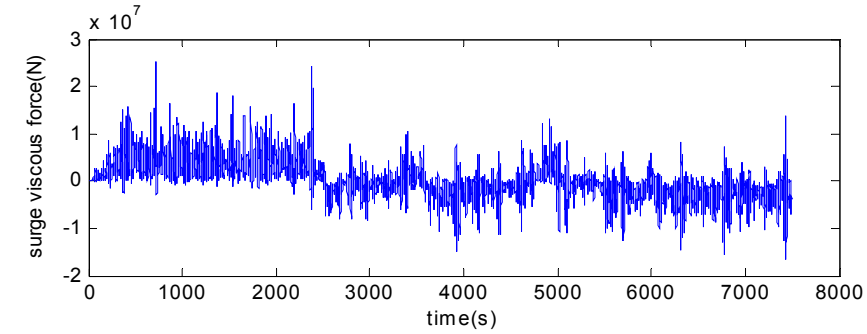

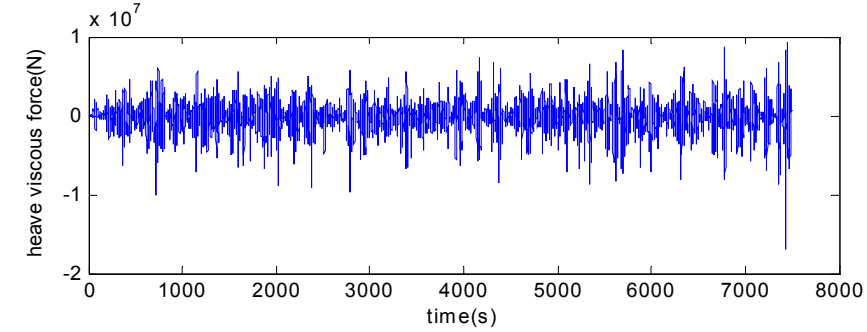

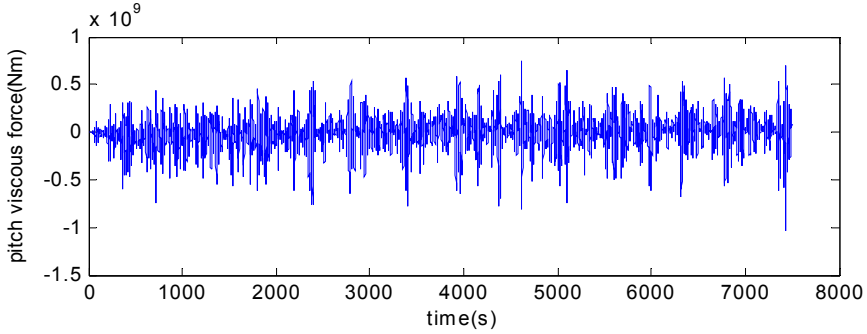

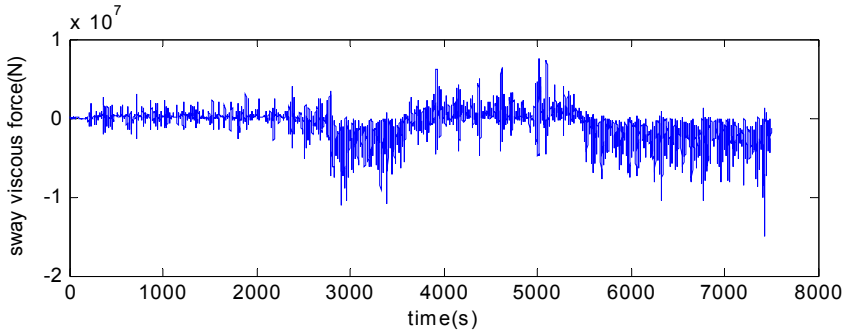

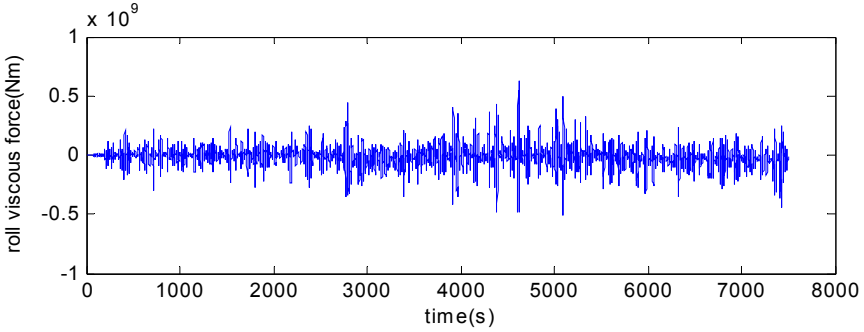

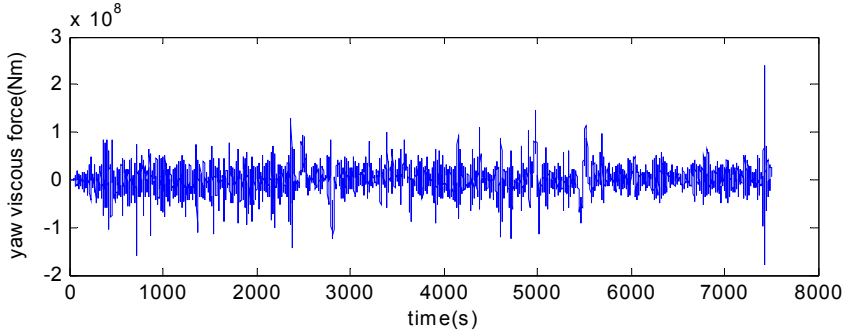

Wind Force:

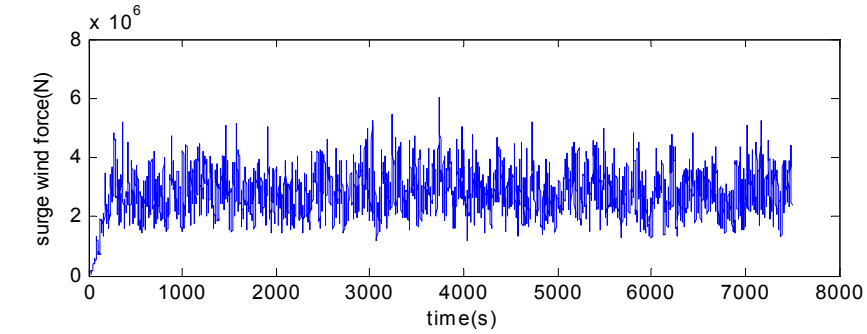
x 10^6
surge wind force(N)
time(s)

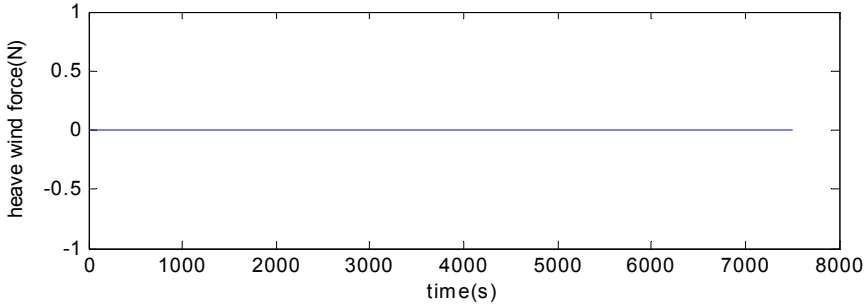
heave wind force(N)
time(s)

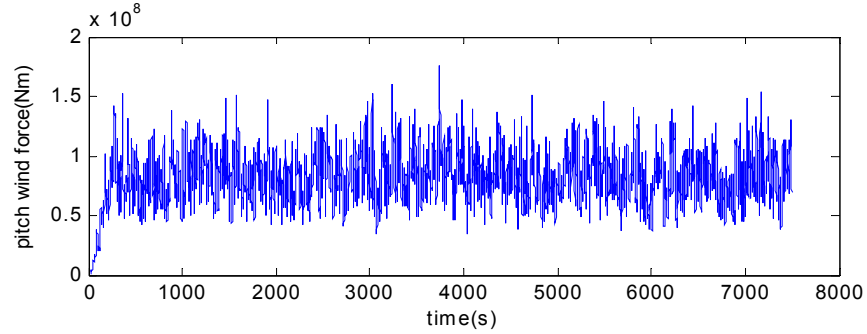
x 10^8
pitch wind force(Nm)
time(s)

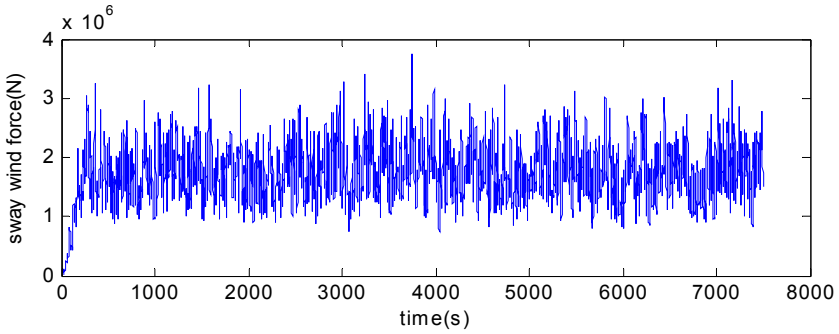
x 10^6
sway wind force(N)
time(s)

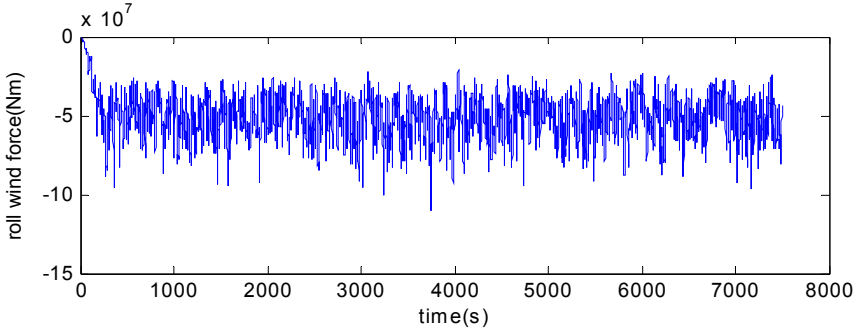
x 10^7
roll wind force(Nm)
time(s)

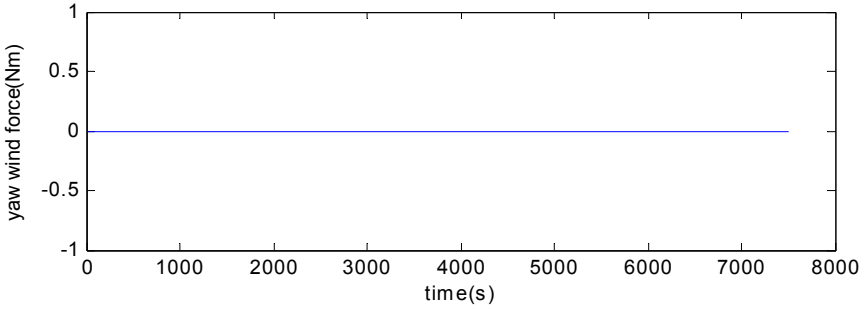
yaw wind force(Nm)
time(s)

Total Force:

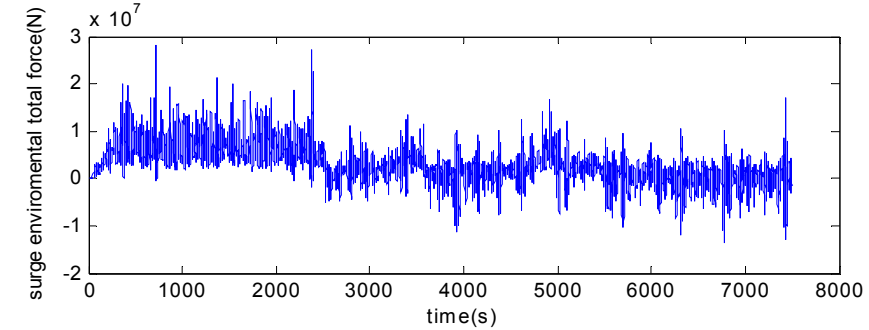
x 10^7
surge enviromental total force(N)
time(s)

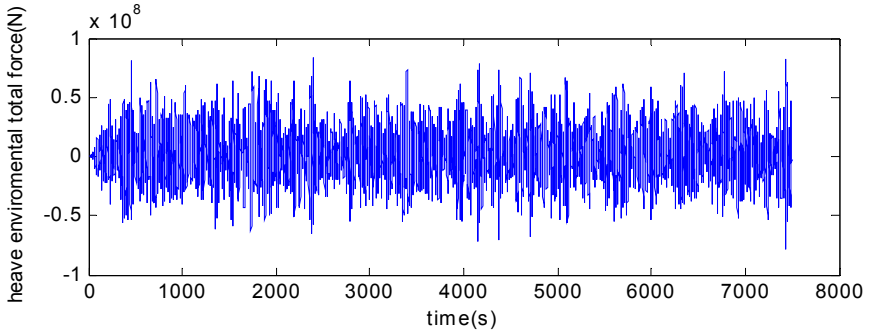
x 10^8
heave enviromental total force(N)
time(s)

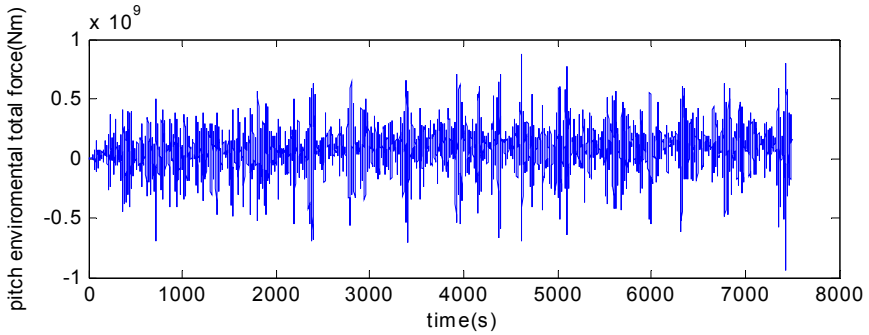
x 10^9
pitch enviromental total force(Nm)
time(s)

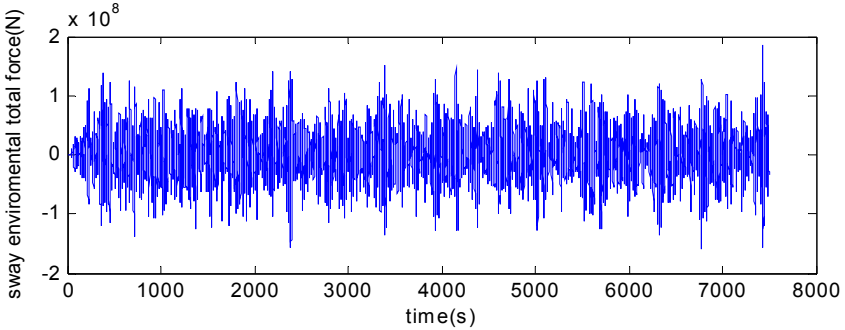
x 10^8
sway enviromental total force(N)
time(s)

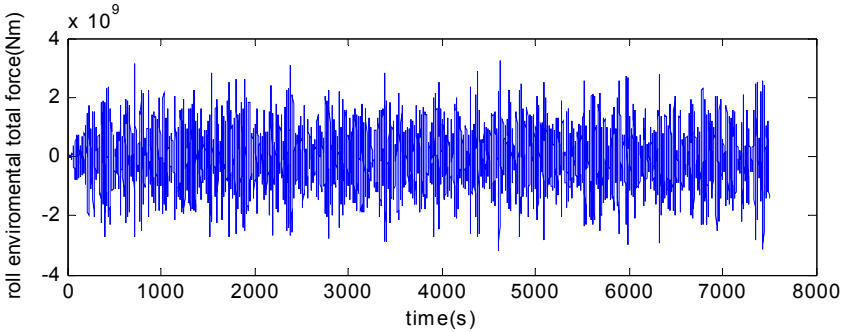
x 10^9
roll enviromental total force(Nm)
time(s)

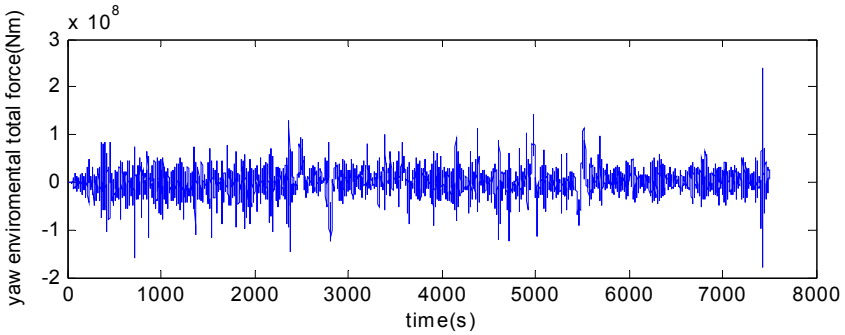
x 10^8
yaw enviromental total force(Nm)
time(s)

Top Tension:

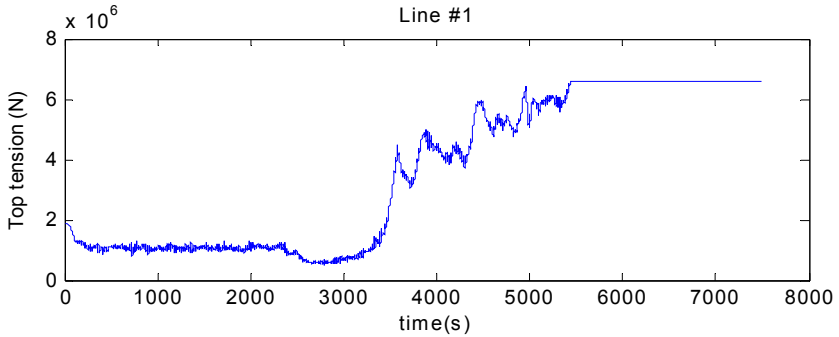
Line #1
x 10^6
Top tension (N)
time(s)

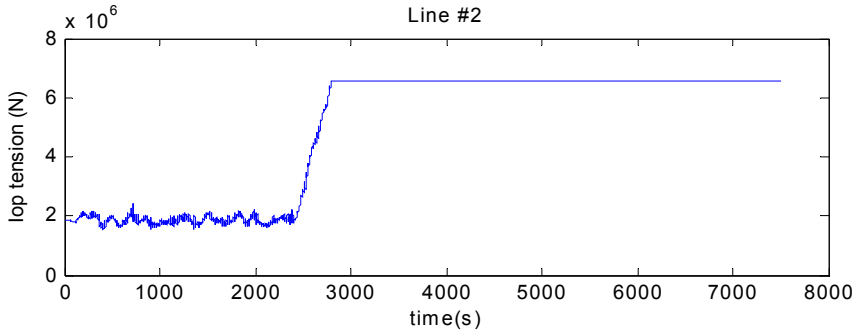
Line #2
x 10^6
lop tension (N)
time(s)

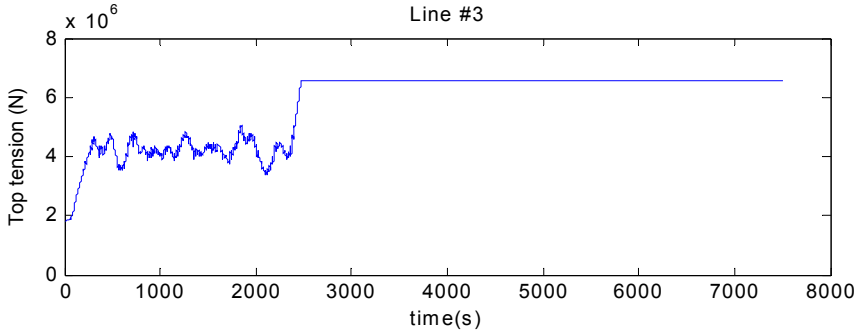
Line #3
x 10^6
Top tension (N)
time(s)

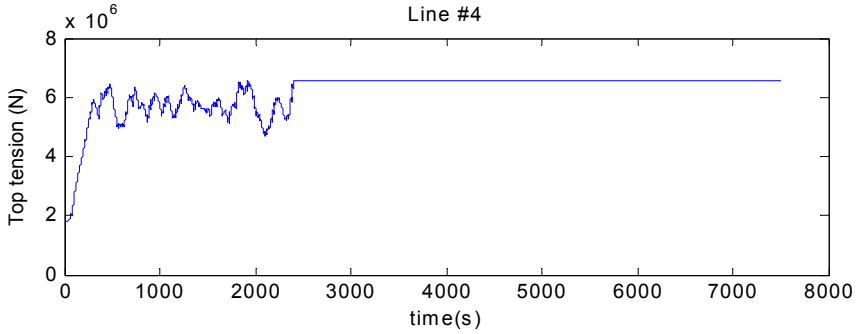
Line #4
x 10^6
Top tension (N)
time(s)

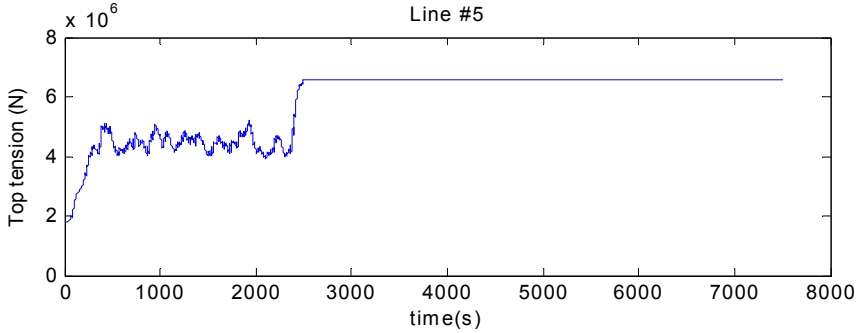
Line #5
x 10^6
Top tension (N)
time(s)

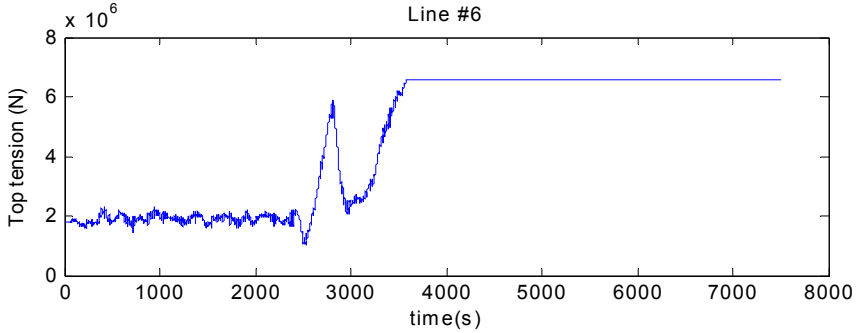
Line #6
x 10^6
Top tension (N)
time(s)

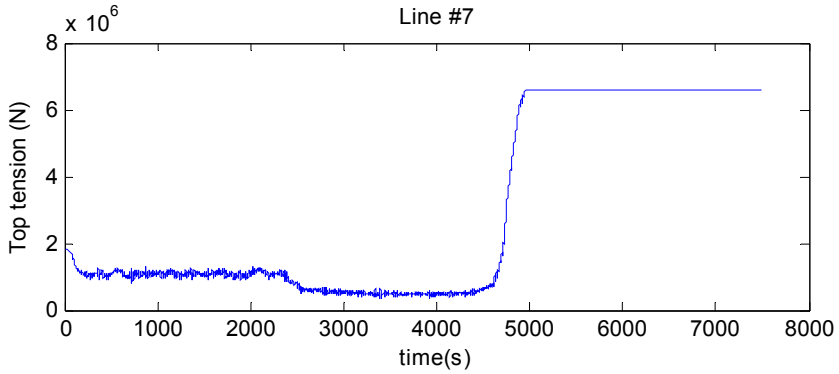

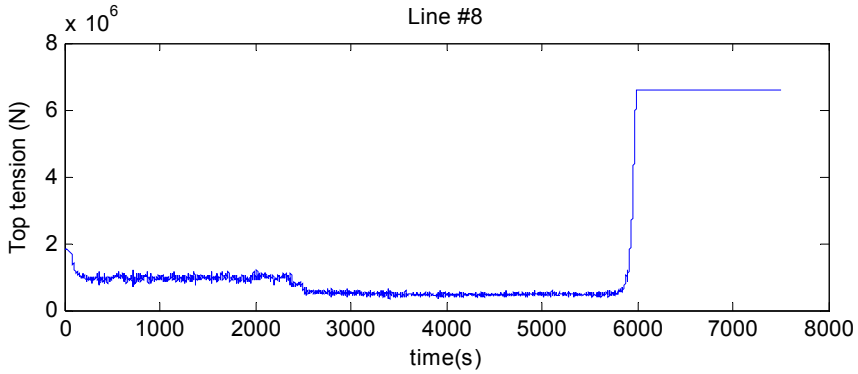

Case B Results: Mooring Failed

Line Broken Sequence:

#4	#3	#5	#2	#6	#7	#1	#8
2398.7 SEC	2470.6 SEC	2494.2 SEC	2789.6 SEC	3573.1 SEC	4951.1 SEC	5434.0 SEC	5991.4 SEC

Figure B16. Case C Collinear: Incident Wind Angle =295 deg. Mooring Survived:

Displacement:

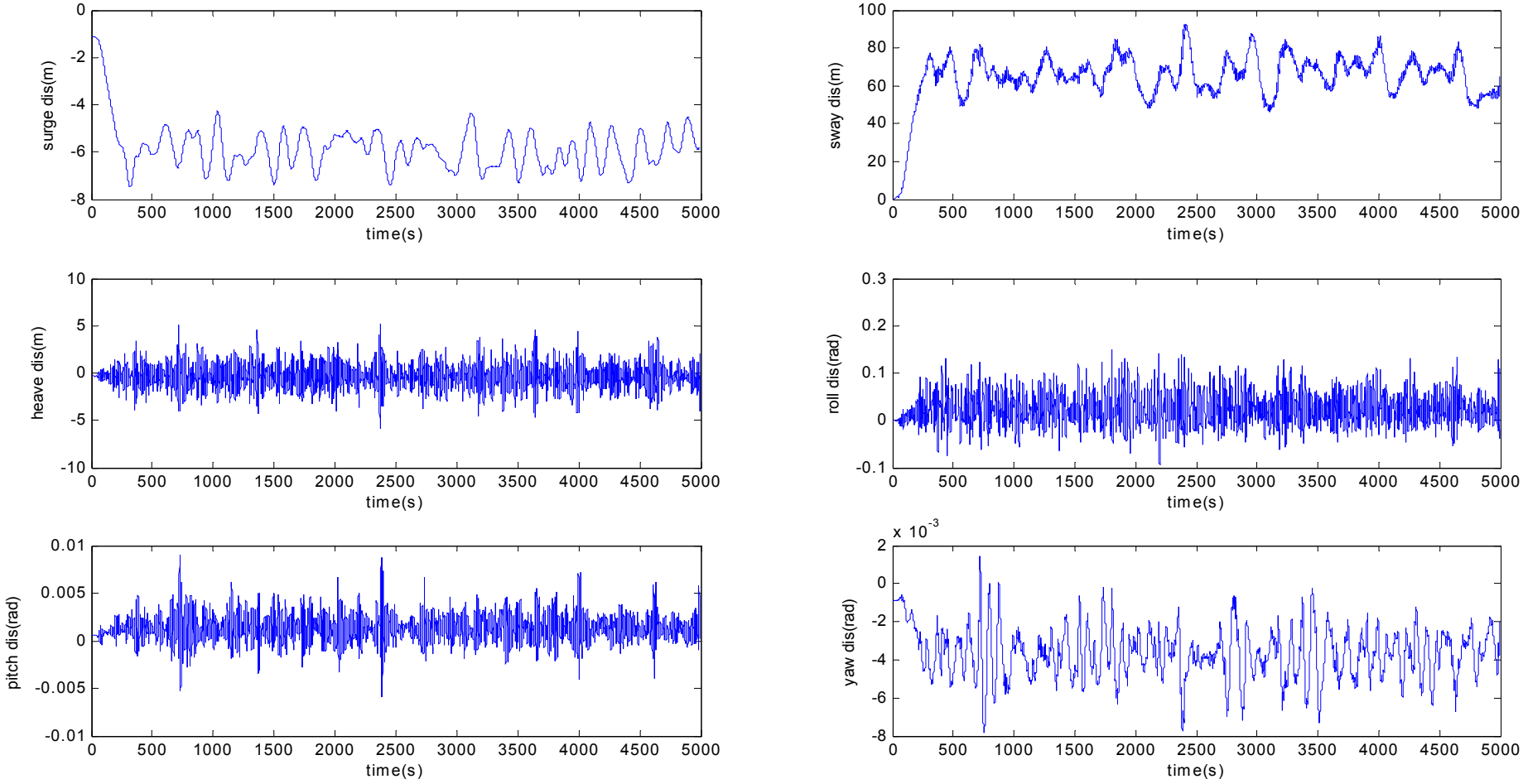

Diffraction Force:

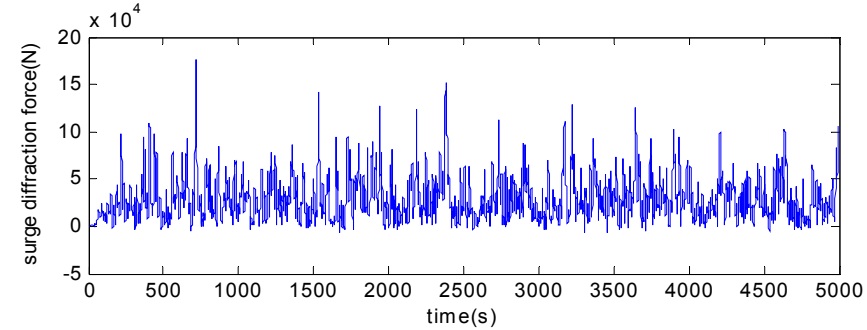

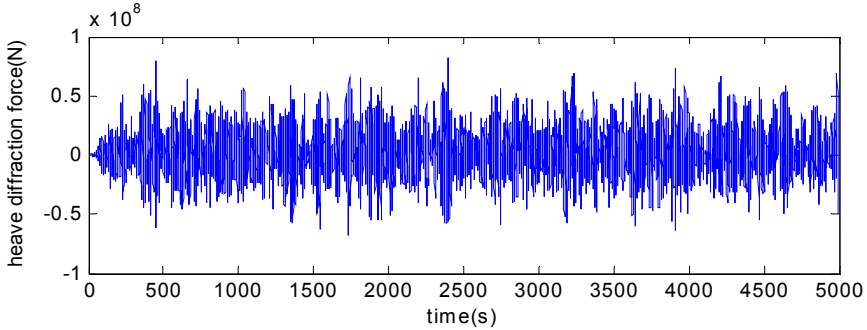

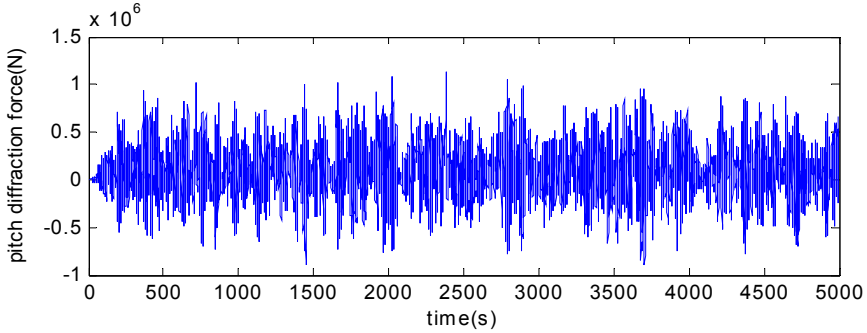

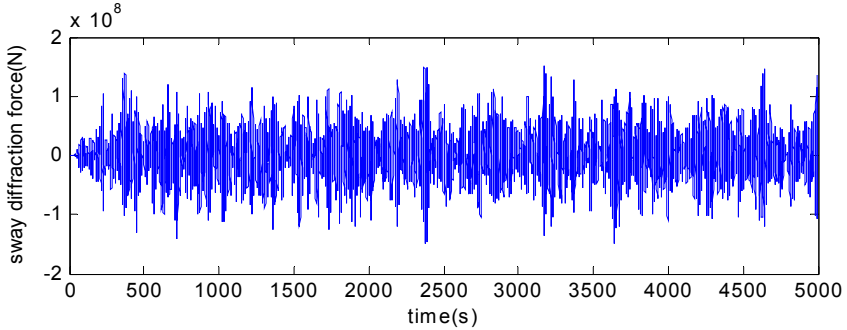

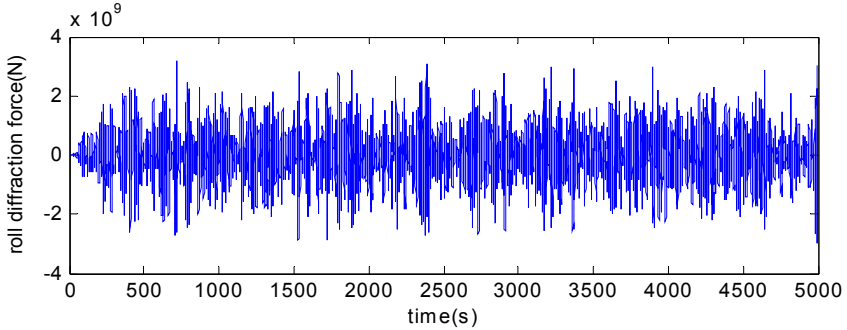

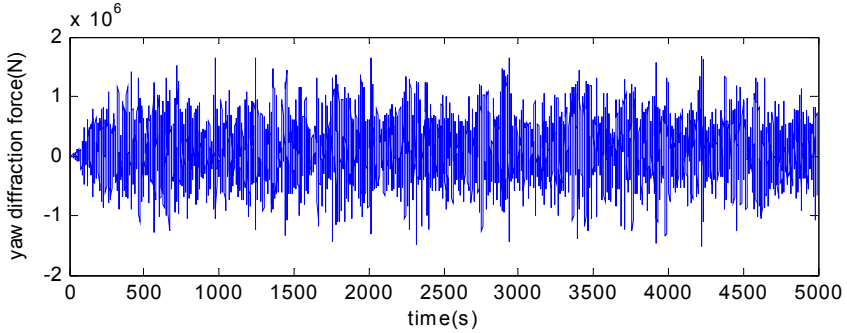

Viscous Force:

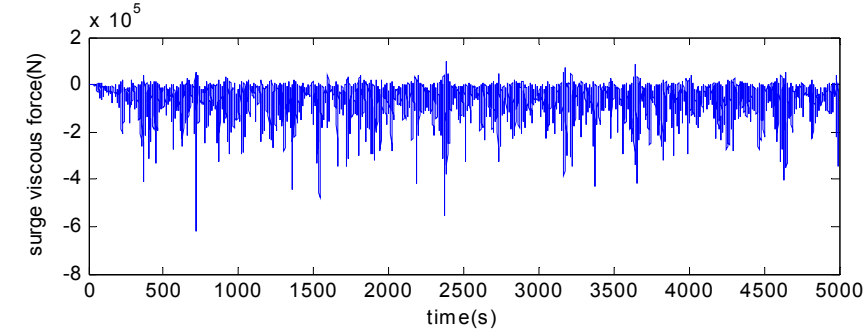

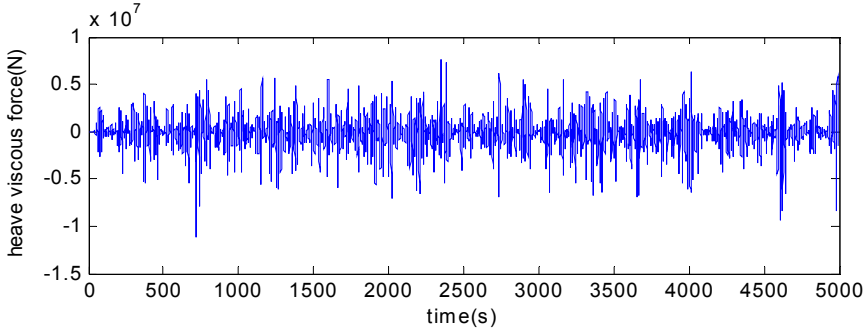

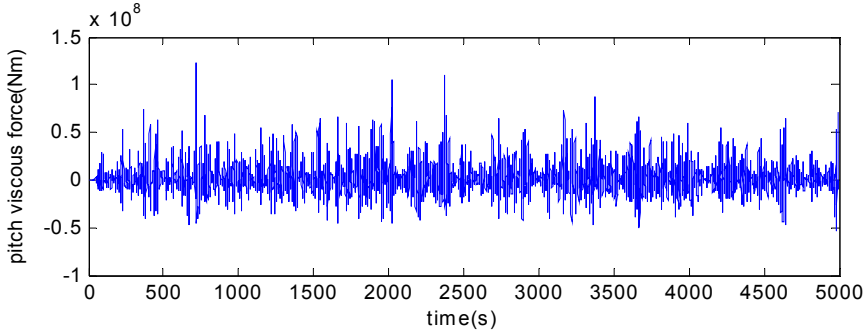

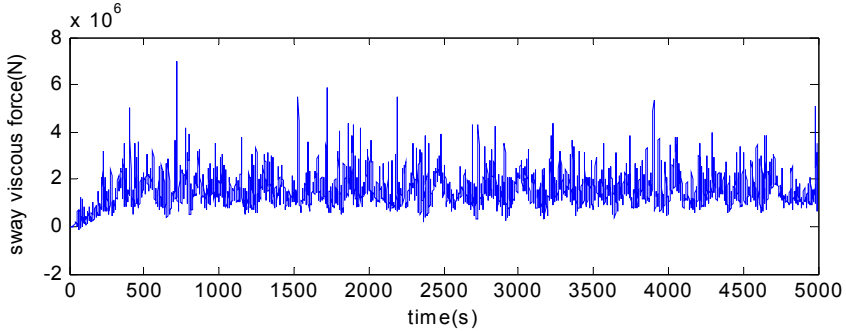

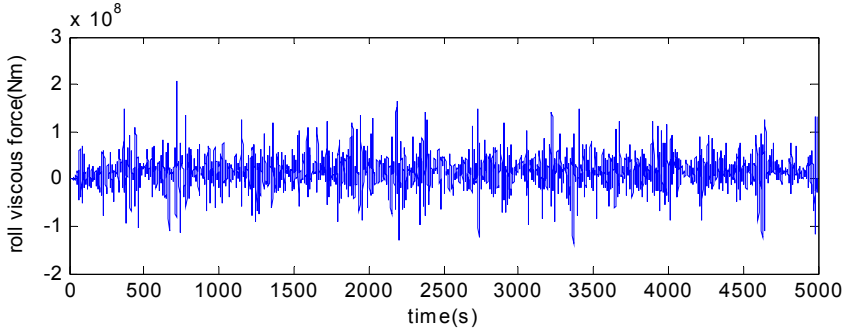

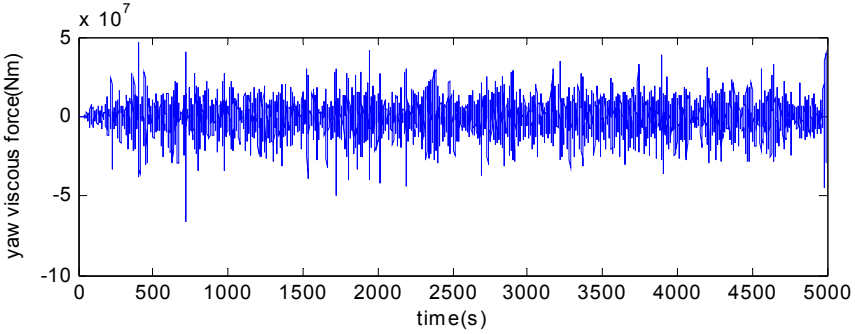

Wind Force:

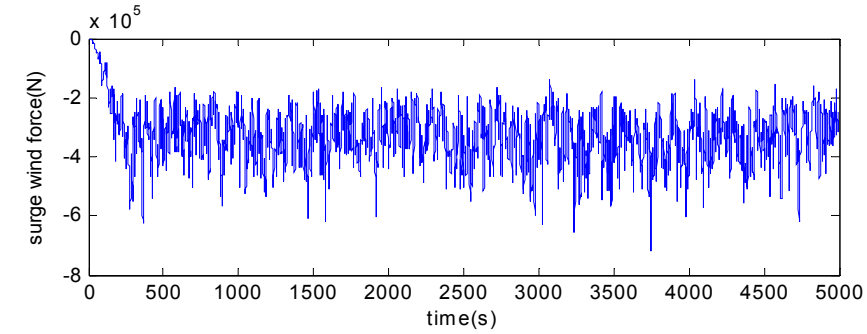
x 10^5
surge wind force(N)
time(s)

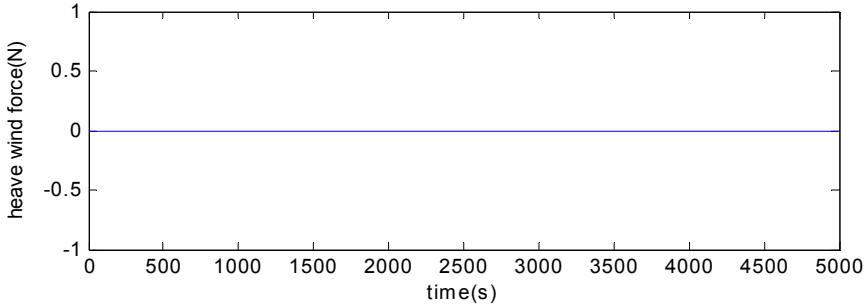
heave wind force(N)
time(s)

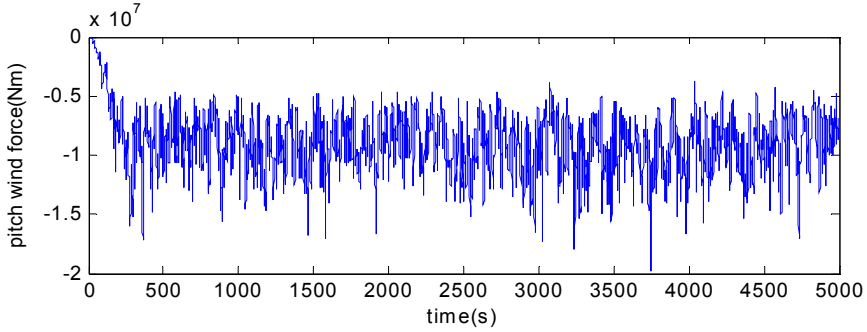
x 10^7
pitch wind force(Nm)
time(s)

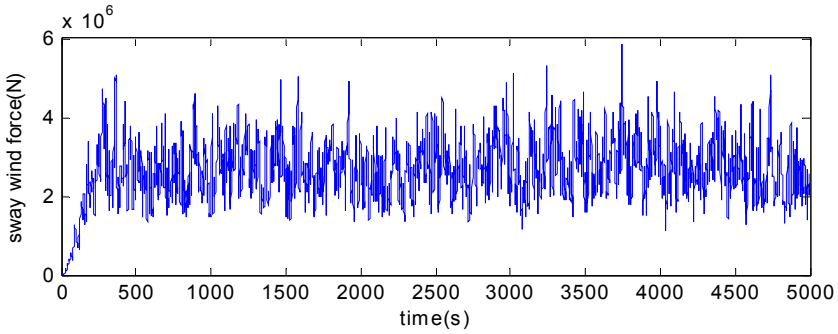
x 10^6
sway wind force(N)
time(s)

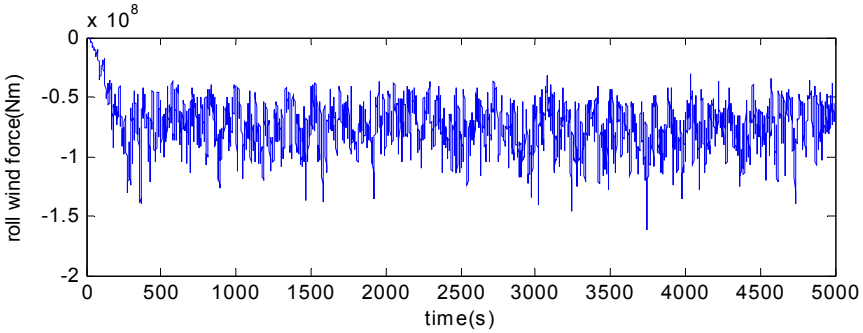
x 10^8
roll wind force(Nm)
time(s)

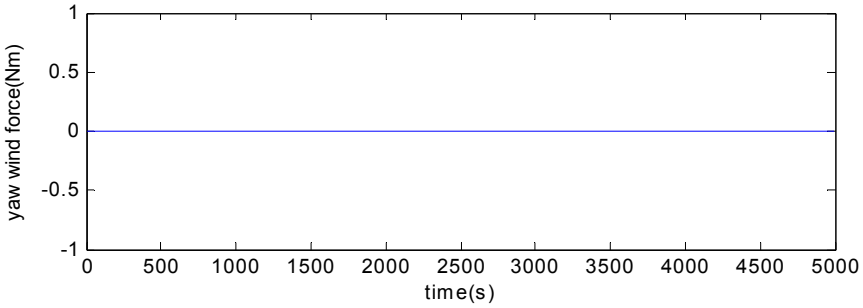
yaw wind force(Nm)
time(s)

Total Force:

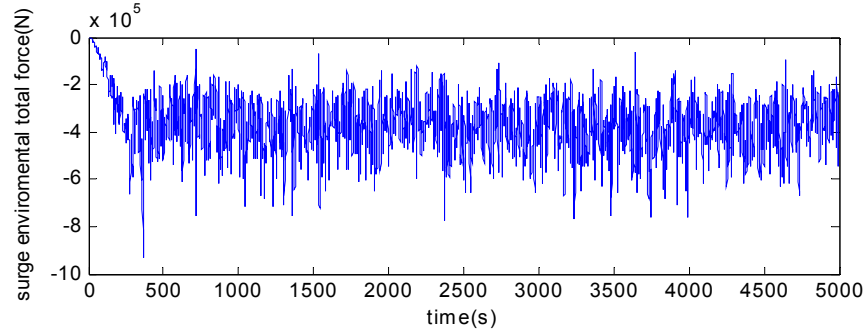
x 10^5
surge enviromental total force(N)
time(s)

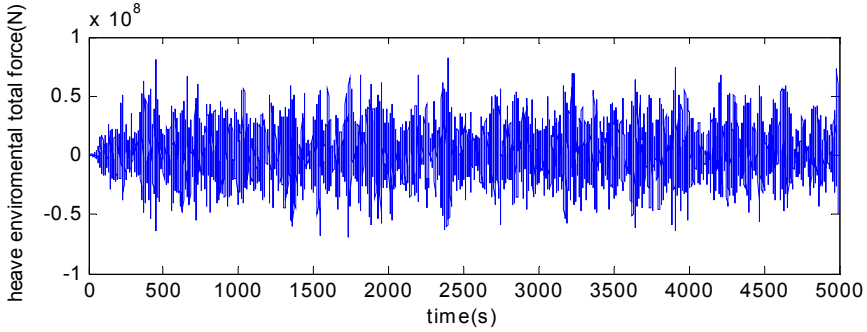
x 10^8
heave enviromental total force(N)
time(s)

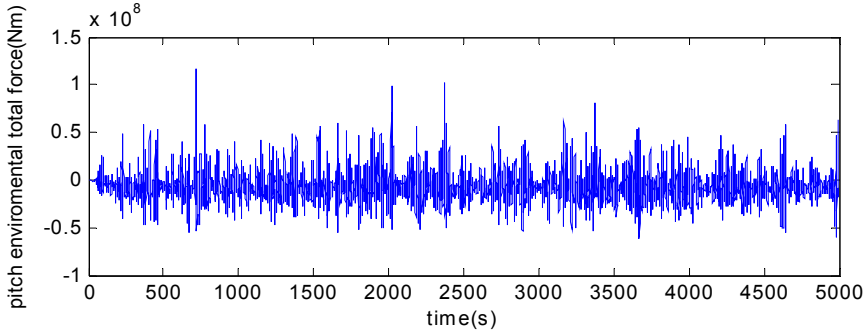
x 10^8
pitch enviromental total force(Nm)
time(s)

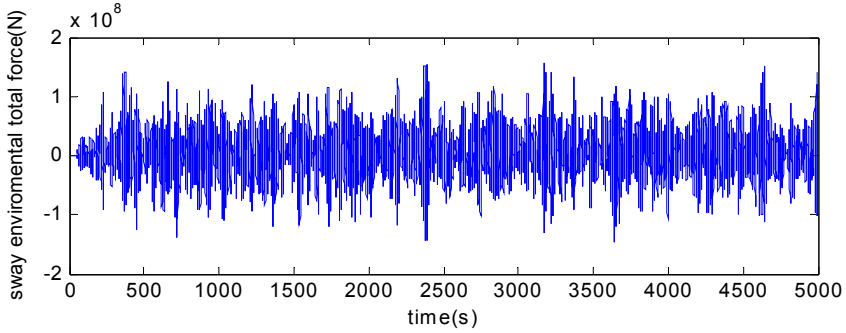
x 10^8
sway enviromental total force(N)
time(s)

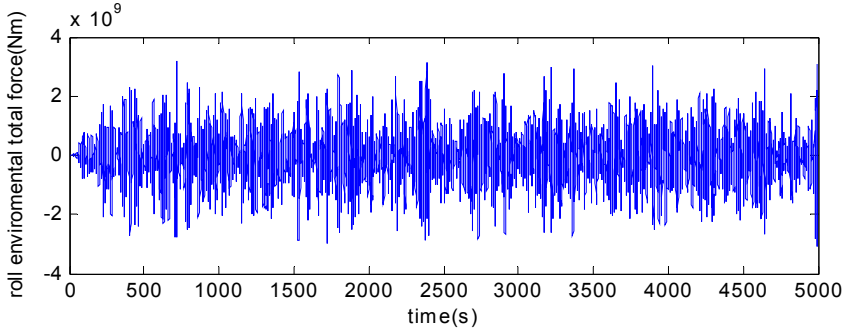
x 10^9
roll enviromental total force(Nm)
time(s)

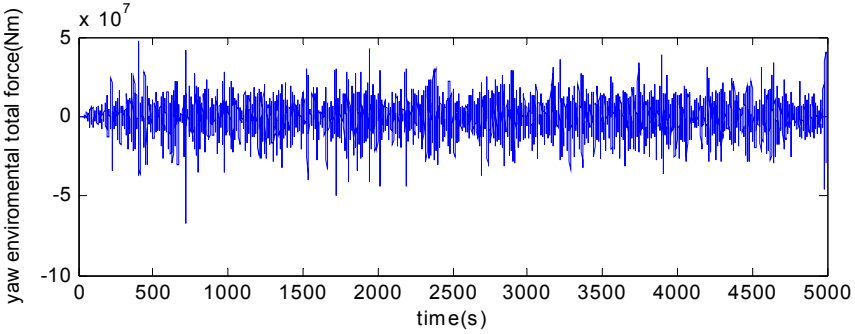
x 10^7
yaw enviromental total force(Nm)
time(s)

Top Tension

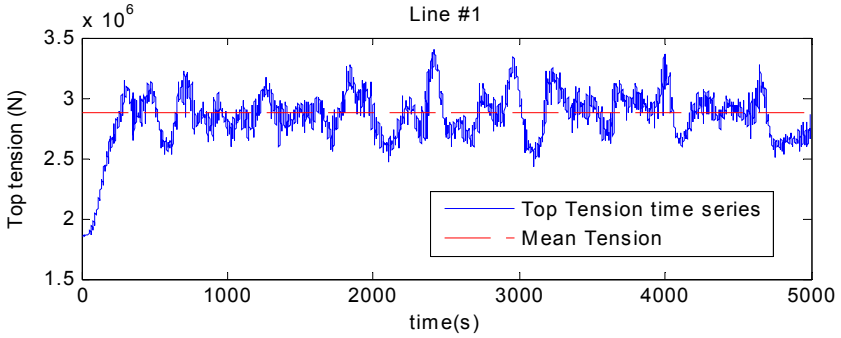
Line #1
x 10^6
Top tension (N)
time(s)
Top Tension time series
Mean Tension

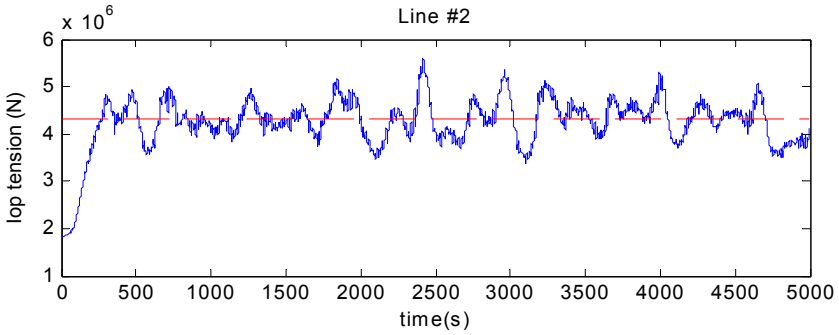
Line #2
x 10^6
lop tension (N)
time(s)

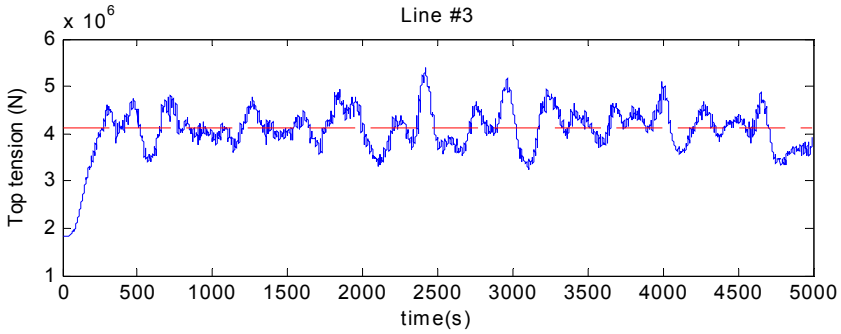
Line #3
x 10^6
Top tension (N)
time(s)

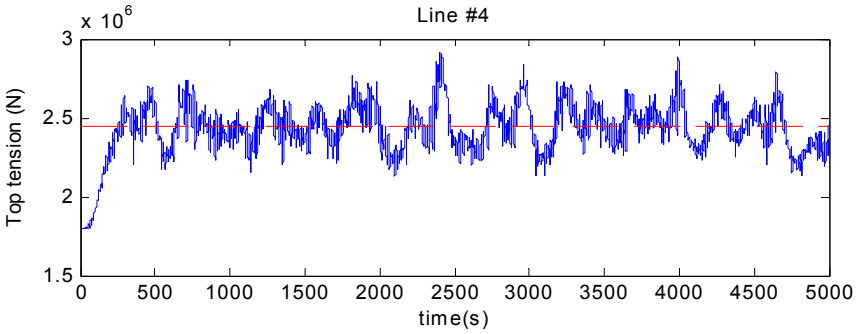
Line #4
x 10^6
Top tension (N)
time(s)

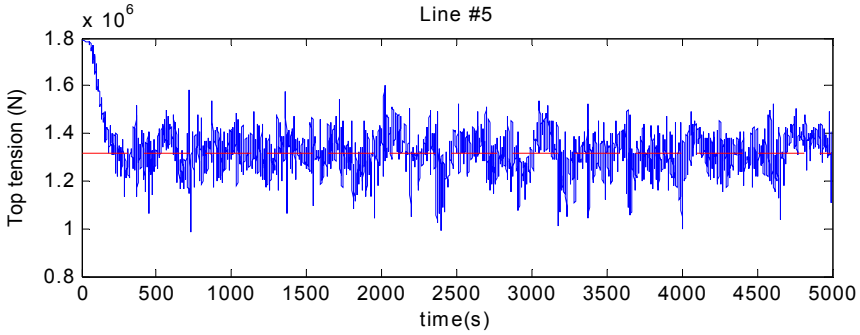
Line #5
x 10^6
Top tension (N)
time(s)

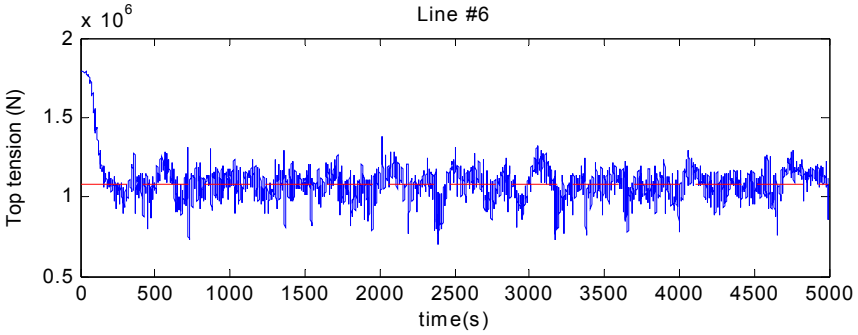
Line #6
x 10^6
Top tension (N)
time(s)

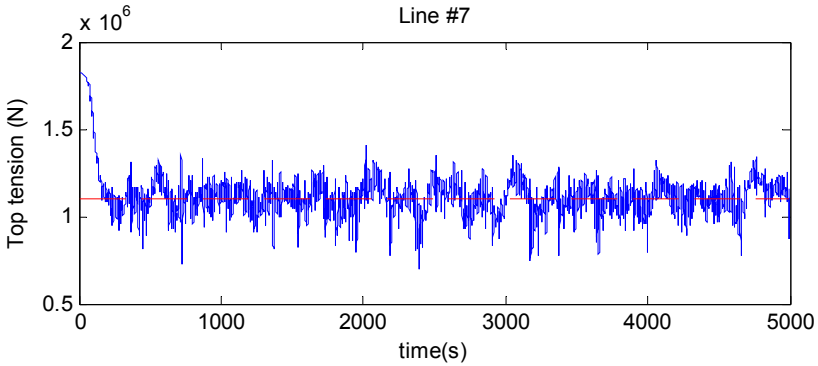

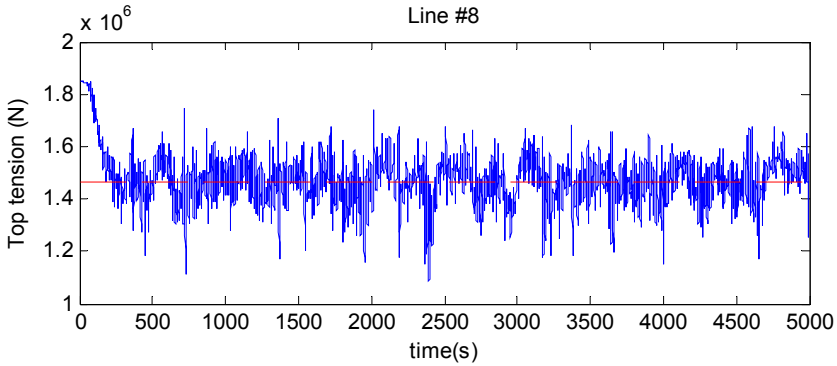

Case C Result - Mooring Survived

Figure B17. Case D: Non-Collinear: Incident Wind Angle = 295 deg. Mooring Survived

Displacement:

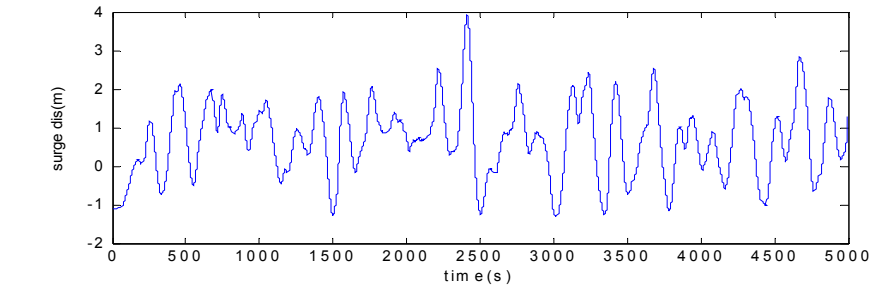

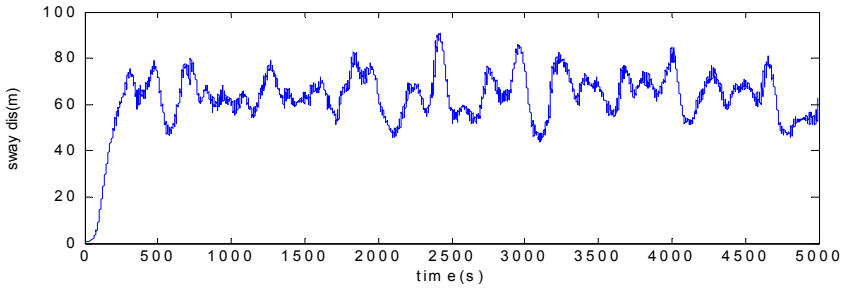

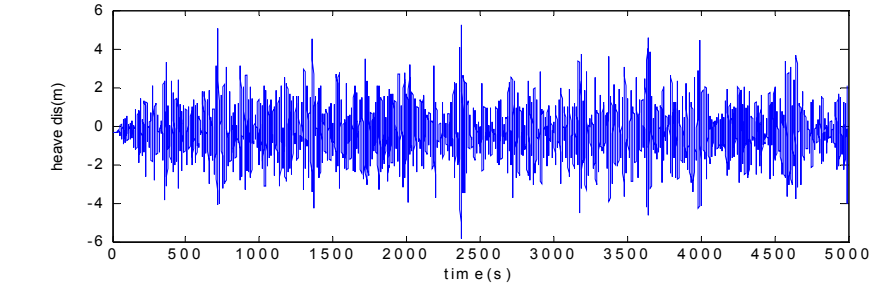

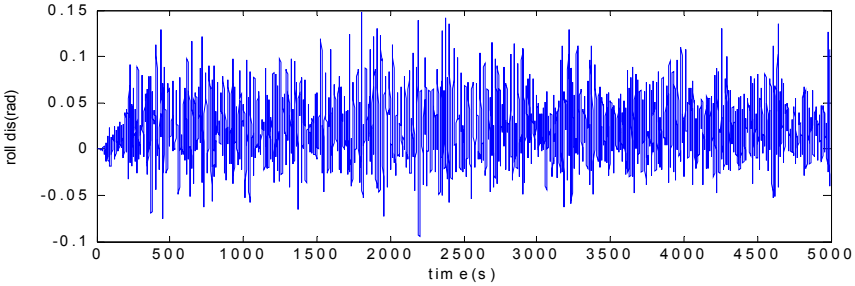

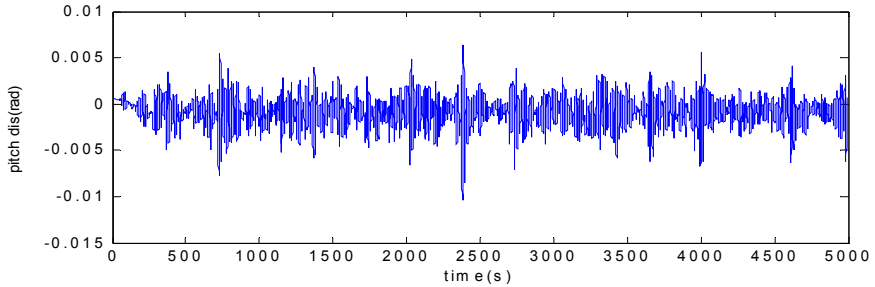

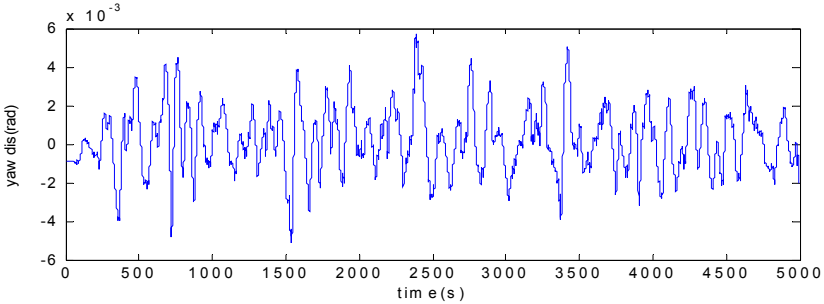

Diffraction Force:

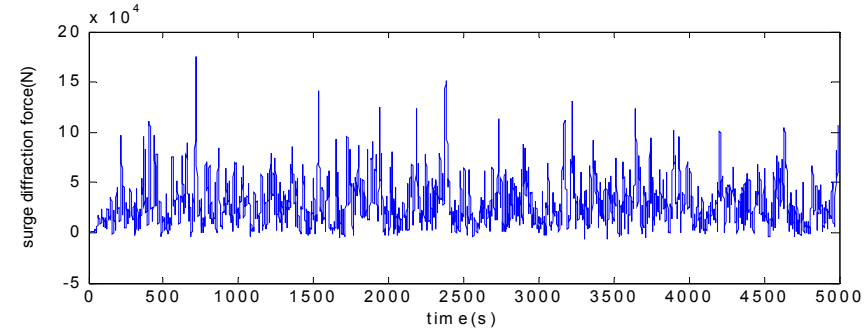

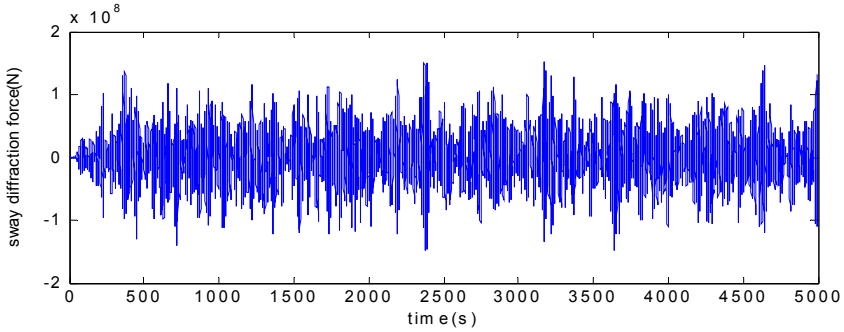

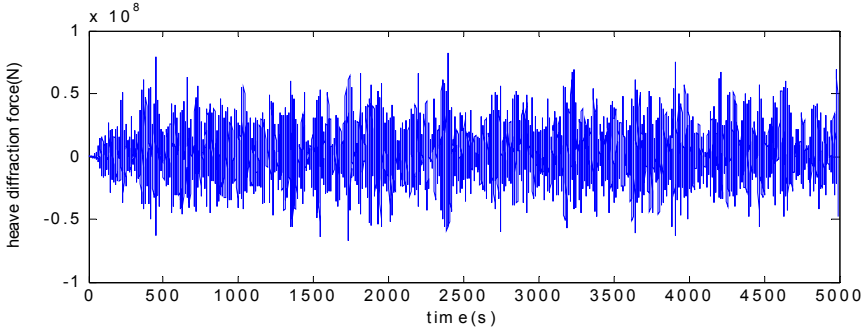

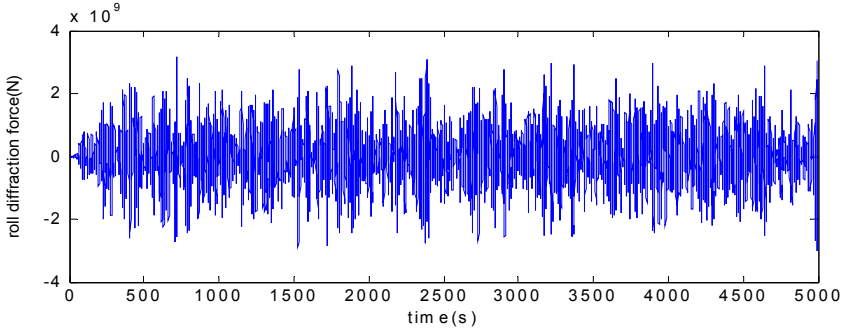

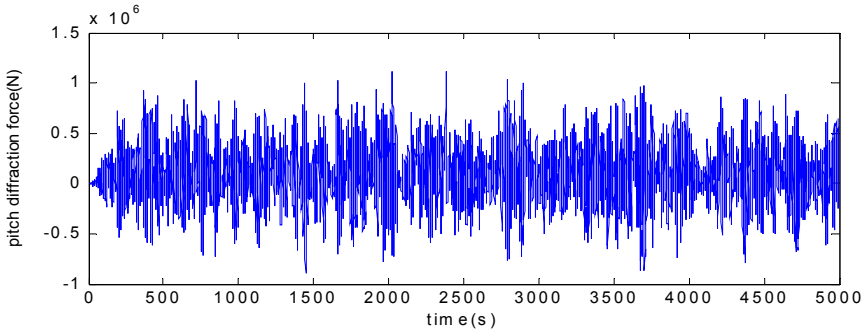

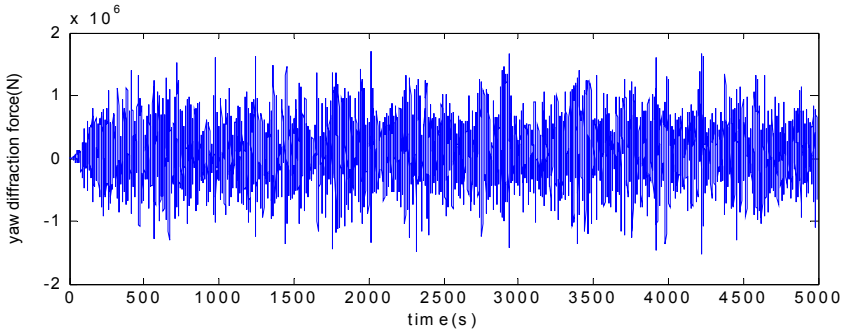

Viscous Force:

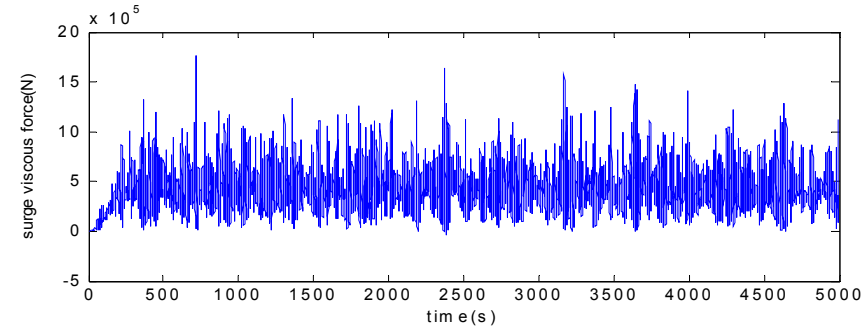

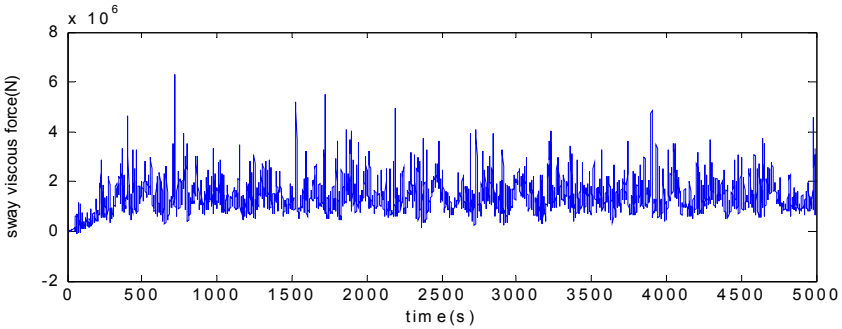

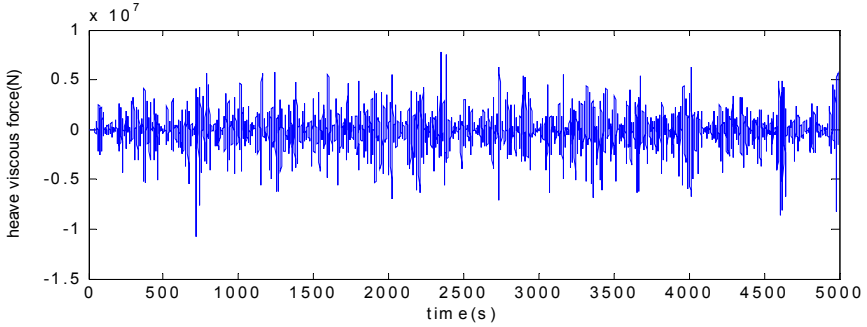

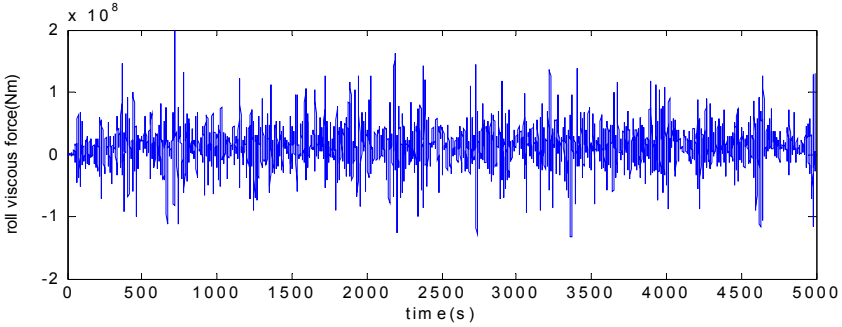

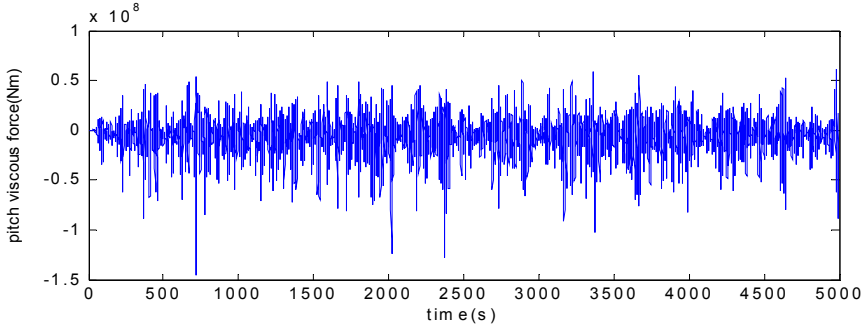

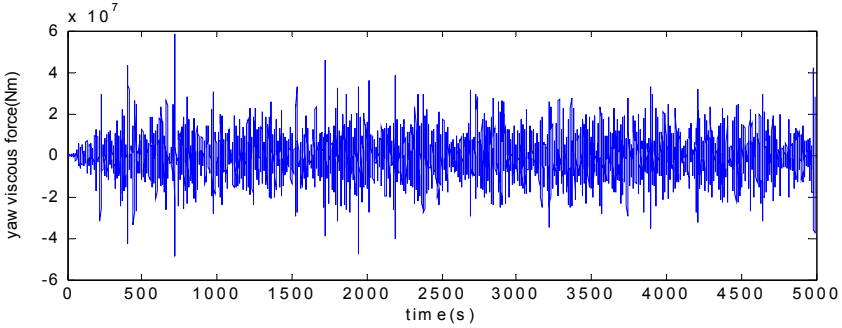

Wind Force:

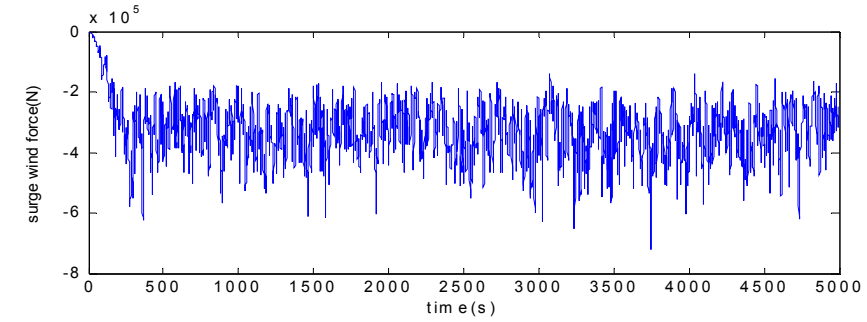
x 10^5
surge wind force(N)
time(s)

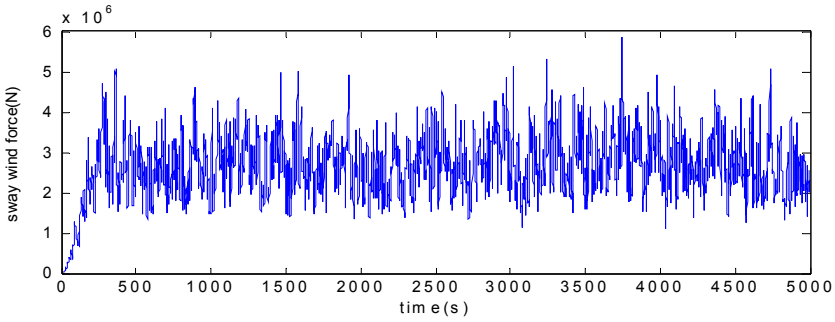
x 10^6
sway wind force(N)
time(s)

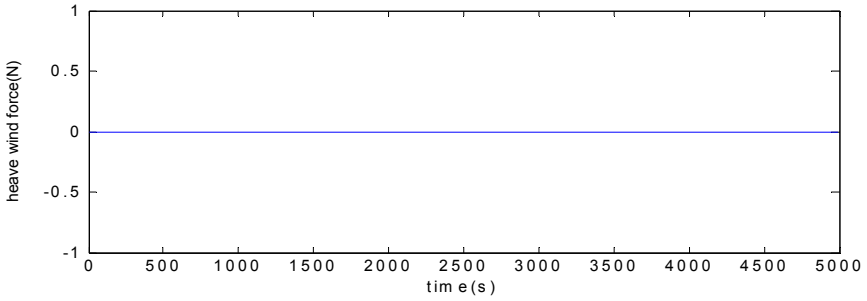
heave wind force(N)
time(s)

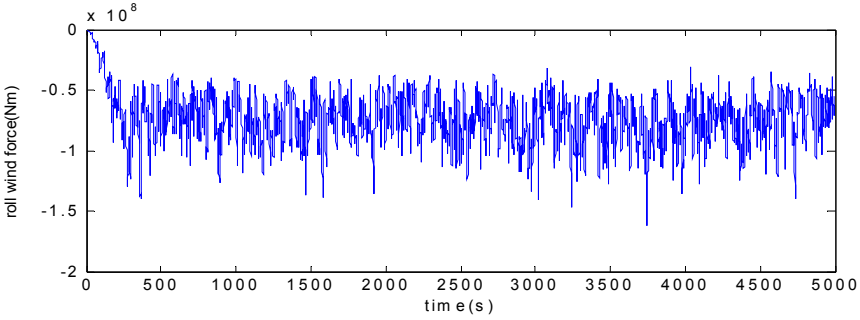
x 10^8
roll wind force(Nm)
time(s)

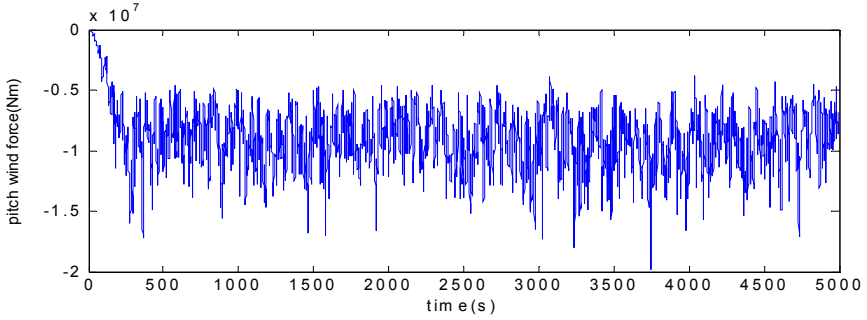
x 10^7
pitch wind force(Nm)
time(s)

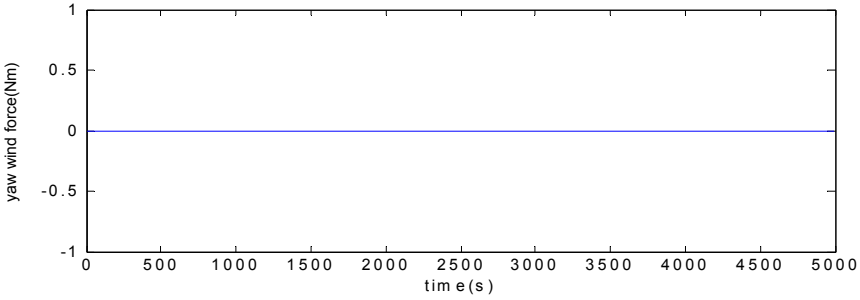
yaw wind force(Nm)
time(s)

Total Force:

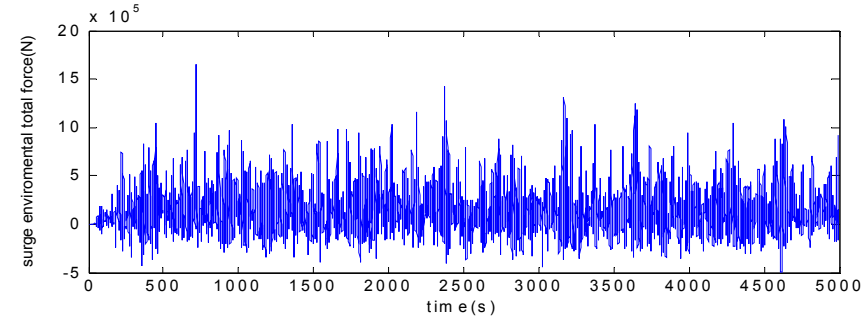
x 10^5
surge enviromental total force(N)
time(s)

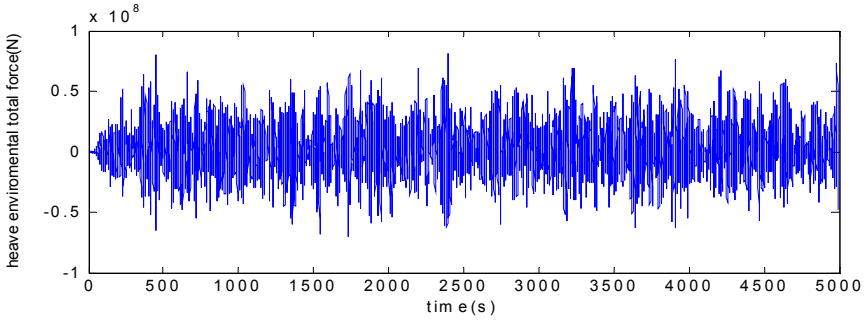
x 10^8
heave enviromental total force(N)
time(s)

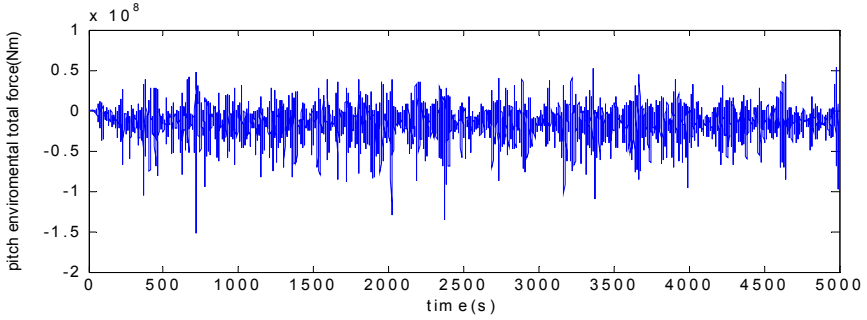
x 10^8
pitch enviromental total force(Nm)
time(s)

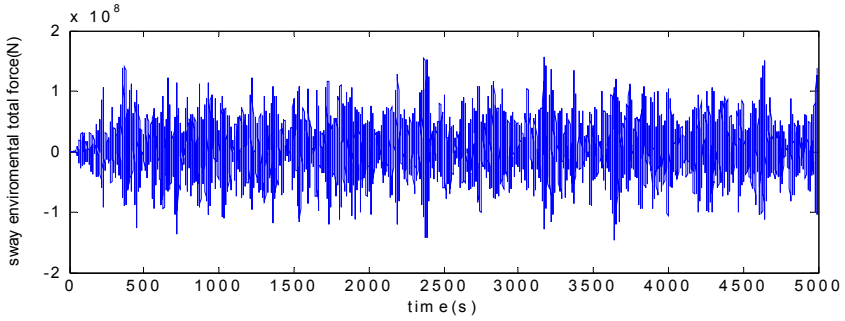
x 10^8
sway enviromental total force(N)
time(s)

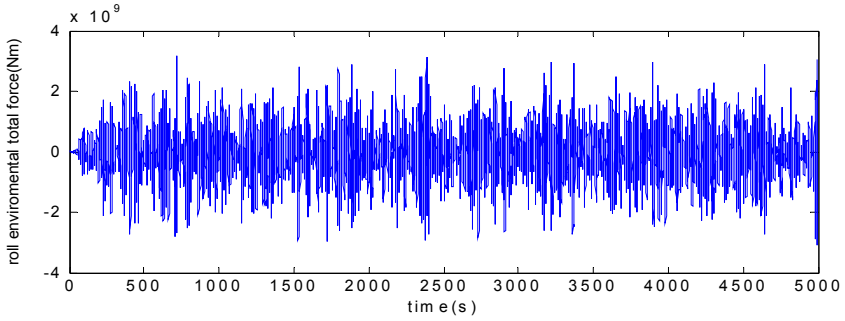
x 10^9
roll enviromental total force(Nm)
time(s)

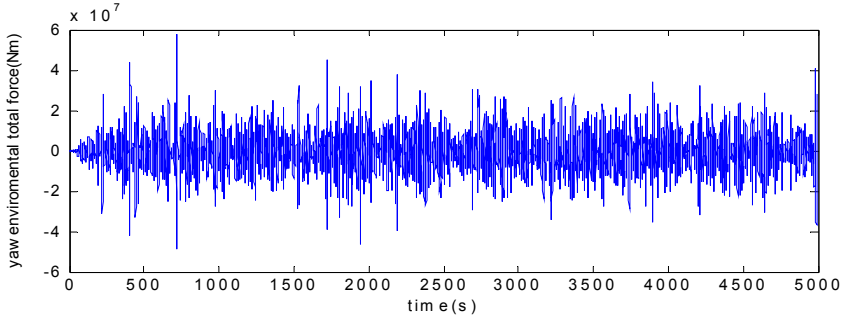
x 10^7
yaw enviromental total force(Nm)
time(s)

Top Tension:

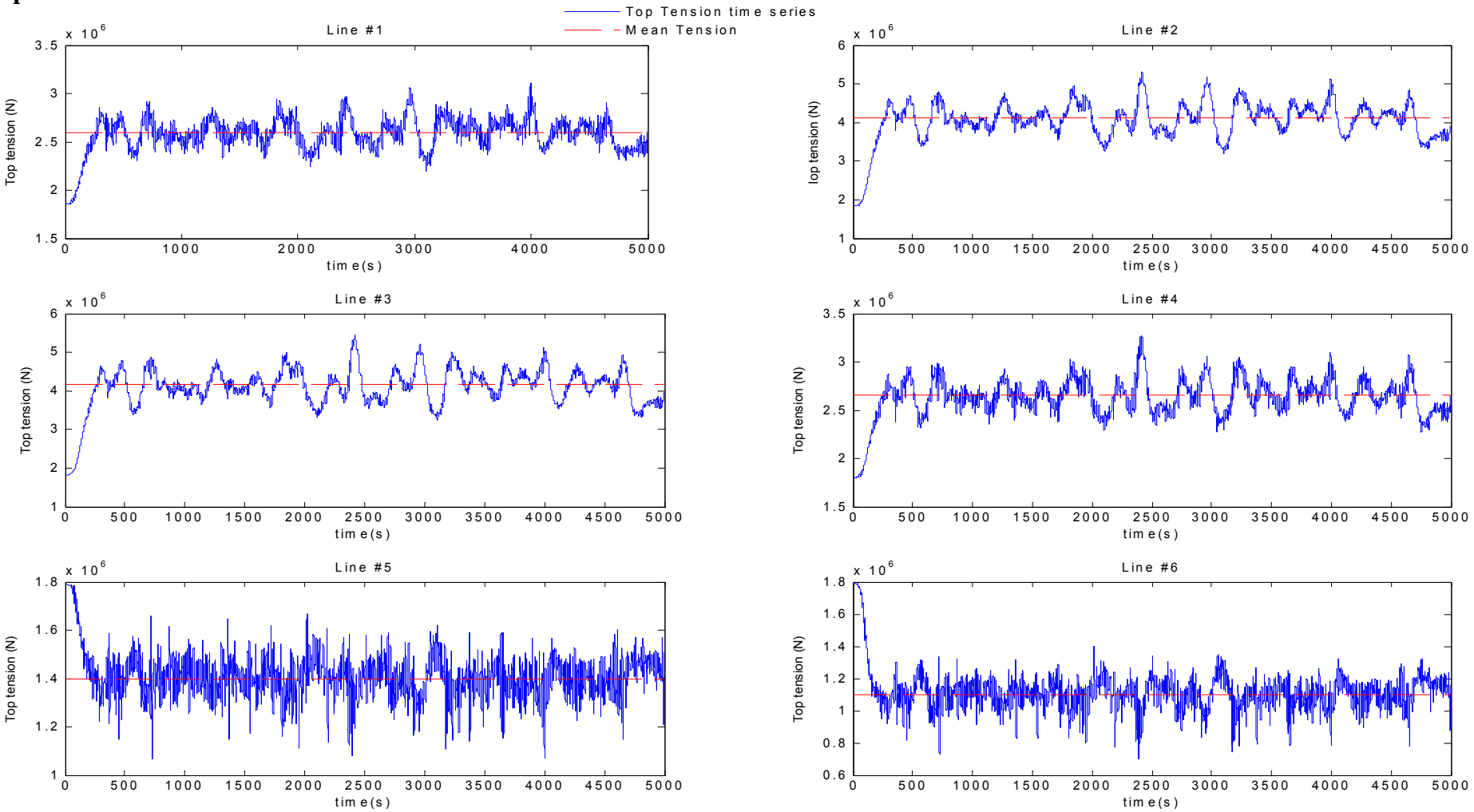
Top Tension time series
Mean Tension
Line #1
Line #2
Line #3
Line #4
Line #5
Line #6
x 10^6
Top tension (N)
Iop tension (N)
time(s)

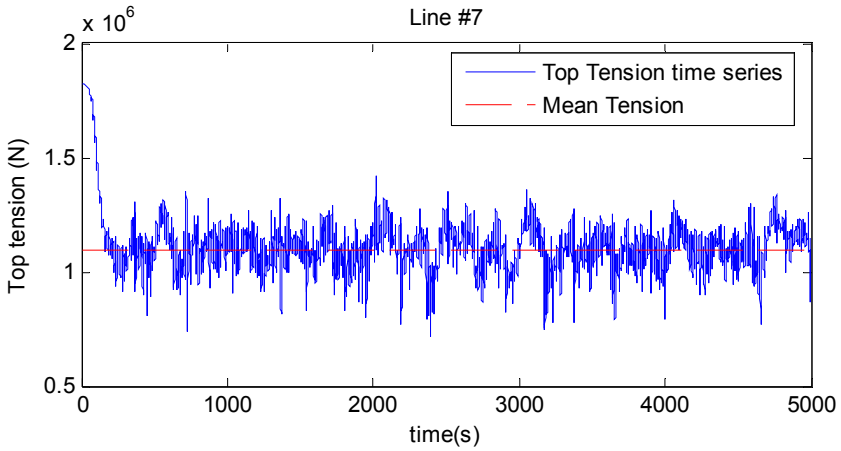

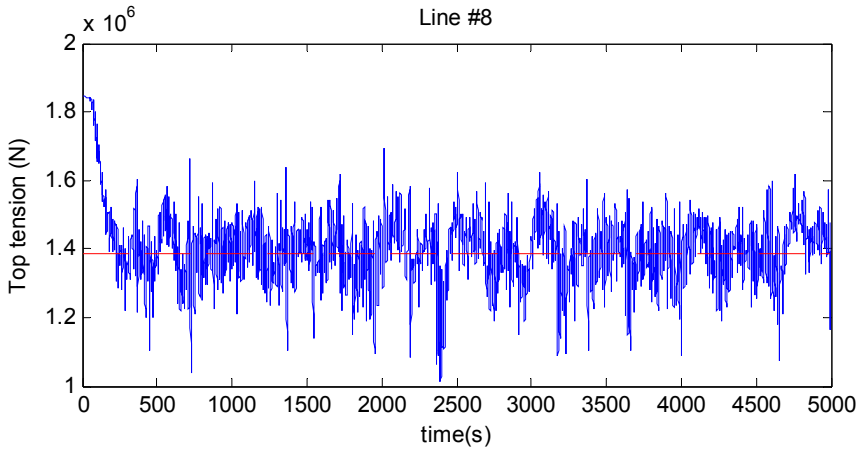

Case D Result: Mooring Survived.

Appendix C: No MODUS Adrift – Geotechnical Issues

Robert B. Gilbert and Charles Aubeny
Offshore Technology Research Center

Introduction

The ability of the anchor to provide a restoring force to a floating Mobile Offshore Drilling Unit (MODU) is limited by the capacity of the mooring line. Under design loading conditions (that is, an intact mooring system or a damaged mooring system with one line missing), each mooring line loads its anchor in the plane it was intended to be loaded ("in-plane loading"). For a suction caisson, in-plane loading means that the line is pulling in the direction of the load-attachment padeye. For a drag embedment plate anchor (DEA) and near-normal or vertically loaded plate anchor (VLA), in-plane loading means that the line is pulling in the plane of the shank.

It is unlikely that the anchor will pull out before the line breaks in in-plane loading. Reliability analyses on mooring systems for permanent, floating production facilities show that the probability of an anchor failure is more than one hundred times smaller than that for a line or chain break (e.g., Gilbert et al. 2005 and Choi et al. 2006). An example set of results for a semi-taut mooring system in 3,000 feet of water are shown on Figure C1. While the absolute magnitudes for these component and system failure probabilities will be larger for a MODU since the design waves are smaller, the relative magnitudes for the various probabilities in comparison to one another provide a crude approximation for a MODU mooring system since a similar design recipe is used.

Therefore, increasing the capacity of the anchors to in-line loading will have very little effect on reducing the probability of a mooring failure. This conclusion is consistent with the performance of floating MODUs in recent hurricanes; all of the mooring systems that failed had failure sequences that initiated above the anchor. However, once several lines in the mooring system break and the rig begins to move off station, the remaining lines

start loading the anchors at an angle to the plane of the intended loading. Out-of-plane loading may mean that a suction caisson will be twisted or that a plate anchor will be pulled over sideways. Under these out-of-plane conditions, the capacity of the anchor can be substantially smaller than the capacity under in-plane loading conditions, and it is possible that the anchor will pull out of the soil before the line breaks. Anchor pull-out is a problem for a MODU that is adrift because it will drag these anchors (weighing tens to hundreds of kips) across the sea floor where wells, flowlines, pipelines, and other mooring systems are located.

The focus of this report is on the capacity of anchors subjected to out-of-plane loading conditions. First, a back-analysis is presented for two case study mooring systems with suction caisson anchors that failed in Hurricane Ivan. These case studies highlight the significance of out-of-plane loading. Next, possible alternatives are presented and analyzed in order to improve the capacity of anchors under out-of-plane loading.

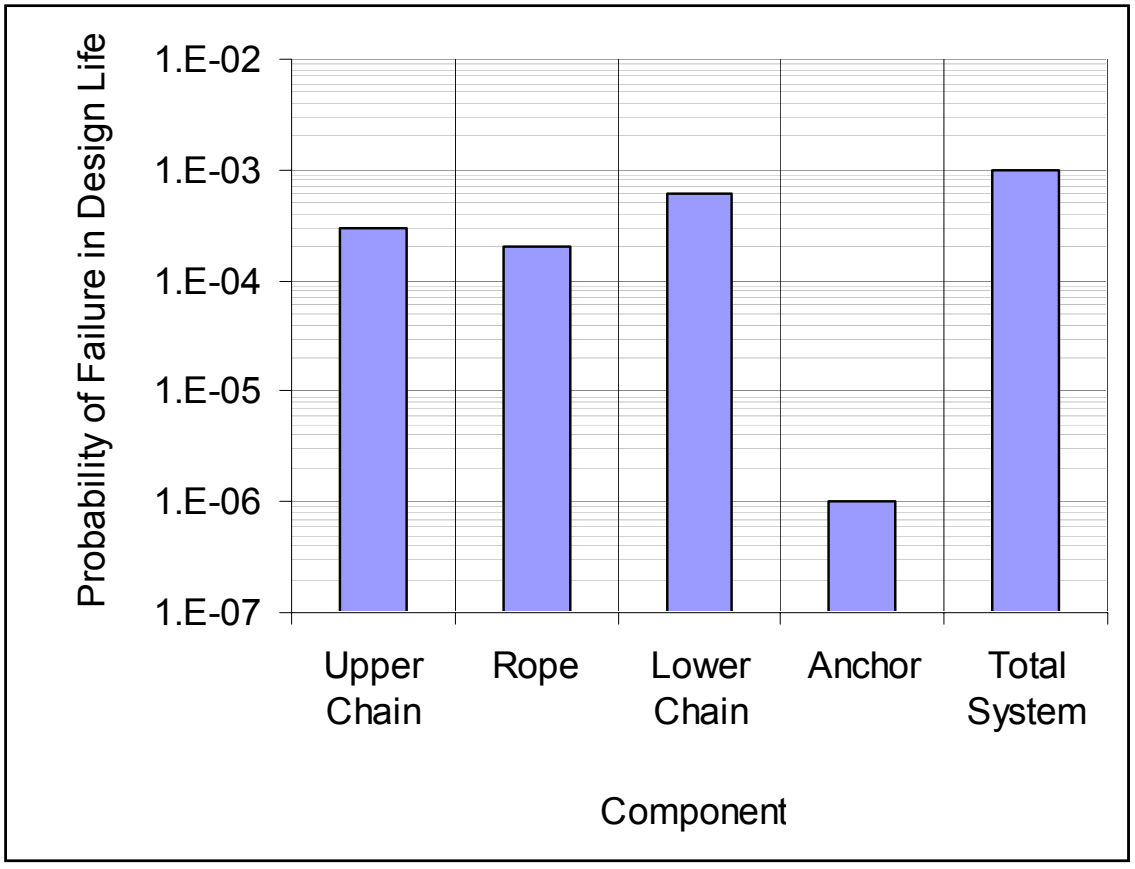

Figure C1. Comparison for Reliability of Components in a Mooring Line (adapted from Choi et al. 2006)

Back-Analysis of Hurricane Performance

We were provided with two reports detailing the performance of the mooring systems for the Deepwater Nautilus and the Noble Jim Thompson in Hurricane Ivan (Delmar 2005a and 2005b). Both mooring systems utilized suction caisson anchors: 9.55-foot diameter by 70-foot long caissons for the Deepwater Nautilus and both 9.55-foot diameter by 70-foot long and 12-foot diameter by 60-foot long caissons for the Noble Jim Thompson. The mooring system for the Deepwater Nautilus was taut with the line loading the caissons at about 40° to the horizontal under design loading conditions, while the mooring system for the Noble Jim Thompson was semi-taut with the line loading the caisson at about 10° to the horizontal under design loading conditions.

Capacity for In-Plane Loading

The capacity of the suction caisson anchors was analyzed as follows. Since both of these caisson dimensions provide similar axial and lateral capacities, a 12-foot diameter by 60-foot long caisson will be used to represent the anchors for each of these systems. The caisson is assumed to be installed to 55-feet below the mudline, with the load attachment padeye located 35 feet below the mudline. It is assumed to weigh 170 kips. In addition, since no data are available for the geotechnical properties of the soils at these two sites, a generic profile of undrained shear strength with depth will be used, as shown on Figure C2. The model developed by Aubeny et al., 2003 was used to estimate the capacity of the anchors for in-plane loading conditions. The results of this analysis are shown on Figure C3, where the curve denotes combination of axial (vertical) and lateral (horizontal) loads that will cause the anchor to move. The anchor capacity for the taut mooring system (the Deepwater Nautilus) is essentially governed by the axial capacity of the suction caisson, while the capacity for the semi-taut mooring system (the Noble Jim Thompson) is essentially governed by the lateral capacity (Figure C3).

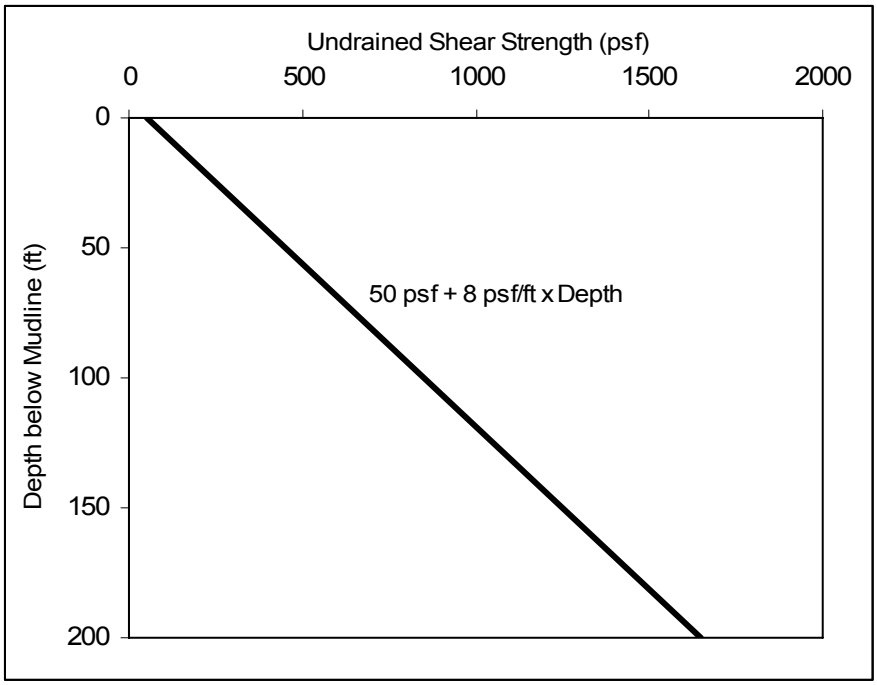

Figure C2. Representative Profile of Undrained Shear Strength versus Depth

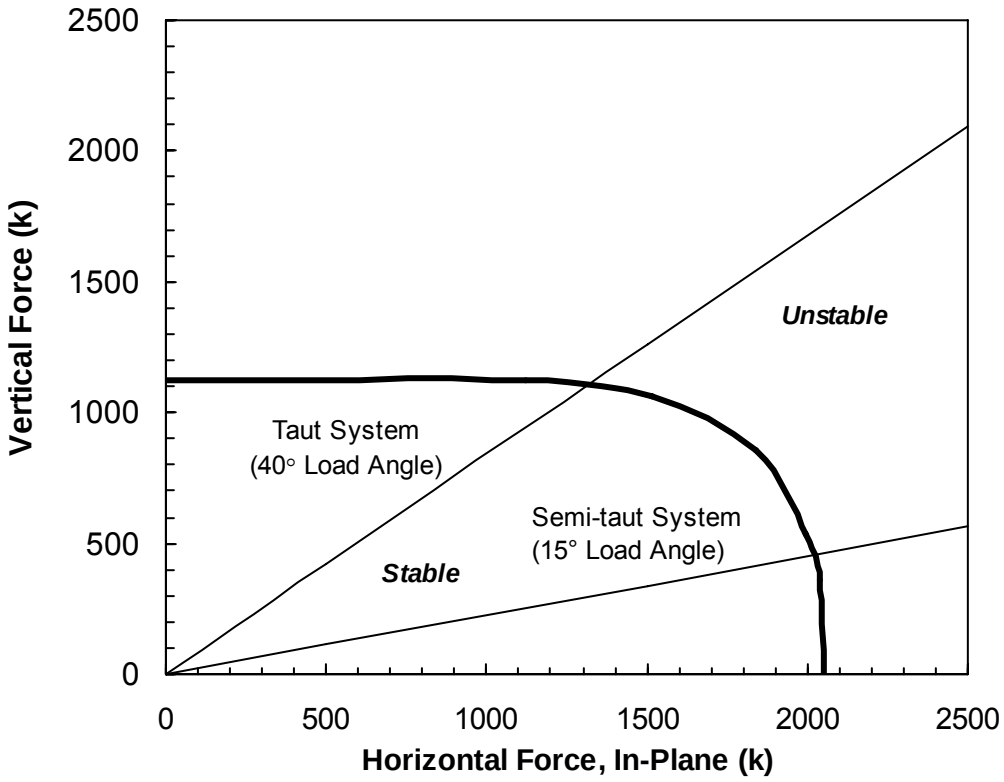

Figure C3. Estimated Capacity of Suction Caisson for In-Plane Loading (12-foot Diameter, 55-foot Penetration, Padeye located 35-feet below Mudline, 170 kip Weight)

The total in-line loading capacity is summarized in Table C1 for the anchors in each of the two mooring configurations. For both configurations, the line is expected to break before the capacity of the anchor was reached in Ivan. This result is consistent with the actual performance of the anchors during all of the recent hurricanes; the initial failures occurred in the lines and not at the anchors.

Table C1. Line Tension at Anchor Capacity for In-Line Loading

Condition	Line Tension at Anchor Capacity (kips)	Maximum Tension at Anchor in Ivan when Line Broke (kips)
Taut	1,700	1,200 to 1,500
Semi-taut	2,100	1,200

Capacity for Out-of-Plane Loading

Out-of-plane loading for a suction caisson produces a torsional moment that can twist the caisson; it also reduces the total axial and lateral capacity of the caisson.

Taut Mooring System – Deepwater Nautilus

The torsional capacity for the suction caisson (assuming a 12-foot diameter, 60-foot long anchor), is about 3,400 kip-ft. For the taut mooring system where the in-plane capacity is governed by the axial (or vertical) capacity (Figure C3), the out-of-plane torsional loading acts along the same failure surface as the axial loading, the circumference of the caisson. In this case, the interaction between axial and torsional loading can be simplistically approximated from force equilibrium, and the results are shown on Figure C4. The results show that the anchor may fail before the line breaks when the out-of-plane angle gets to be greater than about 20 degrees.

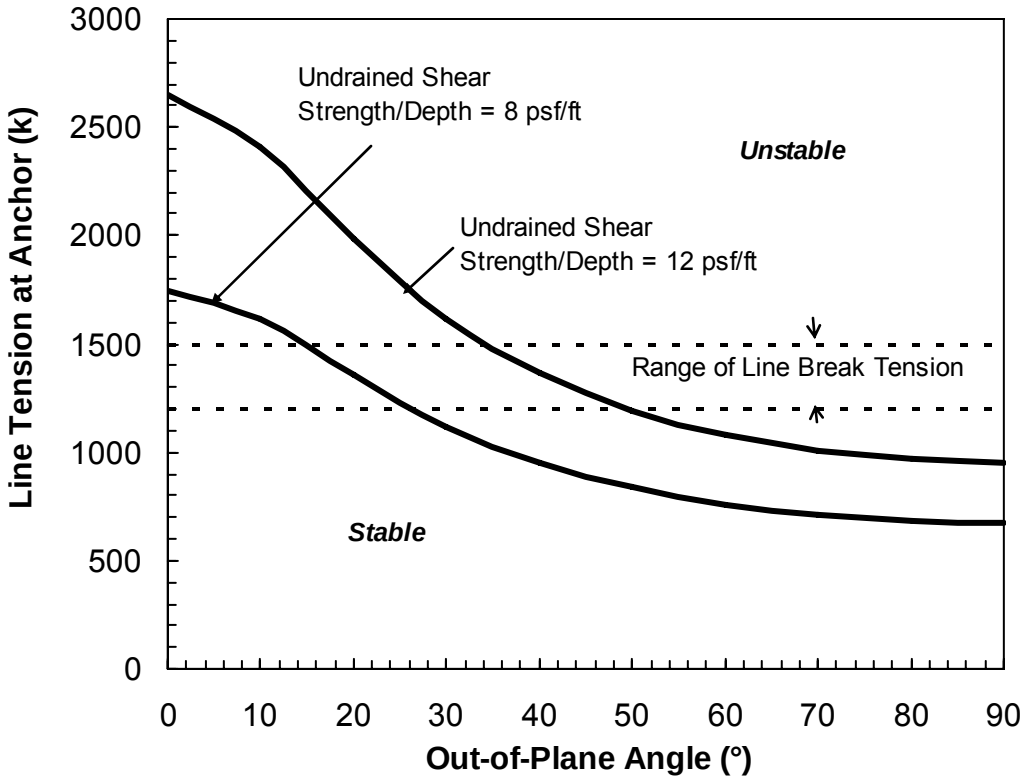

Figure C4. Effect of Out-of-Plane Loading on Suction Caisson Anchor Capacity for Taut Mooring System

In Hurricane Ivan, all of the lines broke in this taut system before any noticeable failure of the suction caisson anchors (Delmar 2005a), even with out-of-plane angles apparently beyond 90 degrees. This result may indicate that the method used to estimate torsional capacity is conservative. This result may also reflect that instability for the anchor on Figure C4 at high out-of-plane loading angles generally means that the anchor will begin to rotate, not necessarily pull-out. Also, the undrained shear strength could be greater than the profile assumed in Figure C2. If the undrained shear strength increases at a rate of 12 psf/ft versus 8 psf/ft, which is within the range of strength profiles in the Gulf of Mexico, then the anchor could hold with out-of-plane angles greater than 50 degrees (Figure C4). More detailed information about out-of-plane angles at line break and about the soil shear strength (say from caisson installation pressures) at this site would be valuable in refining this analysis.

Semi-Taut Mooring System – Noble Jim Thompson

The Delmar (2005b) report for the Noble Jim Thompson (semi-taut mooring system) presents torsional capacity estimates for the suction anchors in terms of three load conditions. The first condition considers lightly loaded anchors for which applied lateral loads are less than 50% of lateral-axial load capacity. For these conditions interaction effects due to the in-plane lateral-axial loads are presumably minor and torsional resistance is greatest. The second condition considers heavily loaded anchors for which applied lateral loads exceed 50% of in-plane lateral-axial load capacity. In this case, lateral-axial-torsional interaction effects are significant and torsional capacity is correspondingly reduced. The last condition considered was a post-breakout condition for which torsional capacity was governed by residual strength conditions. Geotechnical capacity estimates were based on soils data, anchor installation records, and experience. Suction anchor torsional capacity estimates for these conditions were as follows:

Table C2. Suction Anchor Torsional Capacity (Delmar, 2005b)

Condition	Capacity (kip-ft)
Lightly Loaded	3230
Heavily Loaded	2620
Post-Breakout	1190

The capacity estimated here for a suction anchor in pure torsion is 3400 kip-ft. The estimated torsional capacity for a lightly loaded anchor is slightly less than this due to the interaction effect of lateral-axial loading; therefore, the estimates in Table C2 appear very reasonable.

Estimated torsional and lateral-axial loads imposed on each anchor during the storm were determined from a dynamic analysis with Orcaflex (Delmar, 2005b). Table C3 presents maximum values.

Four anchors (2, 7, 8, and 9) failed during the storm due to a structural failure at the pad-eye. None of the anchors failed in a geotechnical sense of anchor pullout. However, evidence of soil yielding did occur in a number of instances, implying that a limit state

had been reached. For purposes of evaluating geotechnical performance, the suction anchors may be considered in terms of three categories:

Category I: No significant evidence of soil yielding was observed. Anchors 3, 5, 6, and 7 are in this group. Note that Anchor 7 failed structurally at the pad-eye, not due to loss of soil resistance.

Category II: The anchor was reported to have experienced a large rotation. Depressions, disturbance, or other evidence of lateral-axial motion (ploughing) associated with lateral-axial yielding was not reported, so yielding is assumed to have occurred in a purely rotational (twisting) mode. Anchors 1, 8 and 9 are in this group. Anchors 8 and 9 failed structurally at the pad-eye.

Category III: Evidence of disturbance or depressions in the soil surrounding the anchor was reported. This type of disturbance is taken as indicative that lateral-axial yielding occurred, where either pure lateral-axial motions or a combined lateral-axial-twisting motion occurred. Anchor 2 failed structurally at the pad-eye.

These groupings are somewhat intuitive and based on limited observations and data. Nevertheless, they can provide a useful framework for characterizing suction anchor performance.

Table C3. Summary of Suction Anchor Performance.

Category	Suction Anchor Number	Maximum Applied Torsion (kip-ft)	Maximum Applied Tension (kips)	Anchor-Soil Condition
I: No Evidence of Significant Soil Yielding	3	6791	1207	Normal
	5	64	1501	Normal
	6	461	957	Normal
	7*	3659	1518	Normal
II: Anchor Rotation - rotational yield mechanism in soil	1	241	30	Rotation
	8*	3258	679	Rotation
	9*	4027	495	Rotation
III: Disturbance, likely lateral-axial yielding in soil	2*	4217	584	Disturbance
	4	725	1439	Depression

*Structural failure occurred at pad-eye.

Comments on the performance summary in Table C3 include:

1. Estimated maximum applied torsion (Table C3) often exceeded the theoretical estimate of torsion capacity (Table C2). In the case of Anchor 3 in Category I, estimated applied torsion was more than twice the estimated capacity. This suggests that the methodology for estimating torsional capacity is generally conservative, which is consistent with the Deepwater Nautilus performance as well.
2. With one exception, even in cases where yielding was evident (Categories II and III), there appeared to be no major reduction in the load capacity. In three cases (Anchors 8, 9, and 2) the anchor appeared to be resisting torsions in excess of estimated capacity, in spite of evidence that soil yielding had apparently occurred. This suggests that suction anchors exhibit a relatively ductile response during yielding under both rotational and lateral-axial plastic deformation conditions.
3. Anchor 1 is the sole case where soil yielding (in this case rotational) appears to be associated with relatively low torsion and tension. The torsional resistance of the soil appears be consistent with a residual soil strength in this case. By contrast, the rotations in Anchors 8 and 9 do not appear to have seriously degraded the torsional capacity of the anchors.
4. Anchor 4 appears to be a fairly clear case of predominantly lateral-axial yielding. The dynamic load analysis indicates a high applied tension with only a moderate level of torsion, and direct observation indicated a depression on the back side of the anchor, indicative of a ploughing (lateral-axial) mechanism of yield.
5. The case for Anchor 2 is more ambiguous. From the high level of torsional loading, one would expect a rotational yield mechanism. The field observation simply noted ‘some soil disturbance’, so it is difficult to draw any definitive conclusion. Given the load levels and observed disturbance, some yielding, possibly combined lateral-axial-rotational occurred.

Foundation Alternatives

Out-of-plane loading can cause problems if the anchor fails and pulls out before the line breaks and then gets pulled across the sea floor with the drifting MODU. Even a structural failure of the anchor (such as a padeye getting ripped off of a suction caisson)

can be a problem if the piece of the anchor that pulls out is large enough to cause damage to infrastructure on the sea floor.

One possible alternative to reduce the effects of out-of-plane loading is a torpedo pile with a load attachment at the top of the pile (Figure C5). The advantages for the load attachment at the top are 1) it is simple and facilitates installation and handling and 2) it prevents an out-of-plane moment from being applied to the pile (either overturning, as with a plate anchor, or rotation, as with a suction caisson). The disadvantage for the load attachment at the top is that the lateral capacity is less because the pile will rotate instead of translate through the soil under pure lateral loading.

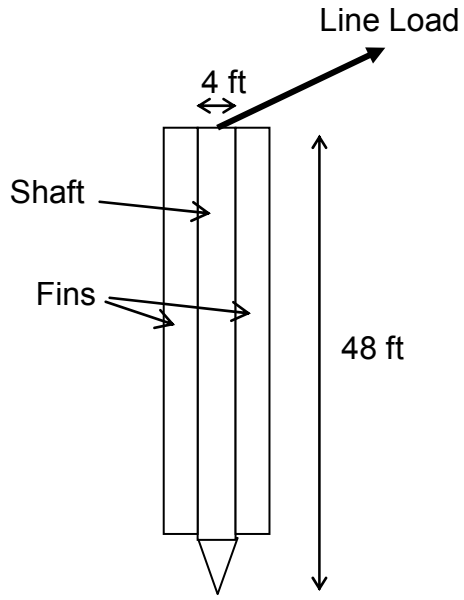

Figure C5. Torpedo Pile

In order to explore the viability of a torpedo pile, we used the profile shown on Figure C2 for the undrained shear strength of the soil. The torpedo pile is dimensioned so that it could be handled with the same vessel as a suction caisson and its weight is the same as the suction caisson, 170 kips. The torpedo pile is dropped from 300 feet above the sea floor. Based on research reported in Gilbert et al. (2008), we estimate that the torpedo pile will penetrate 110 feet below the mudline and have the in-plane capacity shown in Figure C6 and the capacities under pure loading conditions presented in Table C4.

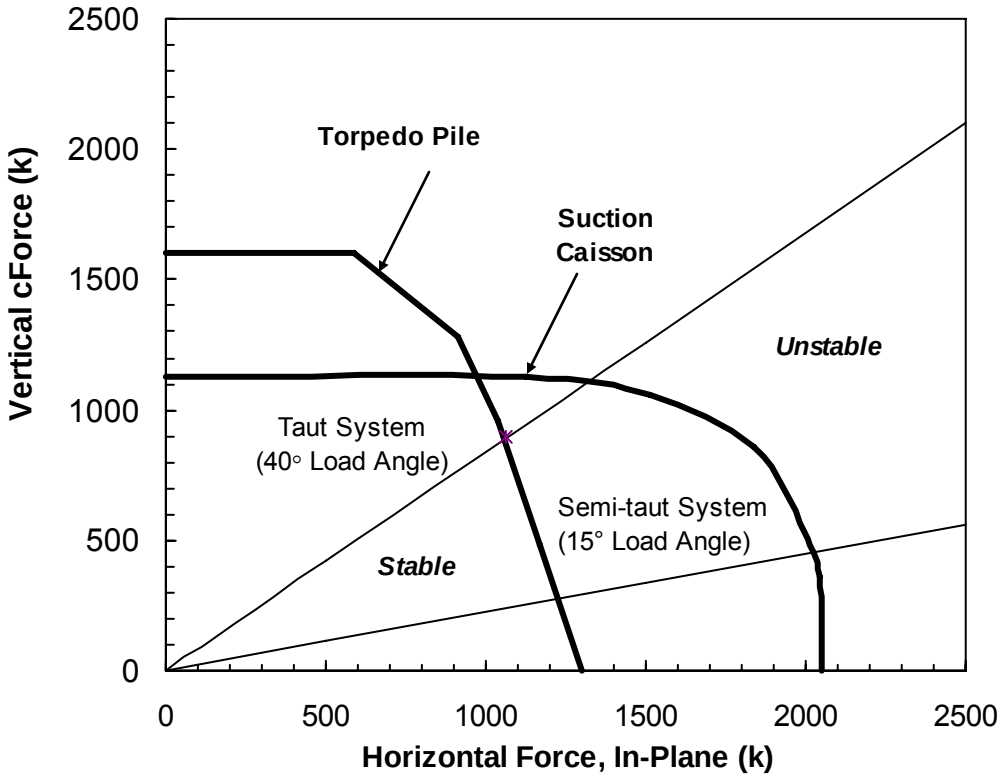

Figure C6. Comparison of Estimated Capacities for Suction Caisson and Torpedo Pile for In-Plane Loading

Table C4. Comparison of Foundation Capacities under Pure Loading Conditions

Foundation	Axial Capacity (kips)	Lateral Capacity (kips)	Torsional Capacity (ft-kips)
Suction Caisson (D=12 ft, L=60 ft, W' = 150 kips)	1,100	2,000	3,400
Torpedo Pile (D = 4 ft, L = 48 ft, W' = 170 kips, z_{tip} = 110 ft)	1,600	1,300	Not Applicable

The torpedo pile configured with the load attachment at the top provides more axial capacity and less lateral capacity under in-plane loading than the suction caisson. It would provide a similar overall capacity for a taut mooring system but a significantly smaller capacity for a semi-taut system. However, the advantage of this torpedo pile is that its capacity is not reduced under out-of-plane loading, as shown on Figure C7 for a taut mooring system..

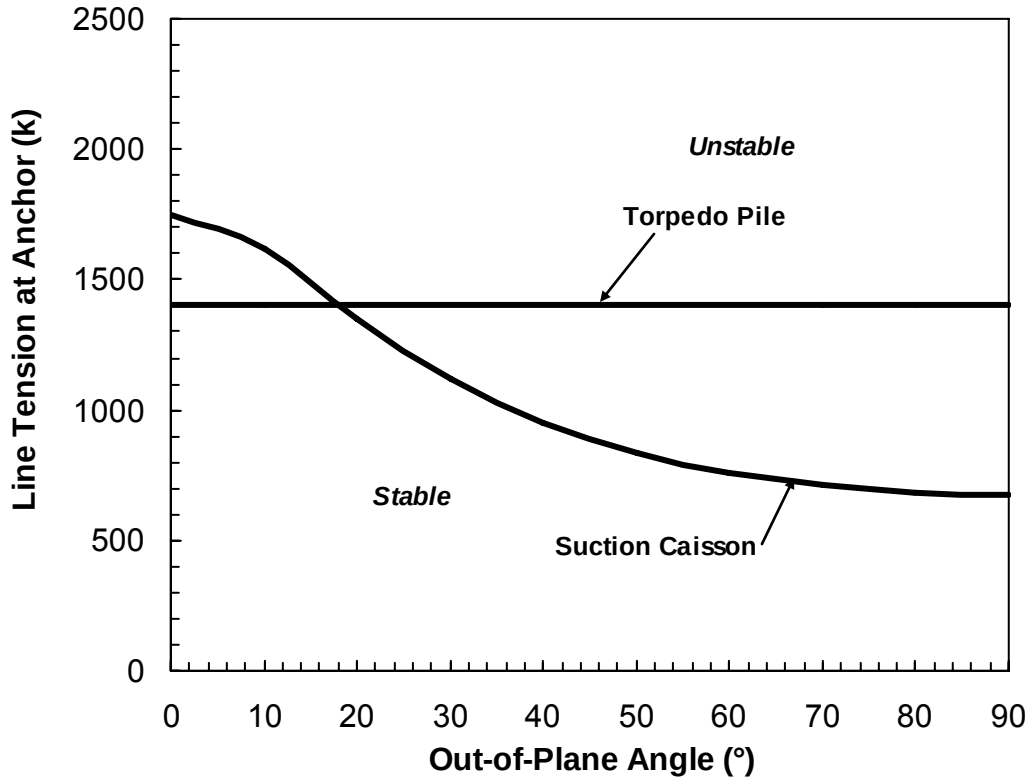

Figure C7. Effect of Out-of-Plane Loading on Suction Caisson and Torpedo Pile Anchor Capacities for Taut Mooring System

While we do not have detailed information concerning the behavior of drag embedment or vertically loaded plate anchors, there were cases in the recent hurricanes where these anchors pulled out under out-of-plane loading. A simplified analysis like for the suction caisson anchor on Figure C7 can be conducted for a plate anchor and it shows that the anchor will move (rotate sideways) with relatively small out-of-plane loading angles, providing that the anchor is loaded to near its capacity. However, these analyses are not very meaningful because the anchor will rotate into the loading and its rotational capacity will increase. Therefore, a more complicated trajectory analysis, that accounts for loading and movements in three dimensions (six degrees of freedom) is required to better understand how these anchors will behave under out-of-plane loading.

An extreme possibility for an anchor that exhibits no dependency on load direction would be a sphere. As an example, consider a 12-foot diameter sphere weighing the same 170 kips as the suction caisson or torpedo pile and dropped from 300 feet above the sea floor

like the torpedo pile. This ball anchor would penetrate 40 feet below the mudline (to its center), and would have an omni-directional capacity of only 600 kips. Therefore, the advantage to having asymmetry in the shape of the anchor is to provide a greater in-plane capacity for a given weight.

Other possible alternatives to reduce the effects of out-of-plane loading on anchor performance are:

- Put the padeye on a suction caisson on a swivel so that it can spin around the circumference;
- Put a constrained hinge between the shank and the fluke on a vertically loaded anchor or a drag embedment anchor to limit the overturning moment that is applied sideways under out-of-plane loading.

Conclusions

The above analyses lead to the following conclusions:

1. When MODU mooring systems are overloaded, the failure sequence is expected to begin in the lines and not at the anchors. Therefore, increasing the capacity of anchors under these “in-plane” loading conditions will not be very effective at reducing the possibility of a station-keeping failure for a MODU.
2. Once a MODU moves off station, the out-of-plane loading on the anchors can reduce the capacity of the anchors, and possibly lead to rotation, pull out, or a structural failure of the anchor.
3. The methodology used for estimating torsional capacity for suction caissons under out-of-plane loading appears to be realistic, but somewhat conservative. Further assessment of the torsional capacity estimate will require a review of the soil strength profile data and the analysis on which the estimate was based. In cases of large rotation about the anchor vertical axis, torsional capacity estimates based upon residual soil strength estimates are most appropriate.
4. Consideration of the cases in Hurricane Ivan where soil yielding appears to have occurred at suction caisson anchors indicates relatively ductile suction anchor behavior for both the rotational and axial-lateral yield mechanisms.

5. A general paucity of field anchor capacity data exists both for anchors subjected to purely in-plane lateral-axial loading as well as anchors subjected to varying components of torsional loading. Practical anchor capacity prediction models require an interaction relationship defining all possibilities of lateral, axial, and torsional load combinations at which yielding commences. A more comprehensive and detailed analysis of field performance data from all of the recent hurricanes, both for MODUs that did and did not lose station, would provide a useful source of data for validating and calibrating suction anchor geotechnical capacity prediction models.
6. Alternatives exist to improve the capacity of anchors under out-of-plane loading conditions, but further study would be required to evaluate their capability and feasibility.

References

Aubeny, C.P., Han, S.W., and Murff, J.D. "Inclined load capacity of suction caisson anchors," Intl. J. for Numerical and Analytical Methods in Geomechanics, Vol. 27, pp. 1235-1254, 2003.

Choi, Y. J, Gilbert, R. B., Ding, Y. and Zhang, J. (2006), "Reliability of Mooring Systems for Floating Production Systems," Final Project Report, Offshore Technology Research Center, Prepared for Minerals Management Service, 90 pp.

Delmar Systems, Inc. (2005a), Deepwater Nautilus Cheyenne Well D LR 399 Mooring Performance During Hurricane Ivan.

Delmar Systems, Inc. (2005b) Noble Jim Thompson Kepler MC 383 in Hurricane Ivan.

Gilbert, R. B., Choi, Y. J., Dangyach, S. and Najjar, S. S. (2005), "Reliability-Based Design Considerations for Deepwater Mooring System Foundations," Proceedings, ISFOG 2005, Frontiers in Offshore Geotechnics, Perth, Western Australia, 317-324.

Gilbert, R. B., Morvant, M., Audibert, J. (2008), "Torpedo Piles Joint Industry Project – Model Torpedo Pile Tests in Kaolinite Test Beds," Draft Project Report, Offshore Technology Research Center, Prepared for Minerals Management Service, 48 pp.